

Term-dependent changes in human milk extracellular vesicle composition and immunomodulatory effects in vitro

Brett Vahkal

Thesis submitted to the University of Ottawa in partial fulfillment of the requirements for the
Doctorate in Philosophy degree in Biochemistry

Supervisor: Dr. Marceline Côté

Department of Biochemistry, Microbiology, and Immunology

Faculty of Medicine

University of Ottawa



Frontispiece – “Ema lapsega” by Otto Friedrich von Moeller, n.d. Art Museum of Estonia.

Abstract

Human milk (HM) provides essential nutrition and immune protection for infants, with a varying composition based on gestational age (GA). The timing of birth – term or preterm, influences infants' vulnerability to inflammatory diseases. Premature infants have an increased risk of developing necrotizing enterocolitis (NEC), a devastating intestinal disease. The contributing factors to the NEC inflammatory cascade include formula feeding and intestinal dysbiosis. HM contains membrane bound extracellular vesicles (EVs), which could prevent the development of NEC via its cargo that includes mRNA, microRNAs (miRs), and proteins. Since mothers deliver infants at varying GA with unique needs, I hypothesized that the contents and biological functions of HM EVs are distinct. I characterized the GA-specific HM EVs using proteomics and RNA sequencing, and investigated the ability of HM EVs to mediate inflammation in cell culture models. The results revealed significant differences in the cargo of EVs isolated from term and preterm HM. While the total number of proteins and mRNAs in EVs was similar between the two types of milk, functional analyses revealed enrichment of immunoregulatory contents in preterm EVs, whereas term EVs were enriched in metabolism-related processes. Similarly, miR profiling identified 12 significantly different miRs between term and preterm HM EVs, with both groups exhibiting functional enrichments in metabolism and immune-related pathways. GA-specific HM EVs had a further differential effect on human gut epithelial cells, primary macrophages, and in a leukemia monocytic cell line – THP-1 cells. Both term and preterm EVs upregulated secretion of epidermal growth factor, while distinct effects were measured for pro-inflammatory cytokines in human intestinal cells and macrophages. Only term EVs inhibited secretion of IL-6, expression of IL-1 β following inflammatory stimuli, and apoptosis, while EVs from both groups inhibited IL-1 β secretion in macrophages and inflammasome-induced cell

death in THP-1 cells. These findings suggest that HM EVs, particularly those from term mothers, may regulate IL-1 β , the inflammasome, and cell death, thereby promoting a tolerogenic response. The results highlight GA-specific differences in HM EV cargo and their specific functional effects. Targeting the EV-mediated mechanisms could support the development of specialized therapeutic interventions to mitigate the risk of NEC and optimize neonatal health.

Acknowledgements

While there are numerous people to whom I owe an enormous thank you over the course of my PhD, this journey would not have been possible without the support of three exceptional scientists and key figures: Dr. Illimar Altosaar, Dr. Marceline Côté, and Dr. Emanuela Ferretti; for *“If I have seen further it is by standing on the shoulders of Giants”* (Sir Isaac Newton, 1676).

I would first like to thank Dr. Illimar Altosaar. You have been a scientific inspiration and have taken me on a multidisciplinary journey throughout the entirety of my PhD that has undoubtedly made me a better scientist and person, for life. Thank you for always reminding me to “see the forest through the trees”, to find the patent-worthy angle in any idea, and to always pursue science with an unyielding curiosity. I will be forever grateful for your guidance. Suur tänu kõige eest!

To Dr. Marceline Côté – thank you for welcoming me, and liters of milk, into your lab and being a pillar of support for the better half of my PhD journey. Your kindness and optimistic spirit are reflected on the positive lab environment, to which I am thankful to have belonged to. You are a master at providing a springboard for your mentees to find the unique facets of their projects, while ensuring scientific rigor and providing support in the stickiest of times. I am grateful to have been able to dip my toes into virology research and explore the similarities between extracellular vesicles and viral particles. I will forever treasure the time spent under your guidance.

To Dr. Emanuela Ferretti – thank you for supporting me since the beginning of my PhD journey. You have always made sure I think about the clinical perspectives and emphasized the importance of translatability in science. I am infinitely thankful for your guidance and inspired by your thorough approach to everything, which has been instrumental to my growth as a scientist. You are a shining light to not only your tiny patients, but to everyone who is fortunate to have your support, whether it be in the hospital, the university, or in life. Thank you for brightness, positivity, and encouragement, always. Until the next project!

I would also like to thank everyone at Dr. Illimar Altosaar’s lab *anno* 2020, and all the past and present members of Dr. Marceline Côté’s lab. Working alongside you has been the best! To my thesis advisory committee members, colleagues, and collaborators at the University of Ottawa and University of Sherbrooke, especially Dr. Jean-Francois Beaulieu, thank you for providing your depth of knowledge throughout this PhD project, technical, and moral support.

I would like to express a special thank you to Dr. Ardeshir Ariana for providing me the knowledge in signaling pathways and immunology as well as the technical training that made the experiments in this PhD possible. Your infinite kindness, helpfulness, and ability to explain even the most complex topics with ease has been essential for my endeavours in science and in life. Thank you for your friendship over the years.

Finally, to my friends, especially Irma and Žanna, family, and parents – *emme* and *issi*, you have been my guiding light and I couldn’t have done it without you. To the two loves of my life, Evan, and our dog, Albert, everything I am, is because of you.

Table of Contents

Abstract.....	iii
Acknowledgements.....	v
List of Figures.....	ix
List of Tables.....	xii
List of Abbreviations.....	xii
Chapter 1. Introduction.....	1
1.1 Human milk.....	1
1.1.1 Milk production and lactational stages.....	1
1.1.2 Human milk composition.....	4
1.1.3 Cells.....	7
1.2 Human milk and infant health.....	9
1.2.1 Infant immune system.....	9
1.2.2 Infant gastrointestinal system.....	11
1.2.3 Necrotizing enterocolitis.....	17
1.3 Extracellular vesicles.....	21
1.3.1 Bioavailability of milk derived extracellular vesicles.....	23
1.3.2 Cargo function of human milk extracellular vesicles.....	27
Hypothesis and dissertation objectives.....	32

Chapter 2. Characterization of term and preterm human milk extracellular vesicle proteins and mRNA	33
2.1 Preface.....	33
2.2 Abstract.....	35
2.3 Introduction.....	36
2.4 Results.....	39
2.5 Discussion.....	62
2.6 Materials and Methods.....	69
2.7 Acknowledgements.....	73
2.8 Data availability	74
Chapter 3. Characterization of term and preterm human milk extracellular vesicle microRNAs	75
3.1 Preface.....	75
3.2 Abstract.....	76
3.3 Introduction.....	77
3.4 Results.....	80
3.5 Discussion.....	93
3.6 Materials and Methods.....	98
3.7 Acknowledgements.....	101
3.8 Data availability	101

Chapter 4. Effect of gestational-age specific extracellular vesicles on inflammation in intestinal and immune cells	102
4.1 Preface.....	102
4.2 Abstract.....	103
4.3 Introduction.....	104
4.4 Results.....	107
4.5 Discussion.....	121
4.6 Materials and Methods.....	126
4.7 Acknowledgements.....	134
4.8 Data availability	135
Chapter 5. General discussion.....	136
5.1 Limitations	140
5.2 Future directions	142
References.....	145
<i>Curriculum vitae</i>	177

List of Figures

Figure 1.1. Lactation in the mammary gland.....	3
Figure 1.2. The infant intestine and protective effects of human milk bioactive molecules.	14

Figure 1.3. Simplified summary of cell death and pathogenesis involved in necrotizing enterocolitis.....	20
Figure 1.4. Biogenesis of small extracellular vesicles.....	23
Figure 1.5. Uptake and fate of extracellular vesicles.....	25
Figure 2.1. HM EV validation and surface marker characterization.....	40
Figure 2.2. Number of proteins in term or preterm human milk EVs.	41
Figure 2.3. Differentially expressed proteins in term and preterm HM EVs.....	42
Figure 2.4. Biological processes identified with PANTHER database for all term and preterm HM EV proteins.....	44
Figure 2.5. Reactome pathways identified with STRING database of all term and preterm HM EV proteins.	45
Figure 2.6. Biological processes enriched in significantly up- or downregulated preterm HM EV proteins.....	46
Figure 2.7. Analysis of proteins derived from HM and term and preterm HM EVs.....	48
Figure 2.8. Analysis of proteins derived from mature HM EVs and transitional term and preterm HM EVs.	49
Figure 2.9. Select HM EV proteins common to skim HM with biological process enrichment analysis.....	51
Figure 2.10. RNA transcripts identified in term and preterm HM EVs following RNA sequencing.....	52
Figure 2.11. Enriched biological processes identified with STRING database of all term and preterm HM EV mRNA.....	53
Figure 2.12. Differentially expressed mRNA in term and preterm HM EVs.	55

Figure 2.13. Biological processes enriched in significantly ($p < 0.05$) upregulated term HM EV mRNA.....	57
Figure 2.14. Biological processes enriched in significantly ($p < 0.05$) upregulated preterm HM EV mRNA.....	58
Figure 2.15. Gene set enrichment analysis of enriched processes, pathways, and functions for differentially expressed term and preterm HM EV mRNA.....	61
Figure 2.16. Single cell gene signatures in differentially expressed term and preterm HM EV mRNA.....	62
Figure 3.1. Human milk extracellular vesicle miR sequencing results.....	81
Figure 3.2. Top 20 most abundant miRs in term and preterm HM EVs.....	82
Figure 3.3. Abundance and functional prediction of top 3 miRs - hsa-miR-148a- 3p, hsa-let-7f-5p and hsa-miR-141-3p in human milk EVs.	83
Figure 3.4. Targets and functional prediction of top 20 term and preterm human milk EVs.....	85
Figure 3.5. Differential expression analysis and functional enrichment of term and preterm human milk EV miRs.....	86
Figure 3.6. Abundance of candidate miRs in human milk EVs that are significantly downregulated in necrotizing enterocolitis.....	90
Figure 3.7. Targets and functional prediction of miRs significantly downregulated in necrotizing enterocolitis with high abundance in human milk EVs.....	91
Figure 3.8. MiR target analysis of dysregulated mRNA in necrotizing enterocolitis intestinal tissue.	92
Figure 4.1. Characterization and super-resolution imaging of CD9, CD63, CD81, and CD14 HM EV surface markers.....	108

Figure 4.2. HM EV surface marker characterization.....	109
Figure 4.3. Effects of HM EVs on Caco-2 intestinal cells.....	111
Figure 4.4. HM EVs regulate expression and secretion of cytokines and signaling proteins in human intestinal epithelial cells.....	113
Figure 4.5. HM EVs regulate expression of cytokines and signaling proteins in macrophages.	116
Figure 4.6. Term and preterm HM EVs regulate inflammasome in macrophages.	118
Figure 4.7. HM EVs regulate cell death in THP-1 monocytes.	120

List of Tables

Table 1.1. Simple summary of human milk components, maternal and infant characteristics following term or preterm birth.	16
Table 2.1. Comparative analysis of differently abundant proteins in term and preterm HM EVs.....	42
Table 2.2. Differential mRNA expression in term and preterm HM EVs.	55
Table 3.1. Significant differentially expressed term or preterm HM EV miRs with log 2-fold change and adjusted p-value.....	86
Table 3.2. Presence of select miRs in prior sequencing studies of human milk cells, lipids, or EVs.....	88
Table 3.3. Human milk donor information.	99

List of Abbreviations

ANOVA	Analysis of variance
APC	Allophycocyanin
CD	Cluster of differentiation protein

cDNA	Complimentary deoxyribonucleic acid
CXCL	C-X-C motif chemokine
DHA	Docosahexaenoic acid
DIA	Data independent acquisition
DMEM	Dulbecco's modified Eagle's medium
EE	Early endosome
EGF	Epidermal growth factor
EMT	Epithelial-to-mesenchymal transition
ER	Endoplasmic reticulum
ERK	Extracellular-signal-regulated kinase
ESCRT	Endosomal sorting complexes required for transport
EV	Extracellular vesicle
FC	Fold change
FDR	False discovery rate
FITC	Fluorescein isothiocyanate
GA	Gestational age
GALT	Gut associated lymphoid tissue
GI	Gastrointestinal
GO	Gene ontology
GSEA	Gene set enrichment analysis
HM	Human milk
HMO	Human milk oligosaccharide
IFN	Interferon protein

Ig	Immunoglobulin
IGF	Insulin-like growth factor
IECs	Intestinal epithelial cells
IL	Interleukin cytokine
ILV	Intraluminal vesicles
JAK	Janus tyrosine kinase family of proteins
KEGG	Kyoto encyclopedia of genes and genomes
LC-MS/MS	Liquid chromatography tandem mass spectrometry
LF	Lactoferrin
LPS	Lipopolysaccharide
MAPK	Mitogen-activated protein kinase
MaxLFQ	Label-free quantification using MaxQuant computational proteomics platform
MFGM	Milk-fat-globule membrane
MHC	Major histocompatibility complex
MiR	MicroRNA
mRNA	Messenger RNA
MS	Mass spectrometry
MVB	Multivesicular body
NEC	Necrotizing enterocolitis
NF- κ B	Nuclear factor kappa b
NICU	Neonatal intensive care unit
PANTHER	Protein analysis through evolutionary relationships
PBS	Phosphate-buffered saline

PT	Preterm milk
qPCR	Quantitative reverse transcriptase polymerase chain reaction
RNA	Ribonucleic acid
RUV	Remove unwanted variation
STRING	Search tool for the retrieval of interacting genes/proteins
SWATH-MS	Sequential window acquisition of all theoretical mass spectra
TGF	Transforming growth factor
TLR	Toll-like receptor
TM	Term milk
TMM	Trimmed mean of M values
TNF	Tumor necrosis factor
VEGF	Vascular endothelial growth factor
WGA	Wheat germ agglutinin

Chapter 1. Introduction

1.1 Human milk

Human milk (HM) is a complex and unique biological fluid tailored for the nutritional and developmental needs of infants. As the gold standard in newborn feeding, HM provides essential micro- and macronutrients, bioactive components, which include stem and immune cells, microRNAs (miRs) and extracellular vesicles (EVs). By providing passive immunity, HM can influence the infant gut microbiome, immune system maturation, and overall short- and long-term health outcomes. Despite decades of HM research, a knowledge gap on the exact mechanisms of action for the numerous milk components remains, especially regarding EVs. The HM-contained EVs have been proposed to systemically influence newborn's metabolism, microbiome, and immune system, while their characterization and exact functional effects are still in their infancy. In the following sections, a general overview of HM will be provided to provide background for the diversity and potential origins of EVs in the context of the milk milieu.

1.1.1 Milk production and lactational stages

The conservation of HM benefits can be explained by the evolution of lactation to support survival of offspring. Functionally, the gland provides essential nutrients, aiding in energy transfer and immunomodulation^{1,2}. The mammary gland contains luminal and myoepithelial cells, which upon interacting with the collagen rich extracellular matrix polarize to basal and apical positions. HM secretion is affected by tight junctions within the mammary gland, in which nutrient passage affects milk's osmolarity. During lactation, differentiated luminal epithelial cells secrete milk components that are passed through the milk duct for expression (**Figure 1.1**)³.

Lactation has been proposed to develop in two stages, with the first in late pregnancy, and full lactation in the second stage at 32 to 40 hours post-birth of a term or preterm pregnancy⁴.

Milk production can be classified into three phases of lactation: colostrum, transitional, and mature. In the first 48-72 hours post-birth, the HM colostrum is especially enriched in immunological molecules, and is lower in lactose, indicating a primary focus on immunoregulation rather than nutrition^{5,6}. Within two weeks of birth, HM is in a transitional stage, where milk volume and nutrient content increase to support infant growth. The first two weeks of lactation are among the most demanding to influence the maturation of the infant's still-developing intestinal immune system, which is largely unexposed to foreign antigens⁷⁻⁹. Starting at one month post-birth, mature HM is secreted, with a marked decrease in immune proteins such as immunoglobulin A, lactoferrin, and lysozyme. Mature HM has been widely studied to investigate HM's response to mother's nutrient intake, circadian rhythm, and various illnesses.

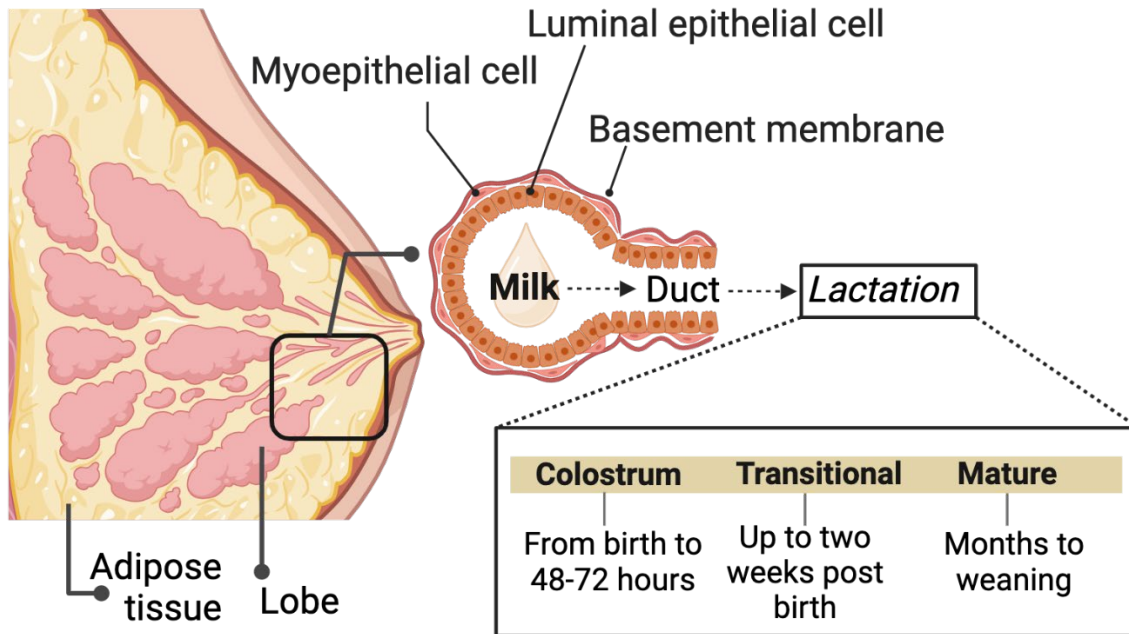


Figure 1.1. Lactation in the mammary gland. The lactating breast contains adipose tissue alongside abundant lobular structures for milk production. Luminal epithelial cells, responsible for secretion of milk components, are surrounded by myoepithelial cells, supported by the basement membrane. Milk is secreted towards the milk duct culminating in excretion. Lactation can be broadly divided into three stages post-birth with colostrum in the first 48 to 72 hours, followed by transitional milk within two weeks of birth, and mature milk secreted within the first month until induction of weaning. Figure created with BioRender.

Timing of milk expression adds further complexity to HM composition. Within a single feed, the initial expression is termed foremilk, which has a lower fat content and higher concentrations of lactose, and essential proteins to promote enzymatic digestion in the infant. Hindmilk, towards the end of the feed, has elevated lipid content, providing high energy nutrients and fatty acids to support development¹⁰.

Infants born at a gestational age (GA) of more than 37 completed weeks are considered at term. However, infants are also born prematurely and can survive as early as 22 weeks at gestation.

Considering HM, preterm birth is associated with delayed onset of lactogenesis, decreased milk production due to incomplete mammary gland development and cell differentiation, limited exposure to growth factors and hormones, and leaky tight junctions^{5,11-13}. Although there may be adaptations to preterm milk's composition, introduced in Section 1.1.2 below, whether the changes result from mechanical differences in the mammary gland, or as a response to a premature infant's needs, remains to be elucidated.

1.1.2 Human milk composition

HM is a colloidal suspension, which can be fractionated upon centrifugation. Key components include micronutrients in the form of vitamins and minerals, and macronutrients comprised of carbohydrates, lipids, and proteins. Lactose is the principal carbohydrate in HM, with oligosaccharides (HMOs) providing a large secondary portion⁵. The dispersion stability is provided by the lipids, which average between 3-5% in HM. Following centrifugation, the fat layer coalesces and floats, the cells pellet, leaving the skim milk in an aqueous interphase. The fat globules, also known as milk-fat-globule membrane (MFGM), consist of nonpolar lipids that are coated with amphiphilic molecules such as phospholipids⁴, and range in size from 0.2-15 μ M¹⁴. The milk fat delivers cholesterol, sphingolipids, and proteins such as lactadherin, butyrophilin and transmembrane glycoprotein cluster of differentiation 36 (CD36)¹⁵.

Three of the most prevalent protein fractions in HM include casein, whey, and mucins which are provided by the MFGM¹⁵. Following fractionation, the middle layer contains both casein and whey proteins, majority of the EVs found in milk, while the precipitated fat layer is enriched in MFGM and contains additional casein proteins. The whey fraction includes a diverse profile of

individual proteins and peptides, with α -lactalbumin, lactoferrin, lysozyme, serum albumin and secretory immunoglobulin A among the highest in concentration. The casein fraction contains β and κ -casein, with lower concentrations of α -casein, all of which predominantly serve a nutrient function together with several whey proteins¹⁵.

Beside the nutrient role of HM, the bioactive molecules help set the stage for ongoing survival and development of the infant. They include cells (epithelial, immune and stem cells), EVs, immunoglobulins (IgA, IgG, IgM), cytokines (IL-6, IL-7, IL-8, IL-10, IFN γ , TGF β , TNF α), chemokines (G-CSF, MIF), cytokine inhibitors (TNFRI and II), growth factors (EGF, VEGF, NGF, IGF, erythropoietin), hormones (calcitonin and somatostatin), anti-microbial proteins (lactoferrin, lactadherin), metabolic hormones (adiponectin, leptin, ghrelin), HMOs, glycans, mucins, and more^{5,15-17}.

Gene regulation by mother to infant crosstalk is evidenced by the presence of messenger RNAs (mRNA) and miRs in milk. Abundant miRs have been extracted from whole and skim milk, lipid fraction, cells, and HM-derived extracellular vesicles (EVs). To understand the downstream effect in infants, HM has been extensively characterized for its miR content, while the mRNA characterization is limited¹⁸⁻²⁰. Milk-derived RNA molecules have been shown to be bioavailable and able to withstand digestion^{21,22}, indicating that their main carrier vehicle may be EVs. A detailed overview of HM and EV-derived mRNA and miRs, in the context of GA and infant health, is provided in Chapters 2 and 3.

Further evidence of HM's ability to respond to the needs of the infant has been sought by investigating any changes to the nutrient and immunomodulatory protein content. The portion of whey and casein fractions in HM changes across lactation, where the ratio of whey/casein is approximately 90/10 in colostrum, declining to 65/35 in transitional, and 60/40 in mature milk^{5,15}. The overall protein levels are highest in colostrum, declining steadily over four to six weeks postpartum, remaining stable in the first year of lactation.

Mothers who delivered preterm infants produce significantly higher levels of proteins and fat in milk⁵. Increased concentrations of several lipids, such as cholesterol, phospholipids, and long-chain polyunsaturated fatty acid and docosahexaenoic acid (DHA) have been measured^{4,23,24}. As for proteins, elevated levels have been detected for epidermal growth factor (EGF), secretory IgA, lysozyme, lactoferrin, and interferons (IFN)^{5,17,25}. Higher levels of fatty acids may confer increased support for neonatal development, cellular membrane integrity, brain cell growth, and myelin formation⁴, while the proteins may have enhanced immunological benefits^{17,25}. HMOs from term and preterm milk, which are critical in regulating microbial colonization, have a generally similar concentration, though variations in specific oligosaccharide profiles have been observed²⁶.

Notably, preterm infants have higher nutrient requirements, wherein donor milk, mainly derived from mature term milk, requires additional nutrient supplementation when fed to preterm infants¹⁰. When compared to term milk, the preterm milk protein levels are mainly elevated in the colostrum stage²⁷. This difference gradually diminishes as lactation progresses, with protein levels in preterm milk aligning more closely with term milk over time. However, the variable

and dynamic nature of HM suggests adaptation to the needs of infant^{5,28} and underscores its importance for supporting the rapid growth and development of preterm infants.

At every opportunity, HM feeding in neonatal intensive care units (NICU) is initiated with mother's own milk, regardless of GA. For premature infants in the NICU, the current recommendations include incorporation of mother's own milk, including the initial colostrum and transitional preterm HM¹⁰. While the overall nutrient profiles between term and preterm HM can be variable^{10,27}, the immunological impacts of preterm HM are still largely understudied. To address this paucity of therapeutically critical data, the GA-based changes to HM EV contents are discussed in Chapters 2 to 4.

1.1.3 Cells

The cells found in human milk originate from the mother's bloodstream or from within the breast tissue²⁹. In HM, populations of epithelial, stem, and immune cells have been identified³⁰⁻³². Epithelial cells comprise the largest portion of cells in HM and include lactocytes that are responsible for synthesis of milk proteins²⁹. The stem cells in are multipotent and able to differentiate into diverse cell types, including epithelial cells, such as the milk-producing luminal cells, adipocytes, and osteoblasts. Populations of HM-derived stem cells also contain markers either on the cell surface or intracellularly that are associated with mesenchymal (CD44, CD90, CD271, and CD146) and embryonic (Oct4, Sox2, Nanog) stem cells^{29,33}. Upon transfer to the infant, the stem cells have been proposed to localize to the neonatal gut and differentiate into epithelial cells, thereby supporting barrier formation³⁴. They may also be able to enter the newborn's circulation, reaching the brain, lungs, spleen, liver, and bone marrow^{29,33,35}. Preterm

HM has been shown to contain differentially expressed stem cell markers when compared to term³⁶, however the functional effects of the different cell types on the infant are unclear.

Immune cells constitute the second largest portion of cells in HM. Based on sequencing analyses^{9,30-32,37}, the abundant populations include monocytes, macrophages, natural killer (NK) cells, and neutrophils of the innate immune system, while a quarter of HM's immune cells are lymphocytes of the adaptive immune system, composed of a T cell majority and B cell minority³⁸. Involved in both innate and adaptive immunity, eosinophils have been detected in HM and their presence linked to infant illness³⁰. The immune cells are proposed to have immunomodulatory roles in the breast itself and also support the infant's innate and adaptive immune responses⁸. For example, passive immunity is provided to the newborn by the B cells that are sequestered in the mammary gland for immunoglobulin (Ig) production. Of the B cells that are trafficked into the milk, the IgG secreting type appears predominant³⁸. In a mouse model, milk-derived B cells were detected in bone marrow and spleen following feeding³⁹, wherein they may continue secreting antibodies to support defense against pathogens.

Based on the overall abundance, macrophages have been found to be in the highest concentration in HM³⁰, containing both pro- and anti-inflammatory populations, which can be broadly classified as M1 and M2 macrophages, respectively⁹. While the mammary gland itself has been shown to have tissue resident immune cells, for example macrophages can facilitate remodeling of the extracellular matrix between lactational stages, the transfer of immune cells from circulation may explain the overall variety of the cells carried by HM^{40,41}. Thus, the concentrations and cell types can be affected by the stage of lactation and health of the mother or

infant. The highest concentration of immune cells is found in colostrum, while transitional and mature milk have a marked decrease in concentration as infant's immune system develops over time^{37,38}. Correspondingly, preterm birth is associated with additional changes in milk immune cell concentrations⁴², which can include a decrease in activated T cell populations⁹.

1.2 Human milk and infant health

The longstanding recommendation of HM-feeding remains highly relevant for infant health⁴³. At birth, the infant's naïve gastrointestinal tract (GI) continues its maturation with environmental exposure, initiating commensal bacteria colonization. Bioactive components of HM facilitate antimicrobial protection and immune modulation through secretory antibodies, oligosaccharides, lactoferrin, cytokines, proteins, and EVs⁴⁴. Thus, HM is associated with various benefits for infants, which includes improved neurodevelopmental outcomes, lower risk of infections, reduction in late-onset sepsis, and protection against necrotizing enterocolitis, a devastating disease affecting premature newborns⁴⁵⁻⁴⁷. Therefore, direct, or indirect supply of HM can support the overall health of the newborn.

1.2.1 Infant immune system

The early development in infants is supported by a tolerogenic immune environment to facilitate exposure to commensal bacteria that occurs during birth and in the first days of life. These environmental interactions encompass maternal milk, which can support a dampened inflammatory cytokine production and a regulatory phenotype for T and B cells. Still, protection against non-commensal microbes is required⁴⁸. As a front line, the innate immune system provides initial defense against pathogens, comprising of neutrophils, monocytes, macrophages,

natural killer cells, and dendritic cells. In newborns, mature neutrophils are present, but demonstrate reduced effectiveness in key immune functions, including bacterial clearance, inflammatory response, and migration to areas of infection⁴⁹. Premature infants have additional deficits in neutrophil functionality^{50,51}. Similarly, the interferon gamma (IFN γ) producing natural killer (NK) cells are an early and effective defense against viruses, but have a lower cytolytic function and activation threshold in neonates than adult NK cells^{52,53}.

Macrophages are considered one of the primary mediators of a newborn's innate immune system⁵⁴. Along with their precursor, monocytes, macrophages are still immature, with limited toll-like receptor (TLR) expression resulting in reduced innate signaling and cytokine responses. TLRs are pattern recognition receptors found on a variety of cell types, including macrophages, that recognize danger signals, such as lipopolysaccharides (LPS) on pathogens *Escherichia coli*, *Streptococcus viridans*, and the respiratory syncytial virus⁵⁵. Upon stimulation, downstream signaling leads to secretion of pro-inflammatory cytokines, such as interleukin 1 beta (IL-1 β) and tumor necrosis factor (TNF). The cytokines then recruit additional immune cells to the site of infection⁵⁶. Notably, macrophages in preterm infants have decreased bactericidal function and less TNF secretion than term infants⁵⁷. Though the macrophages are less potent activators of the adaptive immune system, they quickly reach adult levels in TLR expression⁵⁸⁻⁶¹. Despite this, preterm monocytes are still hyporesponsive to LPS with reduced cytokine secretion⁶². As such, the vulnerability of preterm infants to infections may be partly attributed to these disparities.

Interactions between the innate immune cells and the T and B cells of the adaptive immune system are essential, especially for the activation of T cells. In addition to the limitations in

newborn NK cells and macrophages, the limited responsiveness of neonatal dendritic cells also affects interferon secretion and can lead to attenuated priming of T cells. Following birth, B cells are responsible for antibody production. They can promote an anti-inflammatory Th2 response through secretion of IL-10 and TGF- β . Since neonatal B cells have a lower expression of T cell co-stimulatory molecules, the overall humoral immune response to bacterial polysaccharides is dampened. This can also result in an insufficient cytokine synthesis in response to stimuli. While the diminished responses allow development of tolerance, they can leave neonates vulnerable to infections^{60,63}.

The infant immune system develops rapidly post birth but remains most vulnerable until two to three months post birth. Thus, in this newborn stage, infants are highly reliant on mother's milk for passive immunity. To prevent overactivation of immune response, such as in the case of allergies, but to also support the mounting of an appropriate immune reaction, two key target mechanisms have been proposed for HM: reduction of inflammation, and promotion of tolerance. In the former, HM provides anti-inflammatory cytokines, such as TGF β ⁶³, whereas in the latter, immunomodulatory proteins, including immunoglobulins and sCD14⁶⁴, are transferred. Given the route of HM-intake in infants, the immunomodulatory regulation can occur, but is not limited to, the oral mucosa and gut associated lymphoid tissue.

1.2.2 Infant gastrointestinal system

Gestational age at birth impacts infant's GI maturity anatomically and physiologically. In the stomach, amniotic fluid buffers the gastric acid environment to a pH of 8 immediately after birth, which falls to a pH of 1.5-3, 48 hours post birth, and gradually returns to a neutral range in the

first week of life⁶⁵. The high gastric pH of infants may impede the activity of gastric enzymes thereby affecting digestion. Gastric acid secretion is more reduced in preterm infants, increasing digestion difficulty^{66,67}.

Nutrients are absorbed along the epithelial enterocyte cell monolayer of the small intestine, wherein the depth of crypts and height of villi increase with gestational age. This GI architecture allows for differentiation of intestinal stem cells into several cells including, epithelial, goblet, Paneth, and enteroendocrine cells. The elongation of villi provides increased surface area for nutrient uptake, while the deepening of the crypts creates space for the proliferation and differentiation of stem cells. These processes are fundamental to maintain intestinal integrity and are compromised in the premature infant^{68,69}.

While preterm infants have an increased intestinal permeability, HM feeding is associated with an increase in barrier integrity over the course of the first month of life⁶⁹. To compensate for the immature digestive systems of preterm infants, recent studies have proposed the adaptation of preterm HM to have a higher protease activity when compared to term. The presence of enzymes like plasmin, kallikrein, and thrombin in greater quantities may pre-digest proteins and facilitate a more efficient nutrient absorption^{67,70}. HM also contains abundant immunoregulatory proteins, many of which gain bioactivity following digestion^{71,72}.

Along the intestine, preterm infants have a reduced number of Paneth cells, which are responsible for production of antimicrobial peptides. Near Paneth cells, goblet cells produce mucus and can transfer antigens to intestinal immune cells⁶⁹. These cells by the epithelial barrier

therefore support the innate immune defences that function to control pathogenic bacteria as well as the colonization of commensal bacteria in the intestine⁶⁹. HM has been shown to assist in many of these functions in compromised preterm infants and vulnerable term infants by providing abundant antimicrobial peptides and being a source of mucins to support the intestinal barrier.

The complex interplay between the GI resident immune cells and bacteria shape infants' health⁷³⁻⁷⁵. The intestinal immune system is comprised of inductive and effector sites. Gut associated lymphoid tissue (GALT) and Peyer's patches are among the inductive sites, while the effector site is comprised of the lamina propria – a connective tissue layer containing immune cells^{76,77}. Intraepithelial immune cells reside within the epithelial layer to further facilitate antigen sampling, presentation, and maintenance of intestinal homeostasis⁷⁶. Mucosal immunity is supported by differentiated mucosal macrophages, which display functional phagocytosis and bactericidal activity⁷⁸ (**Figure 1.2**).

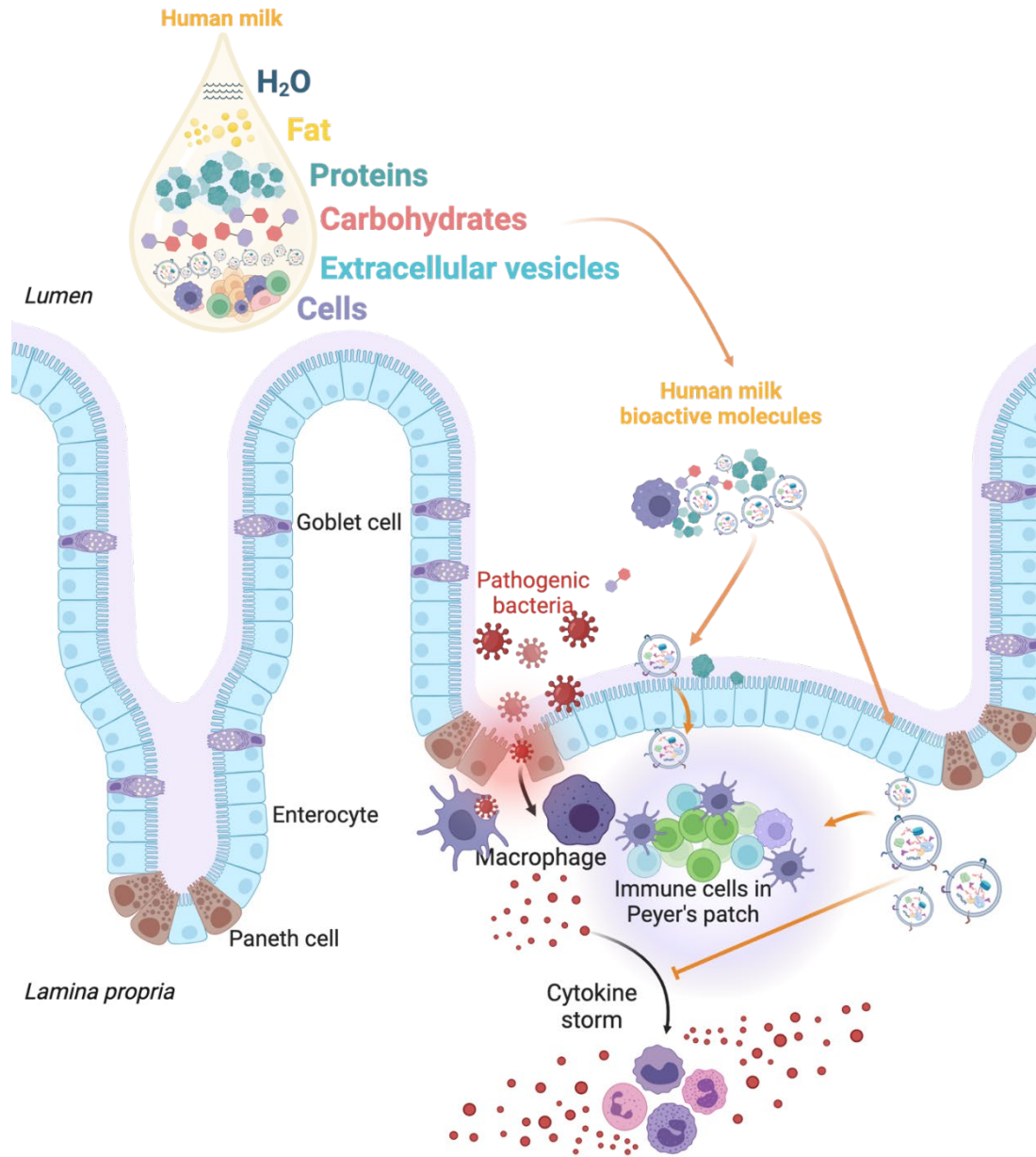


Figure 1.2. The infant intestine and protective effects of human milk bioactive molecules. The epithelial layer of the gastrointestinal tract (GI) contains enterocytes that are interspersed with cells such as mucous-secreting goblet cells and Paneth cells that produce antimicrobial peptides. Tissue resident immune cells are present in the lamina propria and Peyer's patches. In newborns, responses to pathogenic bacteria by immature intestinal and immune cells can result in disruption of the GI barrier culminating in a cytokine storm for additional immune cell recruitment that contributes to systemic sepsis. Human milk bioactive molecules of proteins,

oligosaccharides, and EVs have been shown to mitigate the exacerbated immune response. EVs can be transported through the intestinal cell layers to reach resident immune cells thereby modulating homeostatic responses. Figure created with BioRender.

Introduced in Section 1.2 above, the supply of immune and stem cells by HM can also modulate immune responses in the gut-immune boundary. HM-derived CD8⁺ cytotoxic T cells were shown to be taken up in Payer's patches, where they displayed cytolytic and pro-inflammatory characteristics. Increases in TNF α , IFN γ , IL-18 were intended to support the inefficient response of infant's own T cells^{8,38}. In contrast, maternal antibodies, such as IgG and IgA, could suppress intestinal CD4⁺ T cells⁷⁹. Furthermore, HM-derived IgG can recognize intestinal pathogenic *E. coli* and protect against infection^{73,80}. By shaping and nurturing the interactions between the microflora and immune system, HM has been shown to affect microbial colonization and the microbiome itself⁴³. For example, HMOs can have a prebiotic effect and prevent pathogen binding^{81,82}. In recent years, the immunoregulatory role of HM-derived EVs has added additional complexity to our understanding of mother-infant crosstalk. Thus, many of the research efforts have focused on the maternal educational immunity via HM's components⁸³⁻⁸⁵. The balance and interplay between the microbiome, intestinal epithelial cells, and the gut-associated immune system is especially vulnerable in premature neonates, wherein HM can have a crucial role in modulating the cascades that lead to the development of inflammatory intestinal diseases (**Table 1.1**).

Table 1.1. Simple summary of human milk components, maternal and infant characteristics following term or preterm birth. Human milk composition can differ following term or preterm birth and may respond to the unique needs of infants. Gestational age can further affect maternal characteristics and infant health outcomes.

Characteristics	Term Birth (GA > 37 weeks)	Preterm Birth (GA < 37 weeks)
Human Milk Content		
Proteins	High concentrations of α -lactalbumin, lactoferrin, osteopontin, lysozyme	++ Increased protein levels, including EGF, TGF α , lactoferrin, interferons
Enzymes	Normal levels	++ Increased protease activity may support nutrient absorption via pre-digestion of proteins
Antibodies	Normal levels	++ IgA and other immunoglobulins
Cells	Epithelial, stem, immune cells (monocytes, macrophages, NK cells, neutrophils, T cells, B cells)	++ Higher concentrations of immune cells, differential expression of stem cell markers
Lipids	+ Normal levels of cholesterol, phospholipids, and DHA	++ Increased levels depending on lipid type
Human milk oligosaccharides (HMOs)	+ Normal levels, limited variations	+ Similar concentration to term, variations in specific profiles
Maternal Characteristics		
Mammary gland development	Complete	Incomplete gland development and cell differentiation
Tight junctions	Intact	Leaky
Infant nutrient needs	Human milk meets requirements	Higher nutrient requirements, supplementation and fortification may be needed
Infant Immune System		
Innate immune system	Neutrophils, monocytes, macrophages, NK cells, dendritic cells; mature neutrophils present with reduced effectiveness; limited toll-like receptor (TLR) expression, reduced innate signaling and cytokine responses	Additional deficits in neutrophil functionality; reduced effectiveness in macrophages and monocyte populations; reduced bactericidal function, TNF secretion, monocytes hyporesponsive to LPS

Adaptive immune system	Immature with antigen specific T and B cell responses	Additional vulnerabilities due to more pronounced immaturity
Infant Gastrointestinal System		
Gastric environment	Variable pH post-birth, returning to neutral range within one week	Reduced gastric acid secretion, increased difficulties with digestion
Intestinal development	Improved nutrient absorption with increases in intestinal crypts and villi height with gestational age	Compromised intestinal integrity, increased permeability, reduced number of Paneth cells
Infant Health Outcomes Following Human Milk Feeding		
Neurodevelopmental outcomes	Lower risk	Higher vulnerability with potential enhanced support by human milk's increased fatty acid content
Infection risk	Lower risk	Increased risk which may be reduced by human milk feeding
Necrotizing enterocolitis	Low risk	High risk with protection provided by human milk feeding
Late-onset sepsis	Lower risk	Increased risk, but human milk feeding provides protection

1.2.3 Necrotizing enterocolitis

The concert of protective effects by HM provides substantial support to infants. However, the development of disease is multifactorial, and HM-feeding may not be readily available for preterm neonates in intensive care units⁸⁶. Under these circumstances, newborns have increased risk of developing necrotizing enterocolitis (NEC). Difficult to prevent, detect, and treat, with far reaching complications even after recovery, treatment strategies against NEC are an ever prevalent research area⁸⁷.

NEC has a significant burden on the healthcare system, with an incidence ranging from 1 to 12% in premature neonates^{88,89}, to as high as 22% in infants with a birthweight of <1000g⁹⁰. The overall mortality rate ranges from 10-50%^{91,92}, while cases of rapid NEC progression can result

in up to 80-100% mortality⁹³. During the acute stage of NEC, initial intestinal dysbiosis leads to disruption of the intestinal epithelium, cell death, and immune cell recruitment⁹⁴. Once systemic inflammation has been reached in the chronic stage, effectors such as reactive oxygen species, TLR4-dependent inflammatory activation and neutrophil recruitment, circulatory IFN γ and chemokine CXCL5, lead to further lung and brain injury. As a result, survivors of the disease have additional long-term medical conditions, including short bowel syndrome and neurodevelopmental complications⁸⁷.

Previous sections (1.2.1-1.2.2) provide an overview of the immaturity of a newborn's immune system that can be supported by HM feeding. As is evident in NEC's etiology, neonates, particularly those that are premature, can mount a substantial immune response, leading to disruption of the intestinal epithelium, which can culminate in tissue necrosis and systemic sepsis. The multifaceted pathogenesis of NEC begins at the intestinal epithelium and lumen interface. There, the interplay between TLR4 signaling, intraluminal bacteria and dysbiosis leads to an often irreversible inflammatory cascade^{87,95}. The current consensus of TLR4 being one of the main initial effectors of NEC resulted from numerous animal and human studies. Mice with a defective intestinal TLR4 receptor are protected against development of NEC⁹⁶, while secondary inhibitors of TLR4 can protect against NEC⁹⁷. In clinical studies, 10 out of 17 neonates that had mutations in TLR4 pathway inhibitor SIGIRR, developed NEC⁹⁸. TLR4 expression is also markedly increased in NEC tissue and is overall higher in premature infants' intestinal epithelium due to its *in utero* role of regulating stem cell differentiation via interactions with Wnt and Notch pathways⁹⁹⁻¹⁰². Thus, following premature birth, high levels of TLR4 switch from a protective developmental role to inflammatory activation by the newly introduced intestinal

bacteria. This biological expression pattern may also explain why premature infants are more vulnerable to NEC⁸⁷.

The colonization of the GI microbiome in the first few days of life influences the differentiation of naïve CD4⁺ T cells. The differentiated populations that include T helper (Th1, Th2, and Th17) and T regulatory cells in turn control the response to microbiota¹⁰³. NEC is characterized by the dysbiosis of the microbiome, with a higher concentration of *Enterobacteriaceae* carrying LPS that can trigger the TLR4 cascade¹⁰⁴. The disruptions in the intestinal epithelium allow the microbes to further translocate into the underlying vasculature. As a result, the intestine is infiltrated by pro-inflammatory macrophages, and Th17 cells that release IL-17 and IL-22¹⁰⁰. Increase in these cytokines can lead to additional immune cell recruitment and a systemic response (**Figure 1.3**). Another critical factor of the disease is tissue necrosis, which can be facilitated by different types of cell death in the intestinal epithelium, including apoptosis, necroptosis, pyroptosis, and autophagy, wherein TLR4 signaling has been implicated in all the underlying signaling cascades and in different cell types⁸⁷.

Apoptosis is generally considered a non-inflammatory cell death, whether it is facilitated by death receptor signaling, the intrinsic pathway triggered by mitochondria destabilization, or the proteolytic granzyme molecules. However, the intrinsic pathway has recently been linked to the signaling in pyroptotic cell death via activation of NLRP3, followed by release of IL-1 β and Gasdermin D. Together with pyroptosis, necroptosis, via RIPK1 signaling, are a type of inflammatory cell death that contributes to the cytokine storm observed in NEC^{105,106} (**Figure 1.3**)

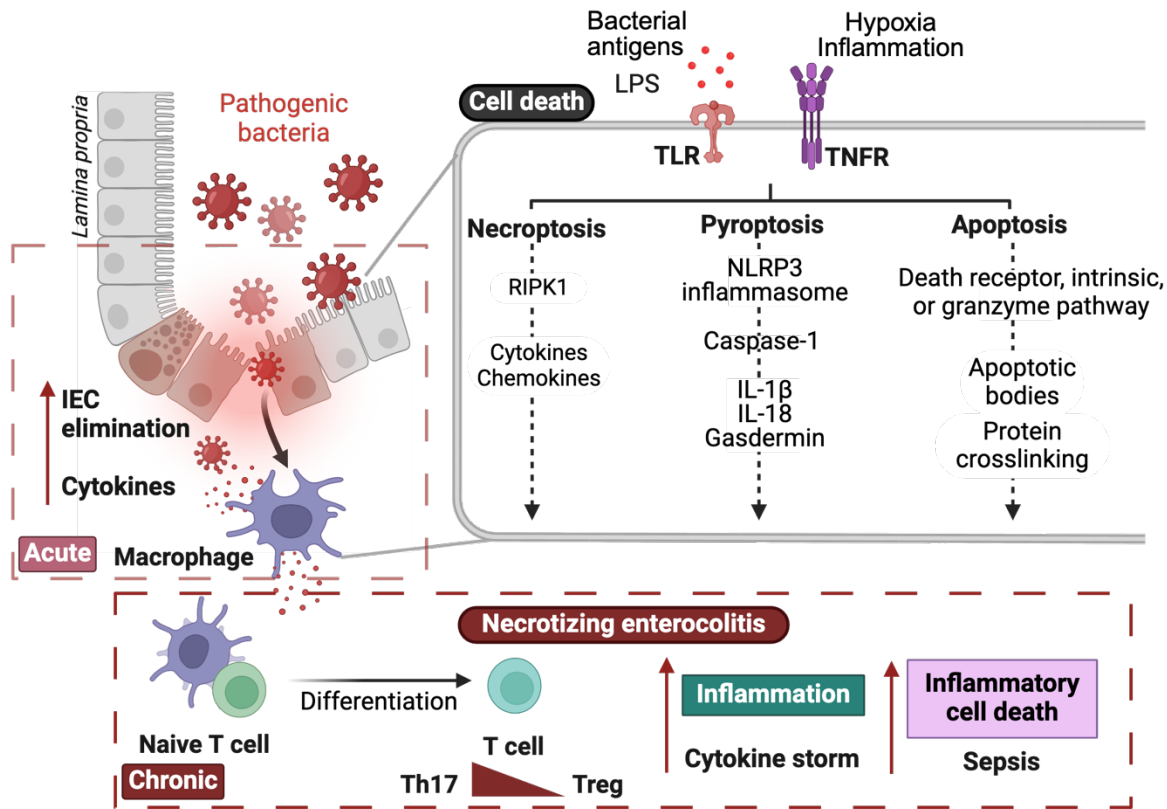


Figure 1.3. Simplified summary of cell death and pathogenesis involved in necrotizing enterocolitis. Upon bacterial invasion, the acute phase of necrotizing enterocolitis (NEC) involves damage to intestinal epithelial cells (IECs) and an elevated level of cytokines, which leads to immune cell recruitment at the site of injury. Cell death involved in the pathogenesis includes necroptosis, pyroptosis, and apoptosis, which are facilitated by signaling cascades initiated by receptors such as toll-like receptor (TLR), and tumor necrosis factor receptor (TNFR). Sustained inflammation with IEC shedding and leakage of the barrier initiates the chronic phase of NEC, characterized by an increased differentiation of Th17 cells, cytokine storm, and systemic complications culminating in sepsis. Figure created with Biorender and adapted from Kanuri et al. 2023⁹⁴.

To combat NEC after its onset, current strategies include surgical removal of necrotic tissue, antibiotics, and removal of oral feeding. Potential therapeutic strategies incorporate TLR4 inhibitors, anti-IL-17, and maternal IgA, which can restore the balance to an anti-inflammatory

environment, though their efficacy and safety remains to be proven⁸⁷. Success in reducing NEC incidence has been shown following incorporation of probiotics and HM-feeding^{107–110}. Notably, the protective effects appear to be facilitated by TLR4 downregulation^{111,112}. As a result, many studies investigating HM focus on discovering the ways in which milk bioactive components can mitigate development of NEC or attenuate its progression. In recent years, the immunoregulatory characteristics and protective role of HM-derived EVs have emerged. EV-related modulation of NEC-related pathways is discussed in Section 1.3.2 below, as well as in Chapters 3 and 4.

1.3 Extracellular vesicles

The preceding sections review HM's ability to modulate infant immune system, digestion, and overall development via free proteins, antibodies, and milk-borne cells. However, longitudinal modulation relies on persistence of bioactive molecules in the digestive system. EVs are established in cell-to-cell communication, but their ability to convey signals from mother to infant is still an emerging research area.

The umbrella term “EVs” encompasses membrane bound, nanosized vesicles that are secreted by cells. EVs carry diverse bioactive cargo, including proteins, lipids, mRNA, miRs, and other non-coding RNAs¹¹³. The cellular origin of HM EVs could greatly affect the EV cargo and requires further exploration¹¹⁴. EV production could be restricted to mammary gland-contained cells, with additional contribution from circulating immune cells. Prior single cell analyses indicate that lactocyte epithelial cells and immune cells are at the highest concentration in HM^{30–32,115}, and could continue secreting EVs even post milk expression.

The biogenesis of EVs involves different pathways depending on the type of vesicle¹¹⁶. Exosomes are small EVs with a diameter of less than 180nm. They originate from the inward budding of the endosomal membrane during the maturation of multivesicular bodies (MVBs) and are released upon fusion of MVBs with the cell membrane¹¹⁷⁻¹¹⁹. Microvesicles, sized 50-1000nm, and small ectosomes with a diameter ranging from 30-150nm, are generated by cytoplasmic membrane budding. Apoptotic bodies are larger vesicles ranging from 1000-5000nm in size and are released by cells undergoing apoptosis^{116,120}. Recently, the existence of an ultra-small class of non-membrane bound particles, sized 35nm, was discovered. The extracellular particles, termed 'exomeres' and their supernatant 'supermeres', are enriched in RNA cargo, including miRs, and encompass distinct proteins¹²¹. Thus, widely used isolation methods such as ultracentrifugation, can lead to co-isolation of a heterogenous mix of vesicles¹²².

To ensure targeted delivery of specific bioactive molecules, the highly regulated biogenesis of small EVs, exosomes, has been described. Proteins such as tetraspanins and dynamin-like proteins have been implicated in the biogenesis of small EVs, influencing cargo selection, cell targeting, and uptake under physiological and pathological conditions. In the canonical MVB biogenesis, invagination of the plasma membrane leads to the formation of early endosomes, which progressively acquire the tetraspanin protein CD63 and undergo secondary invagination events, generating intraluminal vesicles (ILVs) within the endosomes, now termed MVBs¹¹⁶⁻¹¹⁹. The formation and cargo loading of ILVs includes the endosomal sorting complexes required for transport (ESCRT) machinery (ESCRT-0, -I, -II, -III) and associated proteins such as Alix^{123,124}, which has been specifically implicated in the sorting of miRs into ILVs. Within the MVBs, distinct populations of ILV clusters have been proposed, with only a portion of the vesicles being

ultimately secreted. Interaction of MVBs with the endoplasmic reticulum determines whether they are destined for the lysosome or cell membrane. For the latter, the MVBs are trafficked to the plasma membrane where fusion, a process regulated by Rab GTPases, releases the ILVs into the extracellular milieu (**Figure 1.4**)¹¹⁶.

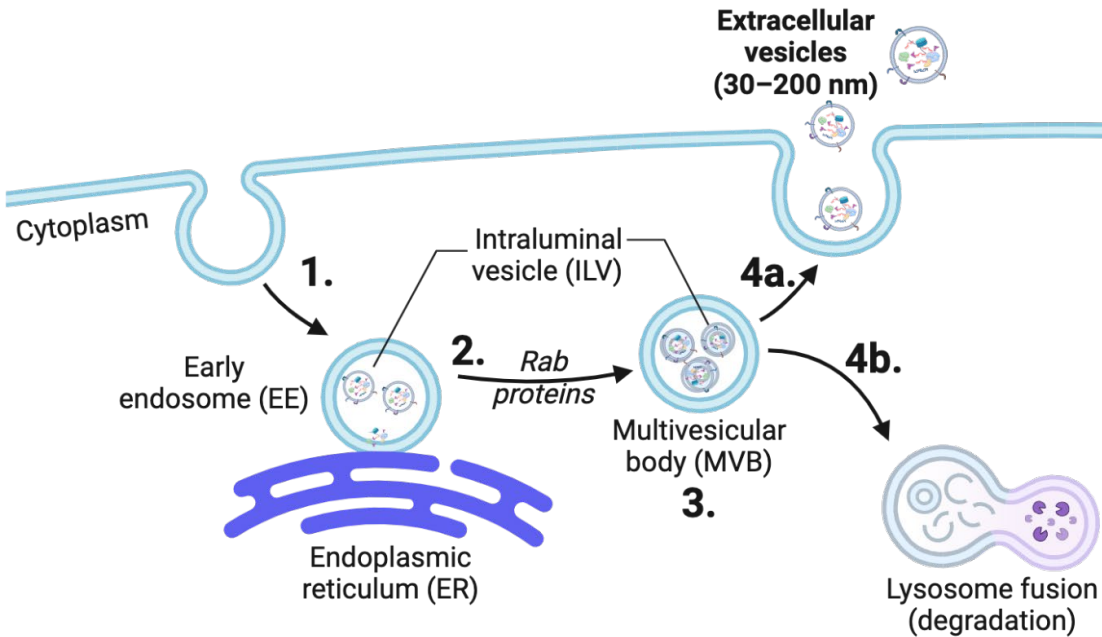


Figure 1.4. Biogenesis of small extracellular vesicles. The canonical biogenesis of small extracellular vesicles, also termed exosomes, begins by formation of the early endosome (1, EE) from the budding of the plasma membrane. After formation of intraluminal vesicles (ILVs) inside the EE, interactions with the endoplasmic reticulum (ER) allow for miR cargo loading. Rab proteins determine the fate of the multivesicular complex by regulating trafficking (2). The multivesicular complex containing ILVs, now called the multivesicular body (3, MVB), can be directed to the cell membrane for secretion of EVs (4a), or to the lysosome for degradation (4b). Figure created with BioRender, adapted from Arya et al. 2024¹¹⁶.

1.3.1 Bioavailability of milk derived extracellular vesicles

There are several fates for EVs upon cellular uptake. The methods by which EVs interact with the target cells include micro- and macropinocytosis, which are non-specific engulfment of

extracellular material by cell movement. Specific uptake by receptor-mediated endocytosis rely on EV surface receptor recognition by the target cell such as clathrin-mediated endocytosis. EVs could also fuse with the cell membrane, thereby releasing cargo into the cytosol. Additional recipient cell stimulation can occur via interactions with EV surface receptors followed by initiation of intracellular signaling¹¹⁶.

In addition to the varied EV uptake and cell stimulation mechanisms, fate of the EV cargo can also take several routes. Following EV incorporation into the endosome, the EVs can be delivered to different organelles, or the EV cargo can be released into the endosome itself following membrane fusion. There is also selective cargo release mediated by interactions with the endoplasmic reticulum, which may allow for more RNA silencing to occur. Fusion with a lysosome will permeabilize the EVs, leading to lysosomal degradation. Lysis is the main outcome for EVs taken up by micro- and macropinocytosis¹¹⁶. Interestingly, the EVs can also be trafficked back to the cell membrane and secreted anew (**Figure 1.5**)¹²⁵.

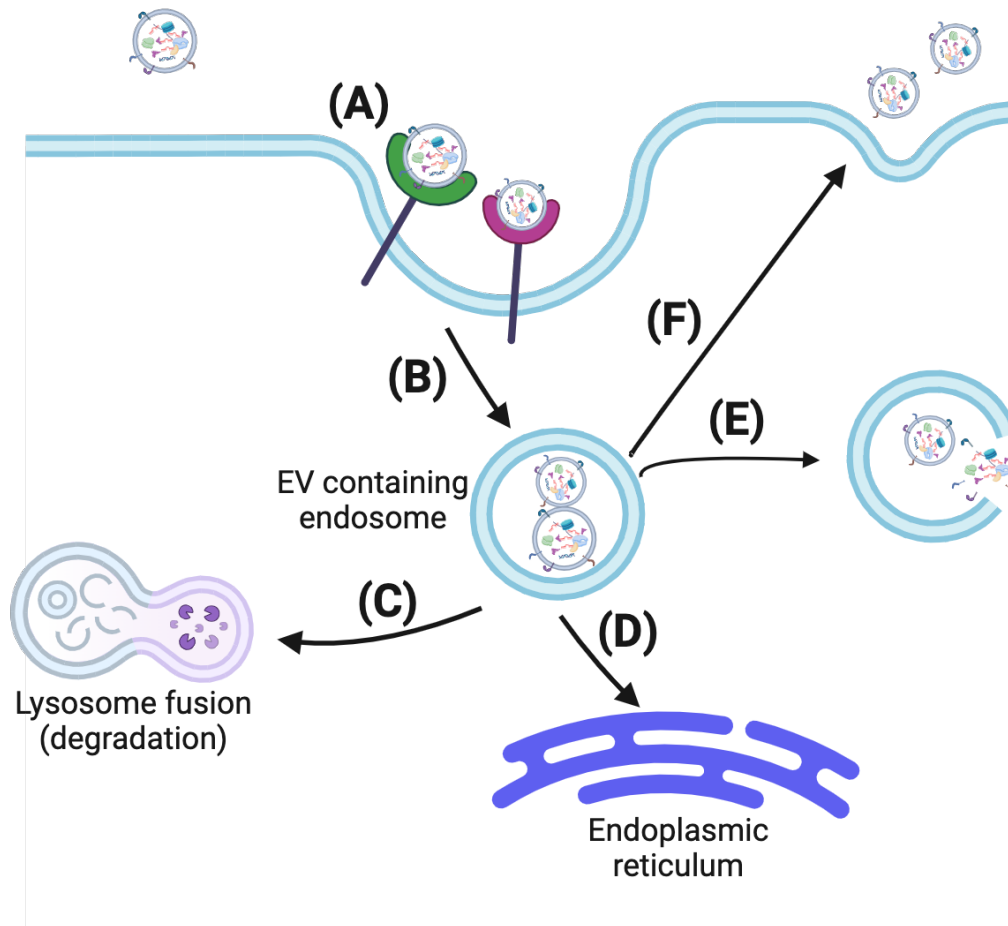


Figure 1.5. Uptake and fate of extracellular vesicles. EVs can enter cells by non-specific pathways or be endocytosed selectively via receptor mediated uptake (A). Following endocytosis, the EV-containing endosome (B) can have several fates: upon fusion with the lysosome, be permeabilized and degraded (C); release select cargo by interacting with the endoplasmic reticulum (D); EVs can internally fuse with the endosomal membrane, thereby releasing their cargo directly into the cytoplasm (E); be re-secreted from the cell through delivery back to the plasma membrane (F). Figure created with BioRender, adapted from Arya et al. 2024¹¹⁶.

The exact intracellular fate and function of milk-derived EVs remain elusive, while movement and distribution of the labelled EVs have been visualized. There is evidence that EVs can be taken up in intestinal^{126,127}, peripheral blood mononuclear¹²⁸, and vascular endothelial cells¹²⁹, as

well as macrophages^{22,130}. In a co-culture study, EVs were also transported across monolayers of a colon cancer cell line, Caco-2¹³¹. Following feeding in mice, fluorescently tagged bovine milk EV miRs were detected in the intestine, spleen, liver, heart and brain tissue¹³². Since HM EVs can survive digestion, the bioavailability of the EVs in infant intestinal lumen¹³³ and transport through the blood-brain barrier are highly likely¹³⁴.

Milk EV-derived miRs are also bioavailable across tissues and could influence immune cell maturation and activation^{132,135,136}. In C57BL6 mice, oral ingestion of human and bovine milk derived EVs, resulted in a 12 and 45% loss in EVs, respectively, after passage through the digestive system. Despite the harsh digestive conditions, the EVs were able to protect mice against colitis and improve intestinal integrity, indicating retained functionality. In the same study, tissue distribution of bovine milk EVs was observed following digestion. One hour post uptake, EVs reached the small intestine, where they were distributed in the villi. Six hours post administration, milk EVs were detected in the colonic tissue. In healthy mice, EVs were also detected in the lamina propria immune cells, while in mice suffering from colitis, triple the amount of milk EVs were found in T cells, dendritic cells, neutrophils and macrophages¹³⁷.

The systemic persistence of milk EVs appears to last no more than 24 hours while levels peak six hours post uptake in biofluids such as plasma, urine and mucosa, and 12 hours post uptake in tissues¹³⁸. Though macrophages have been found to be major eliminators of EVs^{22,139,140}, they are enriched among the immune cells of the lamina propria in the intestine¹⁴¹, wherein uptake of milk EVs may also direct them towards immunomodulation and support attenuation of bacterial infection⁸².

1.3.2 Cargo function of human milk extracellular vesicles

HM-derived EV cargo includes immunomodulatory components that may provide protection against pathogens and promote microbial tolerance in the GI tract of newborns^{142,143}. The cargo and effect of GA-specific HM EVs is explored in detail in Chapters 2 to 4, focusing on mRNA, proteins, and miRs, including their functional enrichments. The effects of EVs isolated mainly from mature term HM have recently been described in epithelial and immune cell lines, and *in vivo* models, which includes experimental NEC.

HM EVs could support defence against microbes via protection of intestinal epithelial cells. Treatment with HM EVs has been shown to significantly increase cell proliferation^{144–146}, and improve survival under cellular stress¹⁴⁷. The pathways through which HM EVs regulate re-epithelization include p38 MAPK with downregulation of adhesion proteins E-cadherin and EPCAM. Epithelial-to-mesenchymal transition (EMT) can also be implicated via TGFβ2 carried by HM EVs¹⁴⁸, and could support repair of the intestinal barrier^{149,150}. In animal models of NEC, disease severity is measured by histologic grading of intestinal necrosis, wherein HM EV administration reduce symptoms^{20,144,151–156}, indicating protection of the epithelial barrier *in vivo*.

In 2007, the first functional study of HM EVs demonstrated their ability to downregulate inflammatory cytokines in peripheral blood mononuclear cells¹⁴². Given the importance of inflammatory signaling in disease processes, regulation of cytokines by HM EVs in varied cell types and animal models of disease have been measured. Across several studies, cytokines such as IL-6, IL-8, CXCL8, IL-1β, and TNFα were downregulated in response to HM EV treatment under inflammatory conditions in either intestinal^{137,152,157}, bronchial¹⁵⁸, and gingival¹⁵⁹ epithelial

cells, endothelial cells¹⁶⁰, macrophages^{137,161}, dental pulp stem cells¹⁶², intestinal organoids^{146,154,163}, or in the rat and mouse intestinal tissue^{152–156,164}. HM EVs can also dampen TLR3 and 9 activation^{158,159} and reduce TLR4 expression¹⁶³. In CD4+ T cells, treatment with term HM EVs regulated cell activation, which was proposed to allow the newborn's immune system to adapt to the new environment and develop tolerance to antigens¹⁵⁹. Milk EVs are also proposed to alter thymic T cell maturation, particularly T regulatory cells¹⁶⁵.

HM EV cargo of over 1000 identified proteins^{142,144,166–168} may exert some of the functional effects seen post treatment. Biological processes that have been found highly enriched among the proteins include cytoskeleton, galactose metabolism, glycolysis/gluconeogenesis, and several immune processes – leukocyte transendothelial migration, regulation of TLR signaling, regulation of T cell activation among several others^{159,167,169}. Enrichment analyses for protein-protein interaction networks relevant for CD4+ T cells found signalling cascades downstream of CD28 for HM EV proteins. Though not tested *in vitro*, these interactions are postulated to result in the inhibition of cell cycle, stimulation of mTOR, and in the retention of the naïve CD4+ T cell phenotype mentioned above¹⁵⁹. On an individual protein level, CXCL5¹⁶⁸, an attractor of neutrophils, and KLK6, an enzyme that regulates immune cell differentiation and survival, are among the many immune-related proteins detected in HM EVs^{168,169}.

Since infants are born at different gestational ages, with varying support requirements¹, the immunomodulatory actions facilitated by the EV cargo in mother's milk can differ. Preterm HM EVs can significantly increase cell proliferation, migration, and mitigate intestinal injury in rats, in comparison to term EVs¹⁴⁴. Corresponding to differences in cargo proteins, the level of

protection against pathogens via term or preterm HM EVs may differ. A pathogenic study using preterm HM EVs showed inhibition of viral activity in epithelial cells¹⁷⁰, although no term group comparison was performed. The cargo differences are further probed in Chapter 2.

The differences and similarities in term and preterm HM EVs are also evidenced by their miR content¹⁷¹⁻¹⁷⁴. HM miRs can have different patterns throughout the lactation period, wherein development and GI maturation¹⁷⁵⁻¹⁷⁸, and regulation of immune signaling¹⁷⁹⁻¹⁸² may be affected. HM EV miRs are reported to have functional similarities to those in whole HM, with a cargo of abundant miRs such as miR-182-5p, promoter of T cell immune response; miR30b-5p, enhancer of immunosuppression; miR-29a-3p, which targets IFN γ and suppresses immune response to pathogens; and miR-146b-5p, which targets the NF- κ B pathway¹⁸³. Comparison of HM EV miRs from healthy mothers versus those with type-1 diabetes, showed that the latter group had more highly upregulated pro-inflammatory miRs, such as miR-4497 and 3178, which are postulated to increase production of TNF α in macrophages¹⁸⁴. These differences indicate that pooling of HM EV samples for miR analysis may not reflect individual variability, which exists among healthy mothers, term and preterm groups⁸⁵. The GA-based characterization of HM EV miRs in the context of infant health is covered in more detail in Chapter 3.

A largely unexplored component of HM EVs is their metabolic cargo. In HM, the metabolome includes all low molecular weight molecules (<1500 Da), which may originate from various metabolic processes of the mammary gland. Due to the endosomal biogenesis of small EVs¹¹⁸, the likely origin of metabolites is from milk secretory cells, or other cells of the mammary epithelium that release vesicles into HM¹⁸⁵. Metabolite analysis in milk vesicles has thus far been

limited. The majority of metabolome studies of EVs originate from cancer cells for detection of biomarkers¹⁸⁶⁻¹⁸⁸. Functionally, EVs from cancer-associated fibroblasts could supply amino acids and increase glycolysis in cultured cells^{186,189}. It is possible that metabolites from HM EVs similarly regulate downstream pathways in infant intestinal epithelial cells.

In bovine, donkey and goat milk, pathway enrichment analyses propose anti-inflammatory roles for identified metabolites in EVs. Among them are group B vitamins, including enriched B2, B3 and B9, all of which have been shown to impact immune responses¹⁹⁰. In HM, a small-scale study has compared lipid metabolites in term and preterm HM EVs, which were found to be highly similar. Bioinformatic analysis of top 50 abundant lipids in both groups indicated regulatory roles via an ERK/MAPK pathway. This was probed in intestinal cells, where treatment with LPS increased p-ERK, levels of which were markedly reduced following treatment with HM EVs¹⁹¹. The highly conserved ERK/MAPK pathway regulates differentiation and growth of cells across the organism, thereby influencing signaling involved in metabolism, immune system, and disease progression¹⁹². While the metabolome was not explored in this thesis, the functional enrichments for HM EV cargo discussed in Chapters 2 and 3 suggest a concomitant effect in line with previous metabolomics studies.

As evidenced by prior research, a consistent supply of functional particles found in HM could sustain newborn health. While EVs are recognized for their role in intercellular communication and effector functions, the transfer of cargo and its ability to mediate mother-to-infant signaling is still not fully understood. Given the disparities between term and preterm infants, and the differences in the corresponding HM, unraveling this mode of communication in the context of

gestational age can provide additional strategies for preterm infant therapeutics, especially in the form of donor milk or formula supplementation to support the specific needs of the premature neonate.

Hypothesis and dissertation objectives

I hypothesized that term and preterm human milk extracellular vesicles have a differential composition of surface markers, proteins, RNA, and that extracellular vesicles isolated from preterm human milk are more potent immunoregulators.

The hypothesis was investigated in the following chapters that are divided by three objectives:

- (1) Characterization of extracellular vesicle proteins and mRNA.
- (2) Characterization of extracellular vesicle miRs.
- (3) Measuring effect of gestational-age specific extracellular vesicles on inflammation in intestinal and immune cells.

Chapter 2. Characterization of term and preterm human milk extracellular vesicle proteins and mRNA

Manuscript 1: Vahkal, B., Altosaar, I., Tremblay, E., Gagné, D., Hüttman, N., Minic, Z., Côté, M., Blais, A., Beaulieu, J.F. and Ferretti, E., 2024. Gestational age at birth influences protein and RNA content in human milk extracellular vesicles. *Journal of Extracellular Biology*, 3(1), p.e128. DOI: <https://doi.org/10.1002/jex2.128>.

Adapted as a re-print from the Journal of Extracellular Biology.

2.1 Preface

There is limited information on the impact of GA on the composition of HM EV cargo. Given a global rise in premature births with a recommendation that all newborns consume mother's milk, addressing these gaps in knowledge may inform feeding strategies. Due to the biological variation, and unknown cargo of EVs, EVs were first characterized in two stages: proteomics, and RNA sequencing. This work builds on prior proteomics studies of term and preterm HM EVs by characterizing EVs from the transitional lactational stage and by using a data independent acquisition method for quantitative proteomics analysis with an increased detection in the number of peptides. For the first time to my knowledge, RNA transcripts in GA-specific HM EVs are described.

The experiments and data analyses in this publication were planned by me and co-authors. Mass spectrometry was performed by Dr. David Gagné, with additional input for proteomics data

analysis by Nico Hüttman, and Dr. Zoran Minic. Dr. Alexandre Blais provided assistance with analysis and interpretation of RNA sequencing data. I prepared all figures except Figure 3, which was prepared by Nico Hüttman, and Figures 12, 15, and 16, which were prepared by Dr. Alexandre Blais. I wrote the manuscript with feedback from all co-authors. This published article includes a corrigendum for Figures 2.2 and 2.7, and accompanying text. The corrected and updated figures are presented in this thesis.

Gestational age at birth influences protein and RNA content in human milk extracellular vesicles

Brett Vahkal¹⁻³, Illimar Altosaar^{1#}, Eric Tremblay⁴, David Gagné⁴, Nico Hüttman⁵, Zoran Minic⁵,
Marceline Côté¹⁻³, Alexandre Blais^{1-3,6-7*}, Jean-François Beaulieu^{4*}, Emanuela Ferretti^{8*}

¹University of Ottawa, Department of Biochemistry, Microbiology and Immunology

²Ottawa Centre for Infection, Immunity, and Inflammation

³Ottawa Institute of Systems Biology

⁴Université de Sherbrooke, Department of Immunology and Cell Biology

⁵University of Ottawa, Faculty of Science, John L. Holmes Mass Spectrometry Facility.

⁶University of Ottawa, Brain and Mind Institute

⁷Éric Poulin Centre for Neuromuscular Disease, Ottawa, Canada

⁸Children's Hospital of Eastern Ontario, Department of Pediatrics, Division of Neonatology

#Current address: Proteins Easy Corp, 75 Campus Drive, Kemptville Agricultural College, North
Grenville, Ontario K0G 1J0

**Co-corresponding authors*

2.2 Abstract

Human milk extracellular vesicles (HM EVs) are proposed to protect against disease development in infants. This protection could in part be facilitated by the bioactive EV cargo of proteins and RNA. Notably, mothers birth infants of different gestational ages with unique needs, wherein the EV cargo of HM may diverge. We collected HM from lactating mothers within two weeks of a term or preterm birth. Following purification of EVs, proteins and mRNA were extracted for proteomics and sequencing analyses, respectively. Over 2000 protein groups were

identified, and over 8000 genes were quantified. The total number of proteins and mRNA did not differ significantly between the two conditions, while functional bioinformatics of differentially expressed cargo indicated enrichment in immunoregulatory cargo for preterm HM EVs. In term HM EVs, significantly upregulated cargo was enriched in metabolism-related functions. Based on gene expression signatures from HM-contained single cell sequencing data, we proposed that a larger portion of preterm HM EVs are secreted by immune cells, whereas term HM EVs contain more signatures of lactocyte epithelial cells. Proposed differences in EV cargo could indicate variation in mother's milk based on infants' gestational age and provide basis for further functional characterization.

2.3 Introduction

Human milk (HM) is the gold standard in nutrition for infants⁵. HM feeding can prevent the development of inflammatory gut diseases^{10,193}, promote antimicrobial protection, and immune modulation, via milk-contained oligosaccharides, RNA, and bioactive proteins such as secretory antibodies, lactoferrins (LF), and cytokines^{5,136,180,194,195}. This biological regulation could extend to HM-contained extracellular vesicles (EVs), which carry proteins and nucleic acids⁸⁴. Uniquely, HM EVs can withstand digestion and are taken up by intestinal cells¹³³. Thus, EV-contained cargo is hypothesized to reach the infant gut lumen, setting the stage for a temporal biological effect – *ut digeratur*. Understanding the composition of proteins and nucleic acids carried by EVs may therefore inform on the downstream outcome of HM feeding.

As infants are born at different gestational ages (GA) – term (>37 weeks) or preterm (<37 weeks)¹⁹⁶, the composition of mother's milk varies. GA-specific differences in dozens of HM

proteins have been measured^{17,70,197–199}. Preterm HM has increased proteolytic activity, which could aid in the digestion of milk nutrients in premature infants²⁰⁰. The increased concentration of epidermal growth factor, transforming growth factor alpha (TGF- α), soluble CD14, immunoglobulin A, LF, and lysozyme in preterm HM^{17,201–203} could modulate the immune system and prevent development of inflammatory disease in the more vulnerable premature infants. The changes in HM composition may arise due to the unique needs of infants and could extend to the HM EV cargo.

Studies of the HM EV proteome have resulted in over 1000 proteins identified, with a total of 1963 proteins identified in mature HM EVs (>2 weeks postpartum)^{142,144,166–168}. In GA-specific HM EVs, 46 proteins have been investigated for differential expression. LF and lactadherin-derived peptides were upregulated in preterm HM EVs and proposed to increase gut epithelial cell proliferation and migration¹⁴⁴. Consistent levels of LF have been previously identified in HM EVs, and the protein content was highly resistant to digestion¹²⁶.

For HM RNA, sequencing has been performed in the HM fat layer¹⁹, and cells^{30–32,115}, where the latter could also provide information about the origins of HM EVs²⁰⁴. Several studies have focused on microRNA cargo^{35,126,127,179,181,195,205–211}, mostly EV-contained, though with limited information on GA-specific changes^{171,173,175}. Two studies have previously characterized GA-specific differences in long-coding, circular RNAs, and mRNAs. For circular RNAs, both term and preterm HM EVs were enriched in VEGF-signalling pathway markers, wherein differentially expressed RNAs regulated inflammatory pathways via their predicted microRNA targets²¹². In long-coding RNA, differentially expressed transcripts were similarly enriched in regulation of the

inflammatory response, specifically those regulated by cell surface receptors. In the same study, EV-contained mRNAs were sequenced. However, differentially expressed mRNA were not functionally characterized by term of birth, but rather described in the context of interactions with long-coding RNAs. These specific interactions focused on upregulated preterm EV mRNAs, which were determined to be enriched in immune, signaling, and metabolic pathways²⁰.

Though differential composition of HM EV cargo of proteins has been described following both term and preterm birth^{20,144,173,191}, an overall limited number of individual proteins with quantitative information have been identified. Additional low abundance proteins remain elusive, but their identification could expand functional interpretations for HM EVs. Prior studies have used label-based, or data-dependent mass spectrometry detection methods. Here, we applied a data-independent approach, which allows for increased proteome coverage²¹³⁻²¹⁵.

Similarly for HM EV mRNA, one study has previously examined EV-contained mRNA in term and preterm EVs, with a full characterization focusing on long-coding RNAs²⁰. As such, quantitative, full-spectrum profiling of GA-specific HM EV cargo is lacking in the current field of HM EV biology.

In this study, we quantitatively measured GA-specific differences in HM EV cargo of proteins and mRNA. By employing mass spectrometry with data-independent acquisition we obtained a deep proteome coverage and quantification of over 2000 HM EV-contained proteins. Using RNA sequencing, total mRNA in GA-specific EVs was detected. With bioinformatic analyses, we postulate significant quantitative differences on individual protein and mRNA levels, wherein

preterm HM EV contents have functional enrichments in immune-related pathways and processes. Term HM EVs contain diverse cargo with highly enriched metabolic-related functions, including pathways and processes implicated in signaling. To postulate the origin of vesicles, we compared the signatures of EV RNA cargo to that of previously published HM single cell sequencing. We show that preterm EVs cluster with immune cell signatures, whereas term EVs have signatures of lactocyte epithelial cells. Overall, our results indicate differences in HM EV cargo based on duration of gestation, wherein the cellular origin and cargo of preterm HM EVs are more immune-related.

2.4 Results

1. Validation of human milk EVs

To investigate small EV surface marker abundance, fluorescence based measurement was used^{119,216,217}. HM EV surface markers CD9, CD63 and CD81 were identified on term and preterm EVs using Exoview R-100 (Nanoview Biosciences, United States). The Exoview platform utilizes three channels of fluorescence for CD9, CD63 and CD81 detection using fluorescently tagged antibodies, and one channel for interferometric sizing. EVs from both groups of samples had presence of CD9, CD81, and CD63 signal (**Figure 2.1A**). The average size for EVs isolated from term or preterm HM was 60 and 59 nm, respectively (**Figure 2.1B**). To visualize EV integrity and size, scanning electron microscopy was performed. Spherical vesicles, up to 200 nm in size, were visible in the field of view (**Figure 2.1C**).

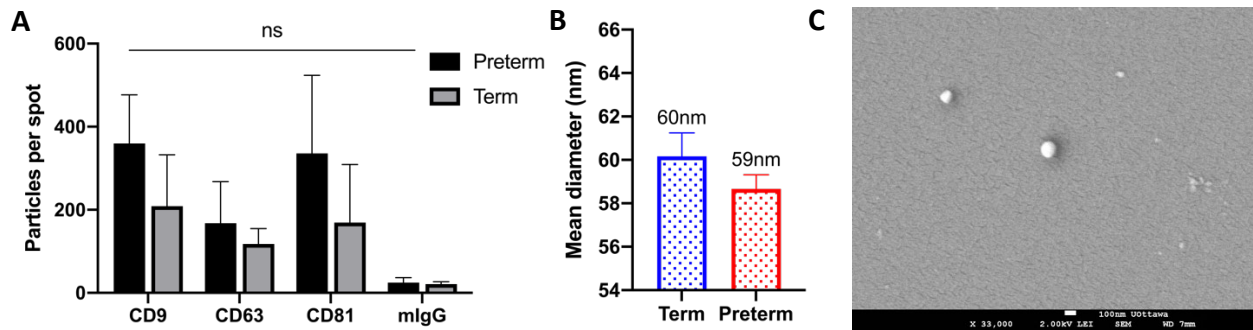


Figure 2.1. HM EV validation and surface marker characterization. (A) Surface markers CD9, CD63, CD81 and mIgG negative control, were identified on term ($n = 2$) and preterm ($n = 4$) EVs. ns, non-significant, two-way ANOVA. (B) Mean size of particles with a cut-off scale of 50–200 nm, bound to CD9, CD63 and CD81 capture probes, measured by interferometry. (C) Scanning electron micrograph of individual HM preterm vesicles, scale bar to 100 nm.

2. Identification and differential expression of proteins from GA-specific human milk EVs

Label-free quantitative mass spectrometry of six HM samples ($n=3$ each term and preterm) was performed using SWATH – a method of data independent acquisition for the detection peptides²¹⁸. Over 19,000 unique peptides and 2,000 protein groups were identified and quantified. Similar number of proteins were identified in term and preterm HM EVs – 1,808 and 1,704, respectively (Supp. 1). In addition to 1662 common proteins, term HM EVs contained 146, while preterm milk samples contained 42 unique proteins. (Figure 2.2).

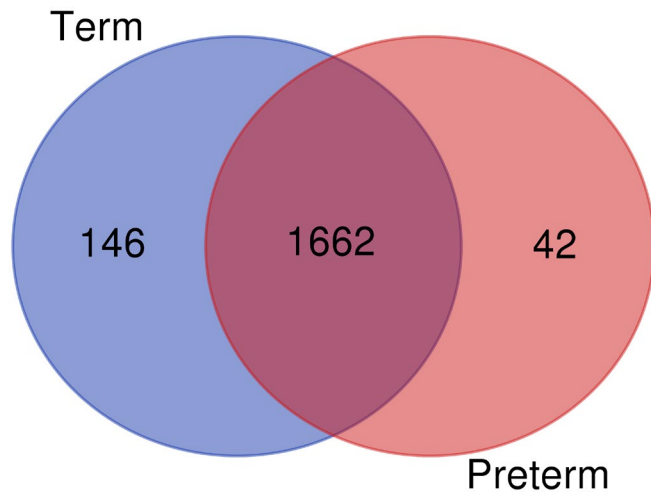


Figure 2.2. Number of proteins in term and preterm human milk EVs. Venn diagram comparing the total number of proteins identified using SWATH method – 1808 in term, 1704 in preterm, after removal of duplicates; 1662 proteins common to both; 146 and 42 unique proteins in term and preterm cohorts respectively; $n=3$. High FDR confidence proteins included in analysis.

Quantitative evaluation of protein abundances was compared between term and preterm HM EV using hierarchical cluster analysis. Large differences between samples and no distant clustering were observed among the two conditions (**Figure 2.3A**). Following differential expression analysis, few significantly ($p<0.05$) up- or downregulated proteins were identified when compared to the total number of identified proteins (**Figure 2.3B**).

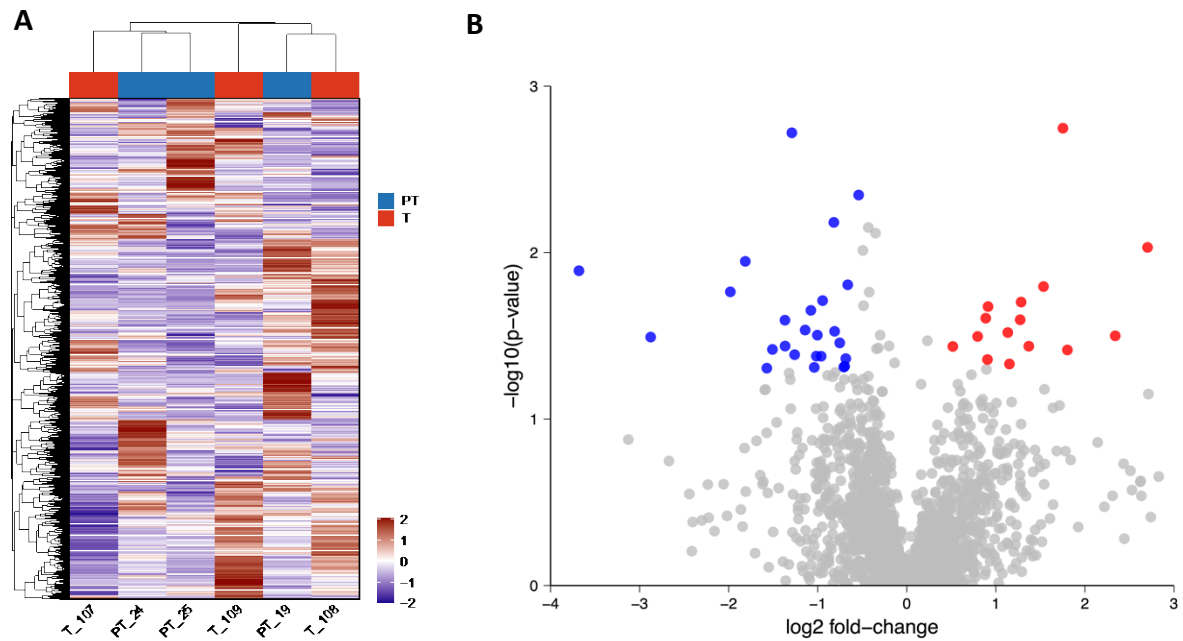


Figure 2.3. Differentially expressed proteins in term and preterm HM EVs. (A) Heatmap showing hierarchical clustering of Z-scored MaxLFQ intensities on protein and sample level. (B) Volcano plot of differentially expressed proteins. Proteins with positive log₂ fold-change value were higher abundant term (red), proteins with a negative log₂ fold-change value were upregulated in preterm (blue), proteins not significantly changed are shown in grey. Significance was assigned to proteins with a $p < 0.05$, pairwise Student's *t*-test.

The results revealed 15 and 25 significantly upregulated proteins in term and preterm HM EVs, respectively (**Table 2.1**). Cathepsin B (CTSB) and serpin family E member 2 (SERPINE2) were the most significantly upregulated proteins ($p < 0.04$) in term HM EVs, with SERPINE2 highest upregulated. In preterm HM EVs, endosulfine alpha (ENSA) was the most significantly upregulated protein, while elastin microfibril interfacier 3 (EMILIN3) and fibroblast growth factor binding protein 1 (FGFBP1) were among the highest upregulated proteins by fold-change.

Table 2.1. Comparative analysis of differently abundant proteins in term and preterm HM EVs. Differential expression was assessed by pairwise Student's *t*-test and proteins were

considered significantly changed based on $p < 0.05$ and absolute \log_2 fold-change > 0.5 . Proteins with positive fold-change value were more highly abundant in term HM EVs, while those with negative fold-change were more highly abundant in preterm HM EVs.

Condition of birth	Protein name	Gene symbol	Fold-change (log2)	P-value	
Term	Cathepsin B	<i>CTSB</i>	1.75	1.79e-03	
	Serpin family E member 2	<i>SERPINE2</i>	2.7	9.31e-03	
	Glycogen phosphorylase L	<i>PYGL</i>	1.53	1.60e-02	
	Argininosuccinate synthase 1	<i>ASS1</i>	1.28	1.98e-02	
	Guanine nucleotide-binding protein G(i) subunit alpha-2	<i>GNAI2</i>			
	Sorting nexin 3	<i>SNX3</i>	0.91	2.11e-02	
	Vitronectin	<i>VTN</i>	0.89	2.48e-02	
	Sorting nexin 2	<i>SNX2</i>	1.27	2.53e-02	
	Cellular communication network factor 1	<i>CCN1</i>	1.13	3.02e-02	
	Heat shock cognate 71 kDa protein	<i>HSPA8</i>	2.34	3.16e-02	
	Solute carrier family 2 member 1	<i>SLC2A1</i>	0.8	3.19e-02	
	CYFIP-related Rac1 interactor A	<i>LOC110522500</i>	1.37	3.65e-02	
	Transmembrane p24 trafficking protein 7	<i>TMED7</i>	0.52	3.66e-02	
	Tax1 binding protein 1	<i>TAX1BP1</i>	1.8	3.85e-02	
	Claudin 8	<i>CLDN8</i>	0.91	4.39e-02	
	Preterm	Endosulfine alpha	<i>ENSA</i>	1.15	4.67e-02
		Vesicle amine transport 1	<i>VAT1</i>	-1.29	1.91e-03
Syntaxin binding protein 1		<i>STXBP1</i>	-0.54	4.51e-03	
Dehydrogenase/reductase 1		<i>DHRS1</i>	-0.82	6.59e-03	
Elastin microfibril interfacier 3		<i>EMILIN3</i>	-1.81	1.13e-02	
Platelet activating factor acetylhydrolase 1b catalytic subunit 2		<i>PAFAH1B2</i>	-3.68	1.29e-02	
Midkine		<i>MDK</i>	-0.66	1.56e-02	
Xanthine dehydrogenase		<i>XDH</i>	-1.98	1.72e-02	
Serine/threonine-protein kinase TAO1		<i>TAOK1</i>	-0.95	1.94e-02	
Albumin		<i>ALB</i>	-1.08	2.22e-02	
Cellular retinoic acid binding protein 2		<i>CRABP2</i>	-1.37	2.55e-02	
Unconventional myosin-VI		<i>MYO6</i>	-1.14	2.92e-02	
Thymosin beta 4 X-linked		<i>TMSB4X</i>	-0.81	2.97e-02	
Fibroblast growth factor binding protein 1		<i>FGFBP1</i>	-1	3.13e-02	
Growth regulating estrogen receptor binding 1		<i>GREB1</i>	-2.88	3.22e-02	
Phosphate cytidylyltransferase 2, ethanolamine		<i>PCYT2</i>	-0.75	3.49e-02	
Mucin-4		<i>MUC4</i>	-1.37	3.64e-02	
S100 calcium binding protein A7		<i>S100A7</i>	-1.51	3.82e-02	
Butyrophilin subfamily 1 member A1		<i>BTN1A1</i>	-1.26	4.11e-02	
Solute carrier organic anion transporter family member 4C1		<i>SLCO4C1</i>	-1.02	4.19e-02	
Caspase 14		<i>CASP14</i>	-0.96	4.19e-02	
Tandem C2 domains, nuclear		<i>TC2N</i>	-0.68	4.33e-02	
Calcium binding protein 39 like C1q and TNF related 1		<i>CAB39L</i>	-0.7	4.82e-02	
	<i>CIQTNF1</i>	-0.71	4.87e-02		
		-1.04	4.89e-02		

3. Functional annotation of GA-specific human milk EV protein cargo

Identified term and preterm proteins were subjected to biological process and pathway analysis. Proteins were queried in the PANTHER database for biological processes analysis, wherein both term and preterm samples revealed the presence of proteins related to immune system processes (Figure 2.4). The total number of proteins involved in each biological process was higher for preterm HM EVs (Figure 2.4 and Supp. 2).

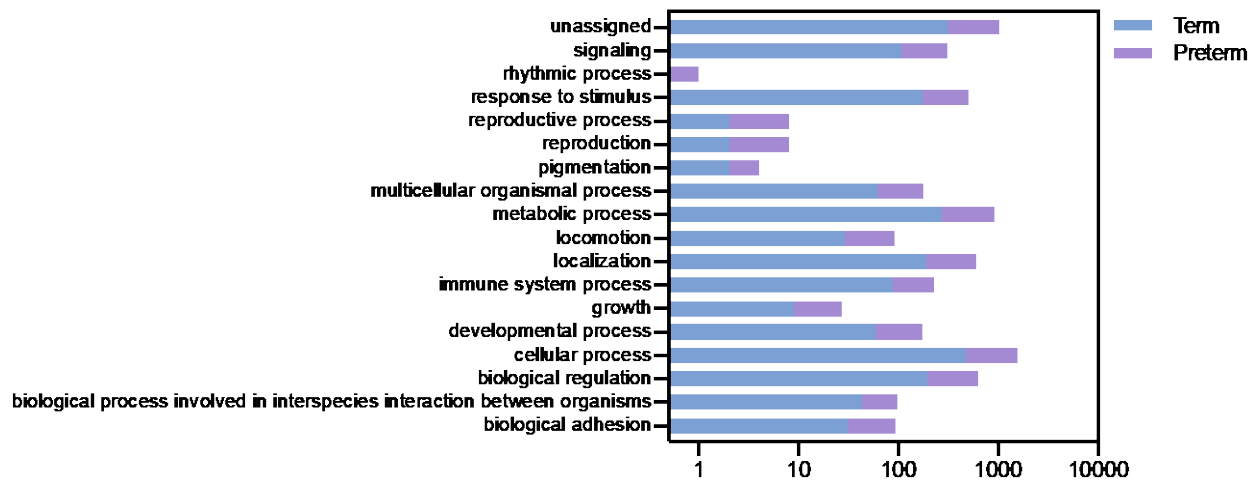


Figure 2.4. Biological processes identified with PANTHER database for all term and preterm HM EV proteins. X-axis represents the log of number of proteins assigned to each biological process that were detected in term (blue bars) or preterm (pink bars) HM EVs. Total number of proteins assigned to biological processes was larger in preterm HM EVs.

Reactome pathway analysis of total protein abundance using STRING database revealed that term EVs had a higher number of unique enriched pathways, including those related to developmental biology, nervous system development and infectious disease (Figure 2.5).

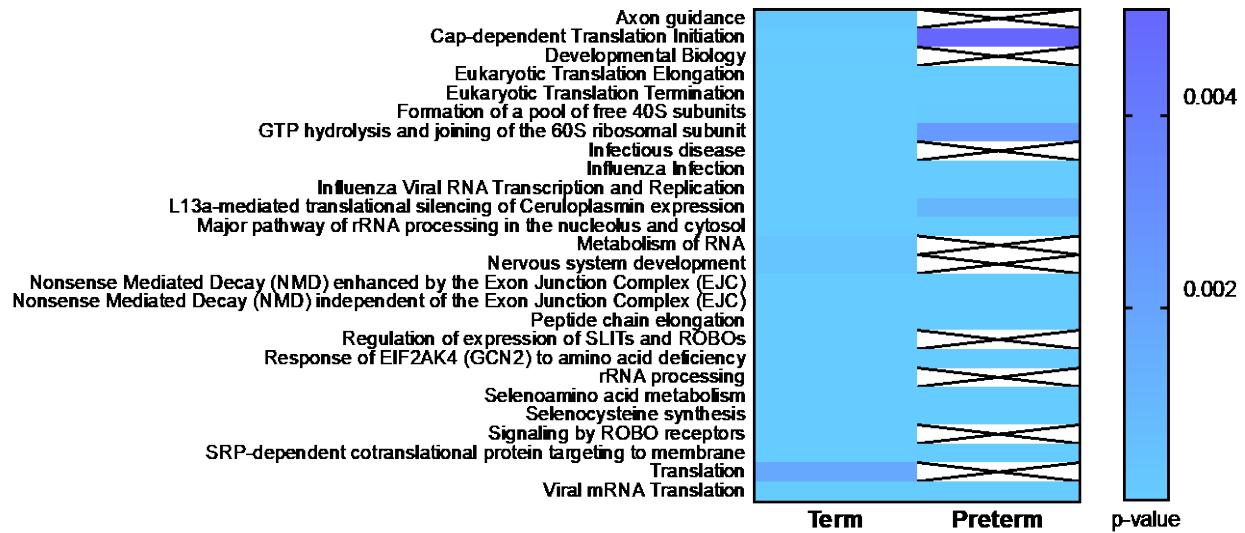


Figure 2.5. Reactome pathways identified with STRING database of all term and preterm HM EV proteins. Blue gradient cells represent the significance of pathway in the dataset. Term HM EV proteins were enriched in more diverse pathways with higher significance. Cells with black lines indicate lack of identification for corresponding pathway. Proteins with abundance values and FDR < 1% were queried.

Differentially expressed proteins with significant up- and downregulation were submitted for combined analysis in STRING. In total, 11 GO biological processes, and neutrophil degranulation Reactome pathway were enriched in the dataset. Among the enriched biological processes, neutrophil degranulation, and leukocyte activation involved in immune response were in the top three of largest enrichment effect in the dataset and included proteins that were both up- and downregulated in preterm HM EVs. Neutrophil degranulation and leukocyte activation processes included upregulated proteins HSPA8, PYGL, CTSB, and downregulated proteins VAT1, PAFAH1B2, RAB6A, GDI1, and MDK, latter of which was specific for leukocyte activation only. The identified biological processes for regulation of signaling and signal transduction contained proteins that were primarily downregulated in preterm HM EVs (**Figure**

2.6). The other enriched biological processes belonged to secretion, vesicle-mediated transport, cell communication and exocytosis functions, which included both up- and downregulated proteins (Supp. 3).

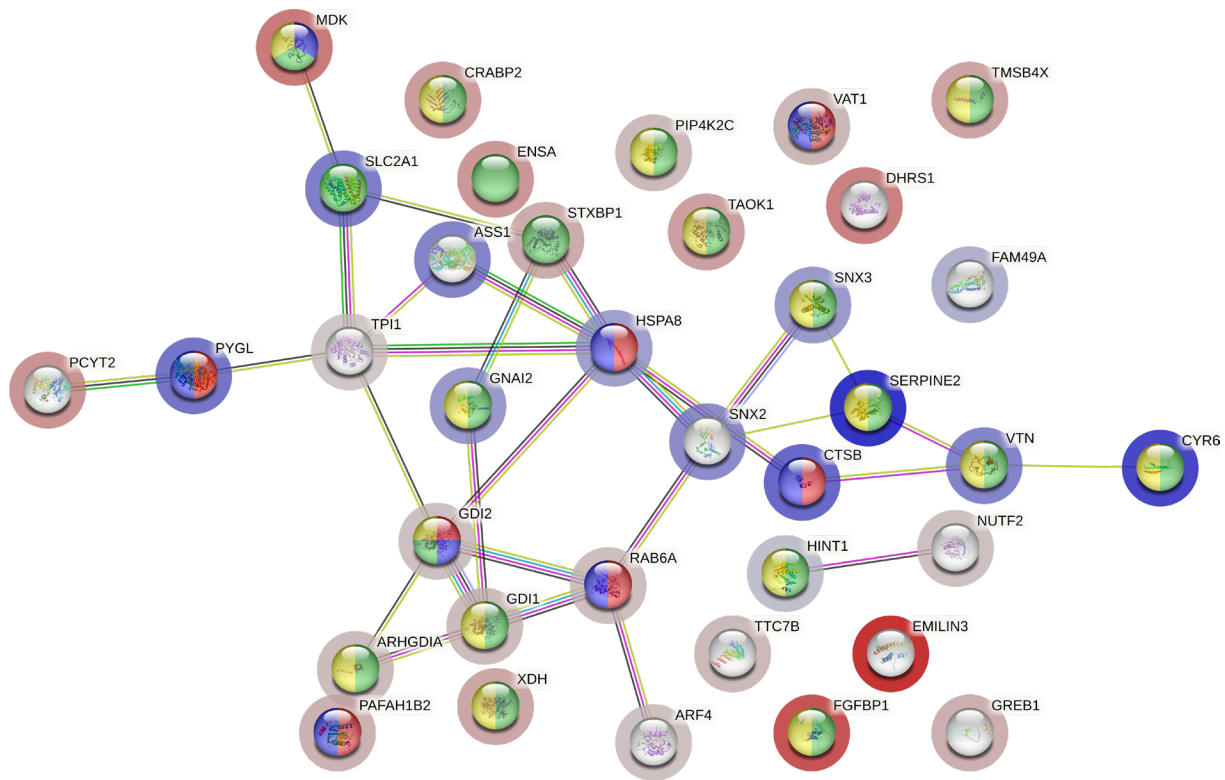


Figure 2.6. Biological processes enriched in significantly up- or downregulated preterm HM EV proteins. Upregulated proteins are annotated with a blue halo, downregulated proteins have a red halo. A total of 11 biological processes were assigned, with strongest evidence for neutrophil degranulation (red filled circles) and leukocyte activation in immune response (blue fill). Majority of proteins enriched signaling (green fill) and signal transduction (yellow fill) were downregulated. $p < 0.04$, Student's *t*-test. Circles include 3D crystal structure of protein, if known. STRING analysis, confidence score > 0.4 - 0.9 with ascending number of connecting lines.

4. GA-specific human milk EV cargo in previously identified human milk proteins

To further validate our proteomics findings, we compared our data to that of previously published proteomics analyses from HM, or HM EVs, whenever publicly available and clearly annotated.

First, we compared our results against all the proteins curated in the Human Biofluid Repository²¹⁹ (human milk with a total number of proteins 2536, last accessed March 14th, 2023). We visualized 1254 overlapping proteins between all three groups, 29 between HM and preterm EVs, 50 between HM and term EVs (**Figure 2.7A**). Proteins unique to only term and preterm HM EVs were queried in STRING database to identify functional enrichments in the unique protein groups. As expected, term EVs had a larger number of enriched processes, 236, compared to the 225 in preterm EVs. A total of 213 processes were shared between the two groups, indicating similarity of preterm contents to term. Relevant to newborn immunity, shared processes included leukocyte mediated immunity, antigen processing and presentation. Further processes related to exo- and endocytosis, protein transport, cellular component organization, and response to wounding (**Supp 4**). Biological processes unique to term EVs included several related to developmental biology, including cell, heart, and circulatory system development, regulation of cell adhesion, and immune effector and activation processes (**Figure 2.7B** and **Supp. 4**). Also present were regulation of metabolic process, organonitrogen compound catabolic process, cellular response to organic substance, cellular response to other organism, and regulation of cell morphogenesis involved in differentiation (**Supp 4**). Biological processes unique to preterm were related to skeletal system and muscle cell development, leukocyte migration, protein and organelle localization. Further processes associated with response to

stress, fatty acid, carboxylic acid and small molecule catabolic processes (**Figure 2.7B** and **Supp. 4**).

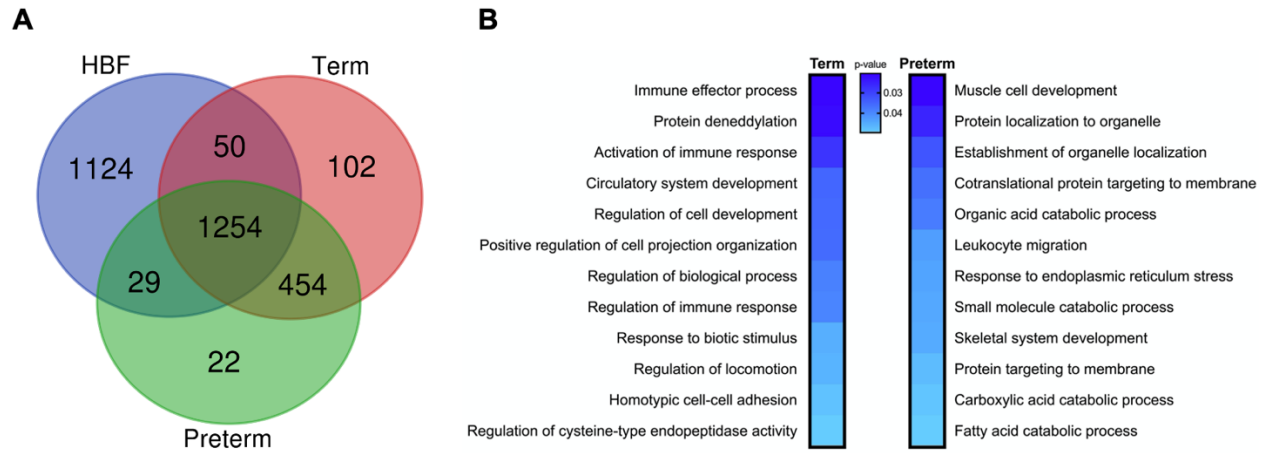


Figure 2.7. Analysis of proteins derived from HM and term and preterm HM EVs. (A) Venn diagram comparing proteins identified in Human Biofluid Repository (HBF) with term and preterm EVs. Out of 2536 proteins identified in human milk (HM), 1254 were present in term and preterm EVs, while term EVs share 50, and preterm EVs share 29 proteins with HM. **(B)** Functional enrichments of proteins not present in HBF and unique to term and preterm EVs. Most significant processes in both term and preterm HM EVs included those involved in cellular processes, including organelle or cell organization, locomotion and protein localization to organelle, catabolic process, as well as immune system processes, such as activation, and leukocyte migration. *STRING* analysis.

Human milk composition is known to differ based on lactation period between colostrum (up to 4 days after birth), transitional (5 days to two weeks after birth), and mature (>1 month after birth) milk^{5,220}. Herwijnen *et al.* have previously characterized the proteome from EVs of mature HM and identified 1964 unique proteins across seven donors¹⁶⁷. To compare the EV proteome of mature HM to that of transitional term or preterm HM, we submitted the list of proteins identified in three donors of term and preterm HM EVs, alongside data obtained from Herwijnen *et al.* to Venn analysis²²¹. In total, 1235 common proteins were identified among the three

datasets. Mature HM EVs contained 728 unique proteins, transitional HM EVs had 615, of which 96 unique proteins were identified in term, and 19 in preterm HM EVs (**Figure 2.8A**). For functional characterization, each set of unique proteins from mature and transitional HM EVs were submitted to STRING for enrichment analyses. In mature HM EVs, 107 GO biological processes, 6 KEGG pathways, and 13 Reactome pathways were enriched (**Supp. 5**). A variety of biological processes were represented, including cell differentiation, metabolic regulation, and immune mediation (**Supp. 5**). In transitional HM EVs, 315 GO biological processes, 35 KEGG pathways, and 223 Reactome pathways were enriched (**Supp. 6**). The enrichments with the highest confidence interaction score were plotted in STRING and included several clusters related to proteasome, immune response, immune system process in GO biological process classification, and metabolic pathways, ribosome-related, and RNA transport in KEGG pathways (**Figure 2.8B**).

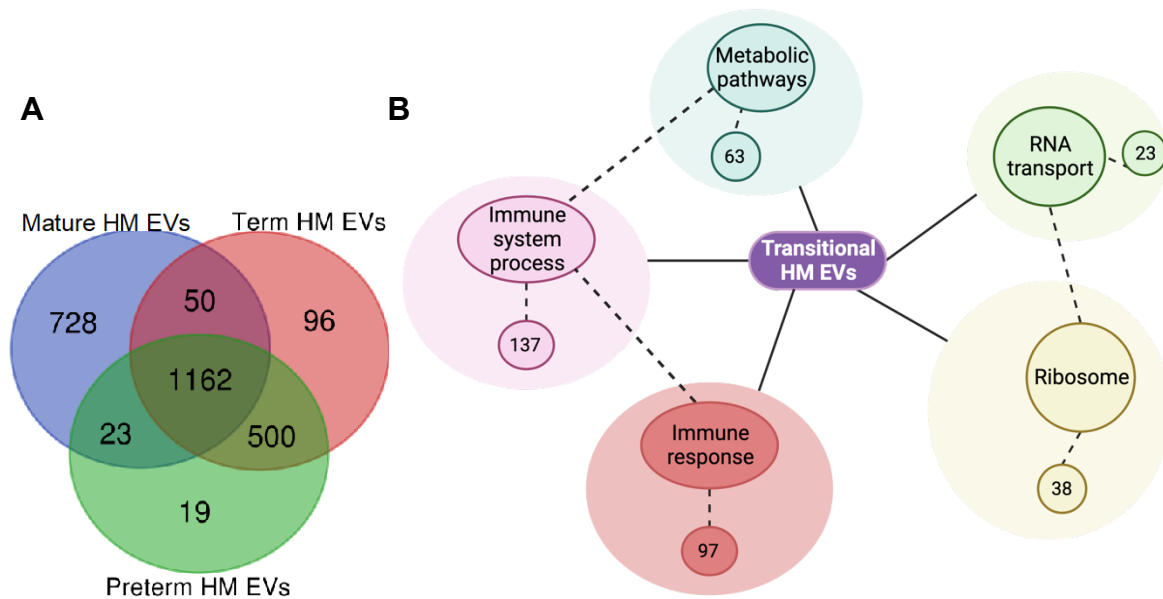


Figure 2.8. Analysis of proteins derived from mature HM EVs and transitional term and preterm HM EVs. (A) Venn diagram comparing proteins identified in mature HM EVs versus transitional term and preterm HM EVs. Out of 1964 proteins identified in mature HM EVs, 1235

were present in term and preterm EVs, with a total of 615 unique proteins in transitional term and preterm HM EVs. **(B)** Functional enrichments of proteins unique to transitional HM EVs. Enriched clusters included pathways in metabolism (blue, KEGG pathway – 63 proteins), immune system process (pink, GO biological process – 137 proteins), immune response (red, GO biological process – 97 proteins), ribosome (yellow, KEGG pathway – 38 proteins), and RNA transport (green, KEGG pathway – 23 proteins), indicated by solid lines. Only high confidence interactions were included in STRING pathway analysis (>0.9 score), dashed lines indicate interactions between clusters.

In addition to total protein identification, previous studies have also measured protein expression quantitatively. We first compared the differentially expressed proteins quantified in the present data to those previously identified in term and preterm skim HM by Molinari *et al*¹⁹⁷. Common significantly upregulated proteins in term HM EVs were cathepsin B and vitronectin. In preterm HM, both lists contained significantly upregulated albumin, and Ras-related proteins – Rab-6 in HM EVs, and Rab-1A, Rab-8A in skim preterm HM. The datasets differed for mucin-4, which was upregulated in preterm HM EVs, but downregulated in preterm skim milk (**Supp. 7**).

To investigate the protein content in relation to previous studies on enzymatic processes and infant digestion, we compared the present dataset to data reported by Nielsen *et al*.²²² obtained from term and preterm human skim milk fractions. When compared with the respective conditions in our data, preterm EVs had 49 proteins in common with preterm skim milk, and term EVs had 22 proteins in common with term skim milk. Although preterm EVs demonstrated more proteins in common with skim milk, those proteins were still found in term HM EVs, but not in term skim milk. Thus, the proteins common to both EVs were analyzed in STRING. As expected, many proteins had enzymatic features. The enriched biological processes were varied,

but the processes with the highest abundance were related to the immune system and to metabolism (**Figure 2.9**, and **Supp. 8**).

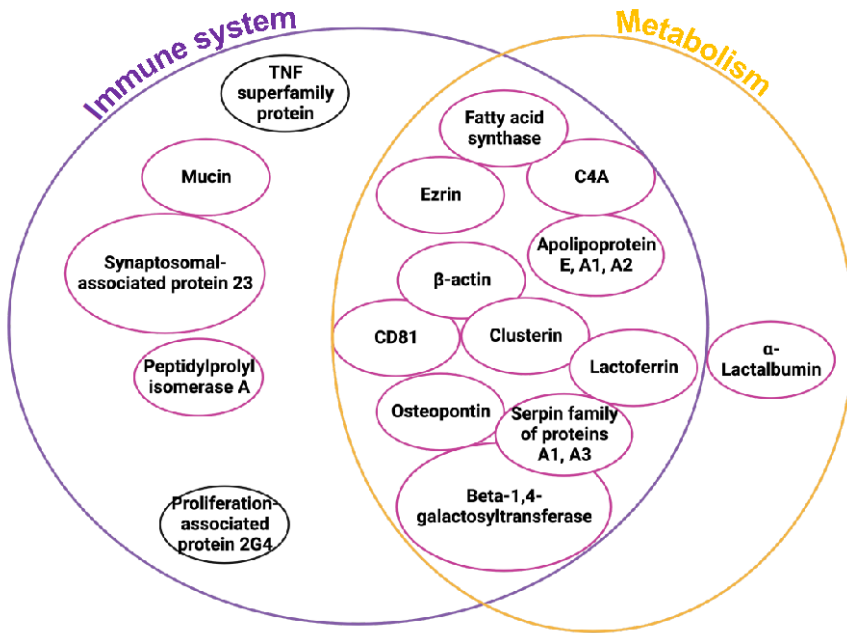


Figure 2.9. Select HM EV proteins common to skim HM with biological process enrichment analysis. Majority of the proteins formed a network of interactions (pink circles) and categorized to both immune system and metabolism-related biological processes. STRING analysis, medium confidence interactions (>0.400 score), total input of 31 proteins.

A study has previously compared the proteomes of term and preterm HM EVs¹⁴⁴. Since the total protein list was not publicly available, we compared the reported significantly up- and downregulated peptides to those differentially expressed in our data. In both datasets vitronectin was significantly upregulated in term HM EVs, and albumin was significantly upregulated in preterm HM EVs. Out of the 16 reported proteins that were differentially expressed in Wang *et al.*, all but RNASE1 and VIMENTIN were found in the present dataset, though not significantly differentially expressed (**Supp. 9**).

5. Quantification of mRNA from GA-specific human milk EVs

RNA of HM EVs from term and preterm samples was sequenced to quantify the mRNA expression. In total, over 12,000 unique transcripts were detected in both term and preterm HM EVs (Figure 2.10A). On the gene level, term and preterm HM EVs shared 5522 genes, with an additional 1067 and 2912 unique genes in each group, respectively (Figure 2.10B).

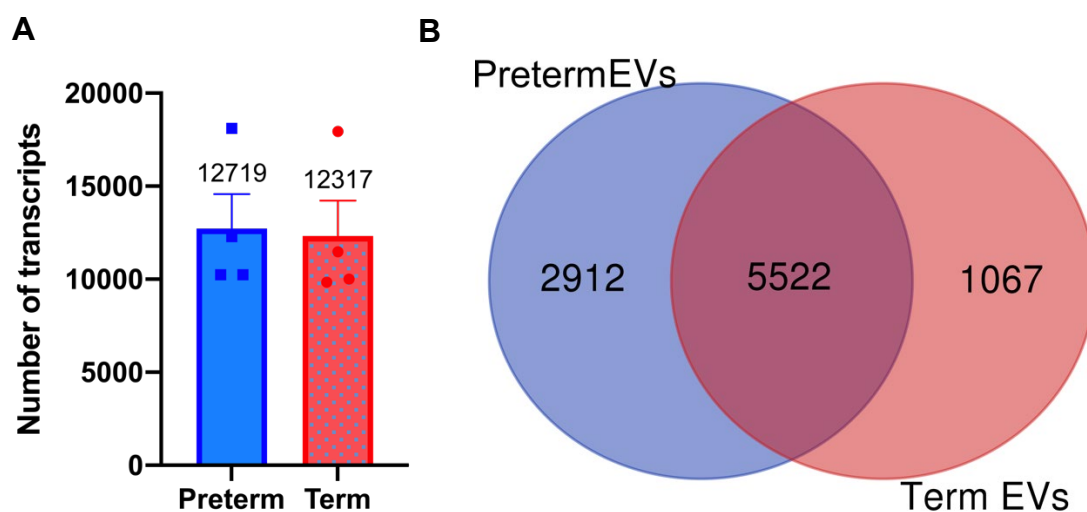


Figure 2.10. RNA transcripts identified in term and preterm HM EVs following RNA sequencing. (A) Number of total transcripts identified for preterm – 12,719 and term – 12,317, average $n=4$ for each preterm and term. (B) In a Venn diagram comparison, 5522 genes are shared between term and preterm HM EVs, while preterm has 2912 and term 1067 unique genes.

Preterm and term HM EV mRNA was then queried in the STRING database to identify enriched biological processes and pathways. Term HM EVs contained double the total number of enrichments in biological processes – 163 versus 80 in preterm HM EVs, but same number of KEGG pathway enrichments (Supp. 1b). Pathway analysis in Reactome database revealed a similar number of pathways between term (191) and preterm HM EVs (189). Both had an

enrichment in IL-1 and IL-12-related pathways (**Supp. 1b**). For enriched biological processes, antimicrobial humoral response, IL-1 response, oxygen level response, and Fc receptor, IL-12, NF- κ B, and Wnt signaling were unique to term HM EVs, whereas cellular response to IL-7 and innate immune response in mucosa were unique to preterm HM EVs (**Figure 2.11** and **Supp. 2b**).

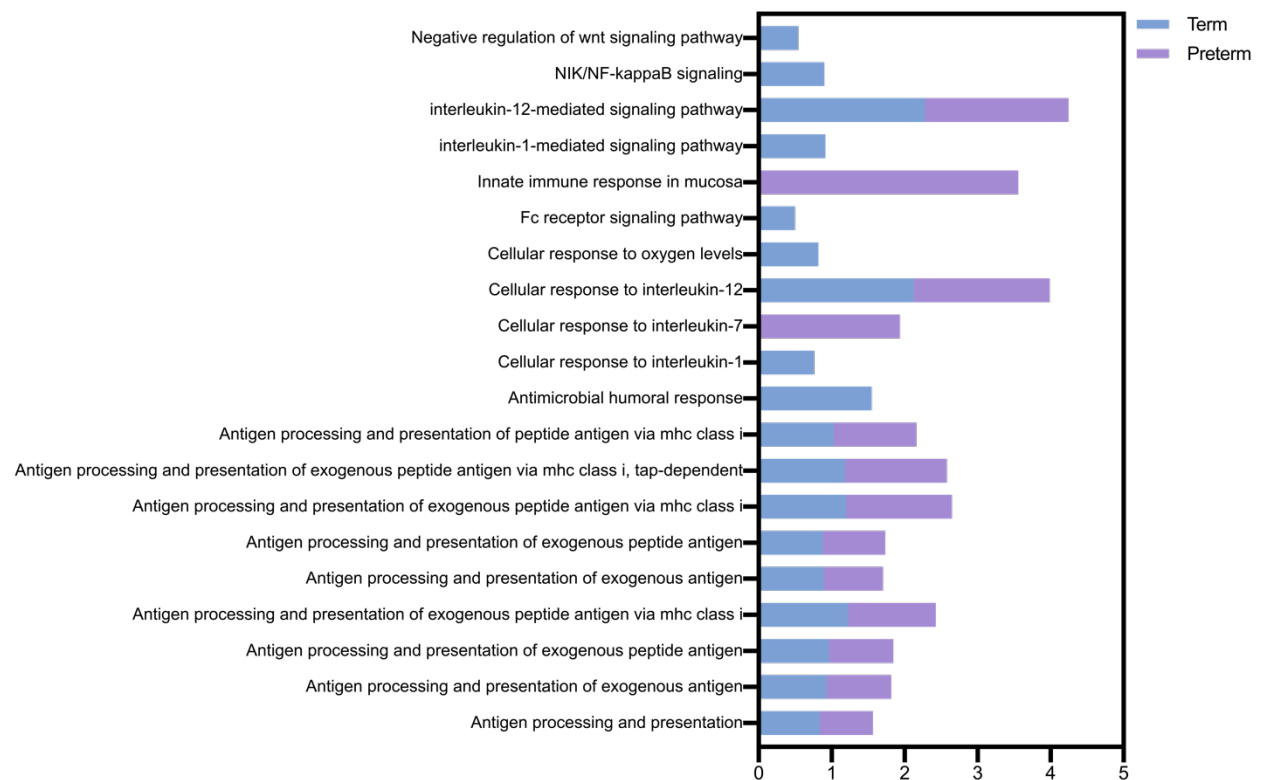


Figure 2.11. Enriched biological processes identified with STRING database of all term and preterm HM EV mRNA. Immune system and signaling related processes were selected for plotting. X-axis represents the enrichment score for term (blue bars) or preterm (pink bars). Enrichment was similar between shared identified biological processes for term and preterm HM EVs. Unique processes for antimicrobial humoral response, IL-1 response, oxygen level response, and Fc receptor, IL-12, NF- κ B, and Wnt signaling were identified for term HM EVs, whereas IL-7 and innate immune response in mucosa were enriched in preterm HM EVs only. Transcripts with a TPM value >0 were queried.

Furthermore, the lists of unique genes from term and preterm HM EVs were queried in the STRING database. In term HM EVs, genes with the highest abundance included translation and ribosomal genes (*EIF3CL*, *RPL34*) as well as cell death related genes (*PDCD5* AND *CASP4*). Enriched biological processes included energy related functions only (**Supp. 3b**). In the unique preterm gene set, one Reactome pathway for translation was enriched (**Supp. 3b**).

6. Differential expression of GA-specific human milk EV mRNA cargo

Next, mRNA raw counts were subjected to differential expression analysis. Term and preterm HM EV biological replicates clustered within their respective groups (**Figure 2.12A**). Overall, high fold-change differences were measured between the two groups, and a modest number of significantly expressed genes were identified, when compared to the size of the total gene pool (**Figure 2.12B**). A total of 153 and 285 genes were significantly (adjusted p-value <0.05) upregulated in term and preterm HM EVs, respectively (**Supp. 4b**). The top 20 most differentially expressed genes in term and preterm HM EVs are listed in **Table 2.2**.

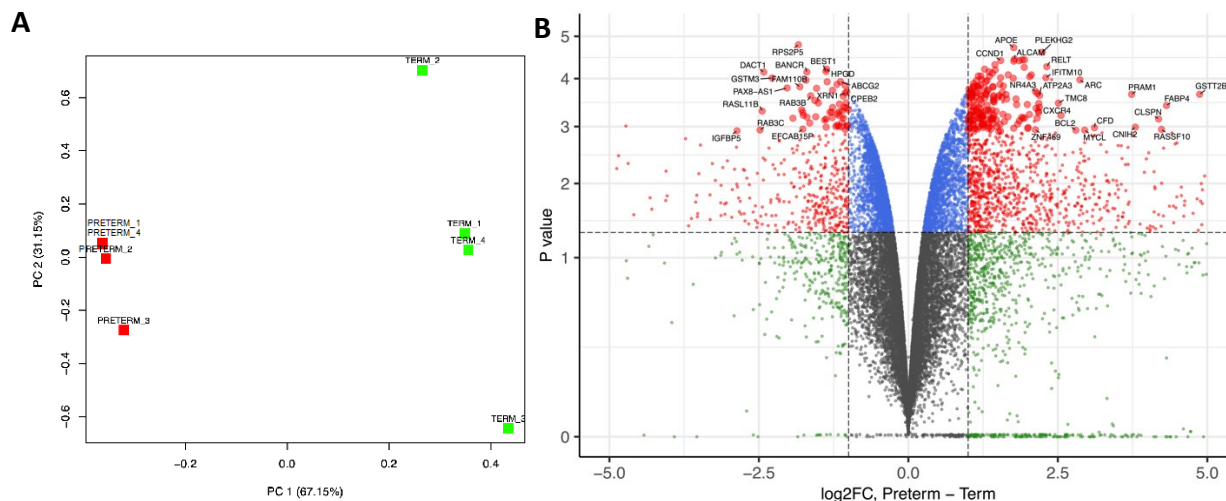


Figure 2.12. Differentially expressed mRNA in term and preterm HM EVs. (A) Clustering analysis of term (green) and preterm (red) HM EVs following TMM RUVr $k=5$ normalization. Both clustered with their respective conditions. (B) Volcano plot of differentially expressed genes. Genes with positive \log_2 fold-change (FC) value were higher abundant preterm, genes with a negative \log_2 FC were upregulated in term, genes not significantly changed are annotated in green and grey. Significance was assigned to mRNA with an adjusted p-value (FDR) of <0.05 (dashed line). Plot is constrained to \log_2 FC <5 , genes with a \log_2 FC >1 and FDR <0.05 are annotated.

Table 2.2. Differential mRNA expression in term and preterm HM EVs. Genes were considered significantly changed based on $p_{adj} < 0.05$ and \log_2 fold-change >1 . Genes with positive fold-change value were more highly expressed in preterm, those with negative fold-change were more highly expressed in term samples. The 20 most differentially expressed genes are displayed.

Gestational Age at birth	Gene symbol	Fold-change (\log_2)	P-value
Term	<i>GSTM1</i>	-12.05	0.045
	<i>RPS14_1_156</i>	-5.89	0.045
	<i>RP4-765C7.2</i>	-4.72	0.047
	<i>IGFBP5</i>	-2.87	0.049
	<i>RAB3C</i>	-2.48	0.047
	<i>RASL11B</i>	-2.45	0.047
	<i>DACT1</i>	-2.42	0.045
	<i>GSTM3</i>	-2.28	0.045
	<i>PAX8-AS1</i>	-2.03	0.045
	<i>PDLIM1</i>	-1.93	0.047
	<i>RPS2P5</i>	-1.84	0.045

	<i>FAM110B</i>	-1.81	0.045
	<i>BEST3</i>	-1.78	0.047
	<i>BTG3</i>	-1.77	0.047
	<i>EFCAB15P</i>	-1.77	0.047
	<i>GLYATL2</i>	-1.76	0.047
	<i>TMEM200A</i>	-1.71	0.045
	<i>BANCR</i>	-1.70	0.045
	<i>GAPT</i>	-1.70	0.047
	<i>RAB6B</i>	-1.65	0.047
	<i>GSTT2B</i>	4.87	0.045
	<i>FABP4</i>	4.32	0.047
	<i>RASSF10</i>	4.23	0.047
	<i>CLSPN</i>	4.19	0.047
	<i>CNIH2</i>	3.80	0.047
	<i>PRAM1</i>	3.73	0.045
	<i>CFD</i>	3.11	0.047
	<i>MYCL</i>	2.95	0.048
	<i>ARC</i>	2.87	0.045
	<i>BCL2</i>	2.80	0.048
Preterm	<i>CXCR4</i>	2.55	0.047
	<i>TMC8</i>	2.51	0.047
	<i>RP11-295K3</i>	2.40	0.045
	<i>RELT</i>	2.32	0.045
	<i>IFITM10</i>	2.30	0.045
	<i>PLEKHG2</i>	2.24	0.045
	<i>ATP2A3</i>	2.19	0.045
	<i>EGR2</i>	2.19	0.047
	<i>WAS</i>	2.18	0.047
	<i>FERMT3</i>	2.18	0.047

All significantly differentially expressed genes were analyzed in STRING for networks interactions and functional associations. Genes more highly expressed in term HM EVs were enriched in 11 GO biological processes, 24 KEGG, and 4 Reactome pathways, with the majority of genes related to metabolic processes only, with no immune enrichment in any of the queried databases (**Figure 2.13** and **Supp.5b**).

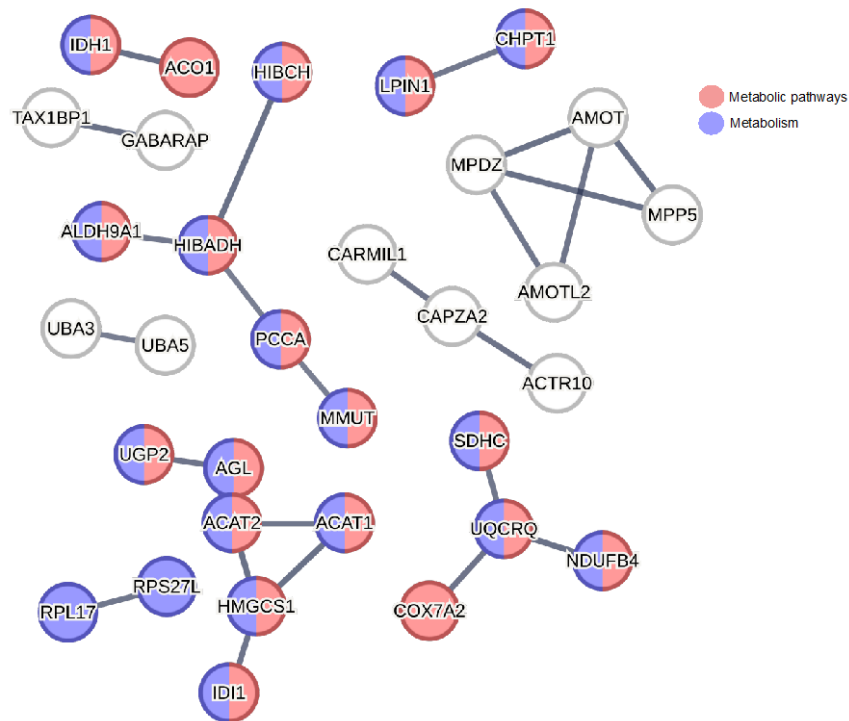


Figure 2.13. Biological processes enriched in significantly ($p < 0.05$) upregulated term HM EV mRNA. A total of 11 biological processes, 24 KEGG, and 4 Reactome pathways were enriched. Metabolism-related enrichment was seen for many differentially expressed genes. KEGG metabolic pathway (red fill) included 33 mRNA in the total dataset, and Reactome metabolism (blue fill) included 42 mRNA in the total dataset. Other significantly increased interacting mRNA are annotated with a white fill. STRING analysis, confidence score 0.9, unconnected nodes removed.

Differentially expressed genes in preterm HM EVs contained genes enriched in 361 GO biological processes, 6 KEGG, and 8 Reactome pathways, with high confidence associations including developmental and immune system processes, and TNF signaling pathway (**Figure 2.14** and **Supp. 6b**). Both conditions resulted in enrichment of sub-cellular compartments – extracellular-exosome for term, and endosome system for preterm.

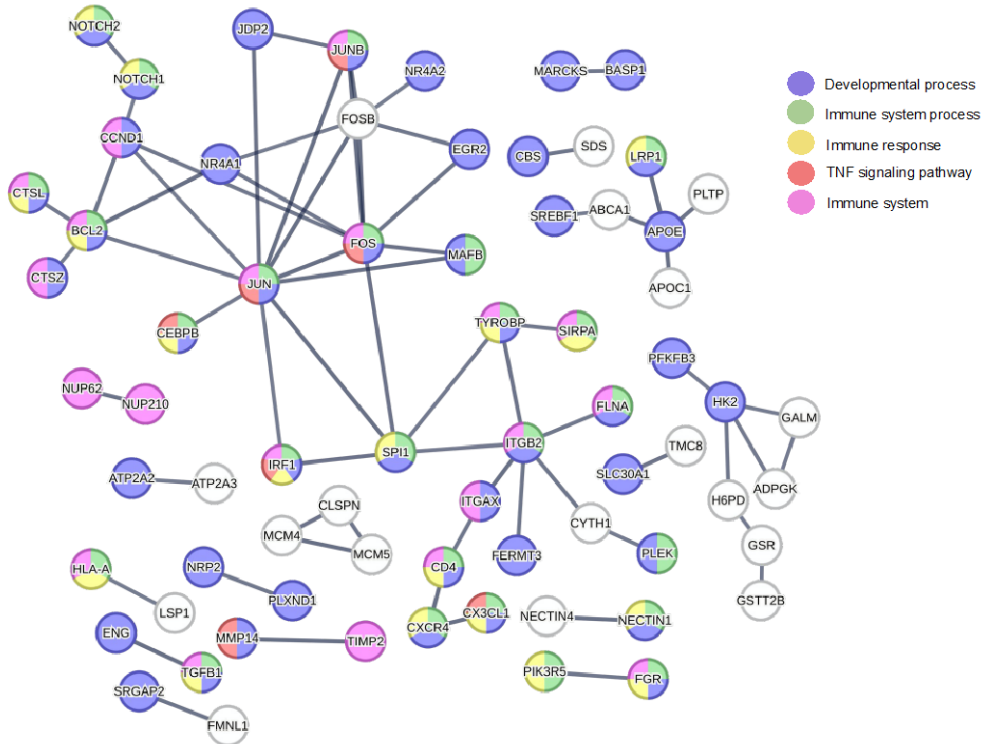


Figure 2.14. Biological processes enriched in significantly ($p < 0.05$) upregulated preterm HM EV mRNA. A total of 361 biological processes, 6 KEGG, and 8 Reactome pathways were enriched. Immune system enrichment was seen for many differentially expressed genes. Total mRNA in the dataset included 118 for developmental process (blue fill), 60 for immune system (green fill), and 38 for immune response (yellow fill, GO biological process). For KEGG database, 8 mRNA in the total dataset were enriched for TNF signaling pathway (red fill). Immune system in Reactome database included 56 mRNA in the total dataset (pink fill). Other significantly increased interacting mRNA are annotated with a white fill. STRING analysis, confidence score > 0.9 , unconnected nodes removed.

To identify meaningful processes and pathways without the limits imposed by arbitrarily chosen differential expression cutoffs, GSEA was performed. In term HM EVs, upregulated genes were constrained to five clusters (**Figure 2.15A**), with an enrichment in metabolic processes, including amino acid metabolism, proteasome regulation, and metabolic cycles. Genes upregulated in preterm HM EVs were constrained to a formation of maximum six clusters

(Figure 2.15B). Many enrichments were immune related, including biological processes in neutrophil activation, antigen processing and presentation, T cell selection, and genomic spatial events in several immune cells (monocytes, CD4⁺ T cells, monocytes).

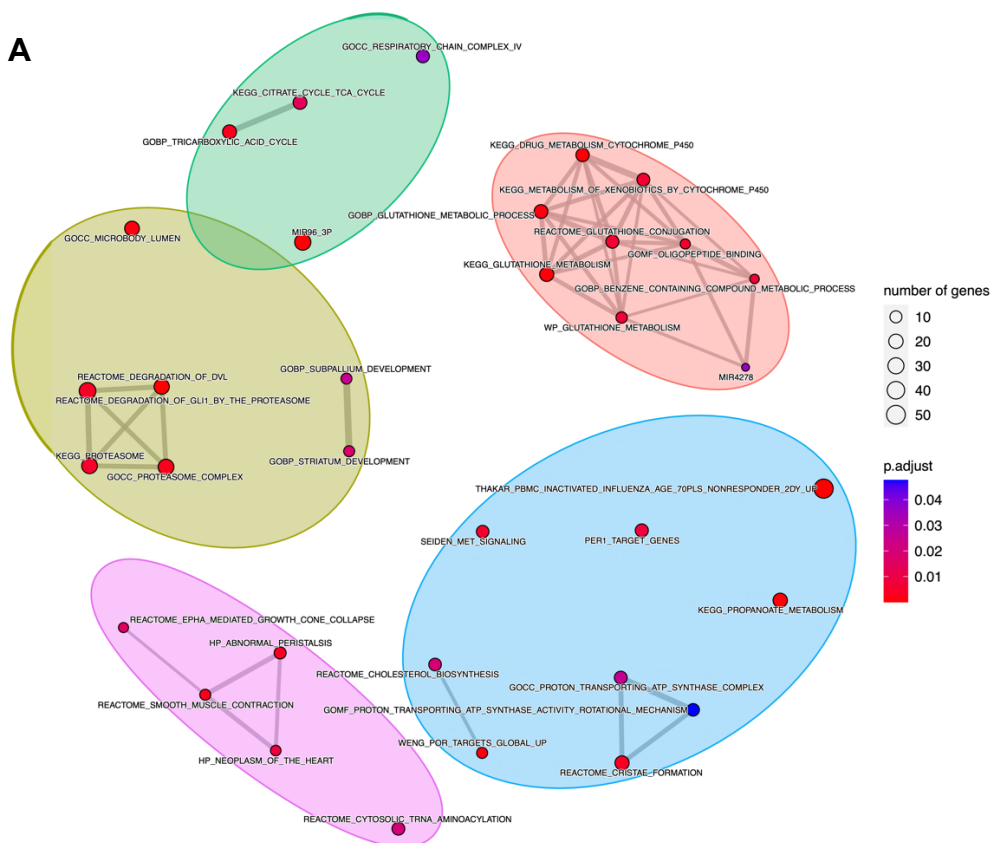
A**B**

Figure 2.15. Gene set enrichment analysis of enriched processes, pathways, and functions for differentially expressed term and preterm HM EV mRNA. (A) Term HM EV-cargo had the highest number of gene clusters for metabolism (red shading). (B) Preterm HM EV-cargo was diverse and shared between several enriched gene sets, indicated by overlapping borders. Immune-related functions (light blue and pink shading) were highly enriched. Gene sets with an adjusted p -value of <0.05 were plotted.

7. GA-specific human milk EV cargo in previously identified human milk mRNA

Since cellular origin of EVs can determine the cargo and downstream biological effects, we sought to compare the gene signatures of term and preterm EVs to human milk single cells. The marker genes listed by Nyquist *et al.* were clustered with term or preterm HM EVs. The gene signatures corresponding to T cells, neutrophils, dendritic cells, fibroblasts, lactocyte epithelial cells (clusters LC1 and LC2), and macrophages (GPNMB+ and CSN1S1) were included³⁰. Briefly, gene lists with fold-change >1 and percent distance >0.5 were retained. Any gene not detected in our dataset was removed from the gene sets. Following GSEA analysis of retained gene sets, any gene set smaller than 10 genes or larger than 500 genes was eliminated.

Macrophages (GPNMB+) and neutrophils were the most upregulated in the preterm group, when compared to term samples (**Figure 2.16A**). In addition to the highest upregulation seen for signatures of GPNMB+ macrophages and neutrophils in preterm HM EVs, they too contained the highest count of differentially expressed genes (**Figure 2.16**). Also significantly increased were T cell, CSN1S1p+ macrophages, LC1 lactocyte epithelial cells, and fibroblasts. Term HM EVs were enriched for LC2 lactocyte epithelial cell gene signatures (**Figure 2.16A**). GA-specific gene enrichment data was also processed with TMM only, and TMM RUV ($k=5$), wherein signatures for LC1, LC2 and fibroblasts were more enriched for term HM EVs (**Supp. 7b**).

However, in all analyses, preterm HM EVs consistently displayed high enrichment for immune cell signatures (Supp. 7b and Figure 2.16).

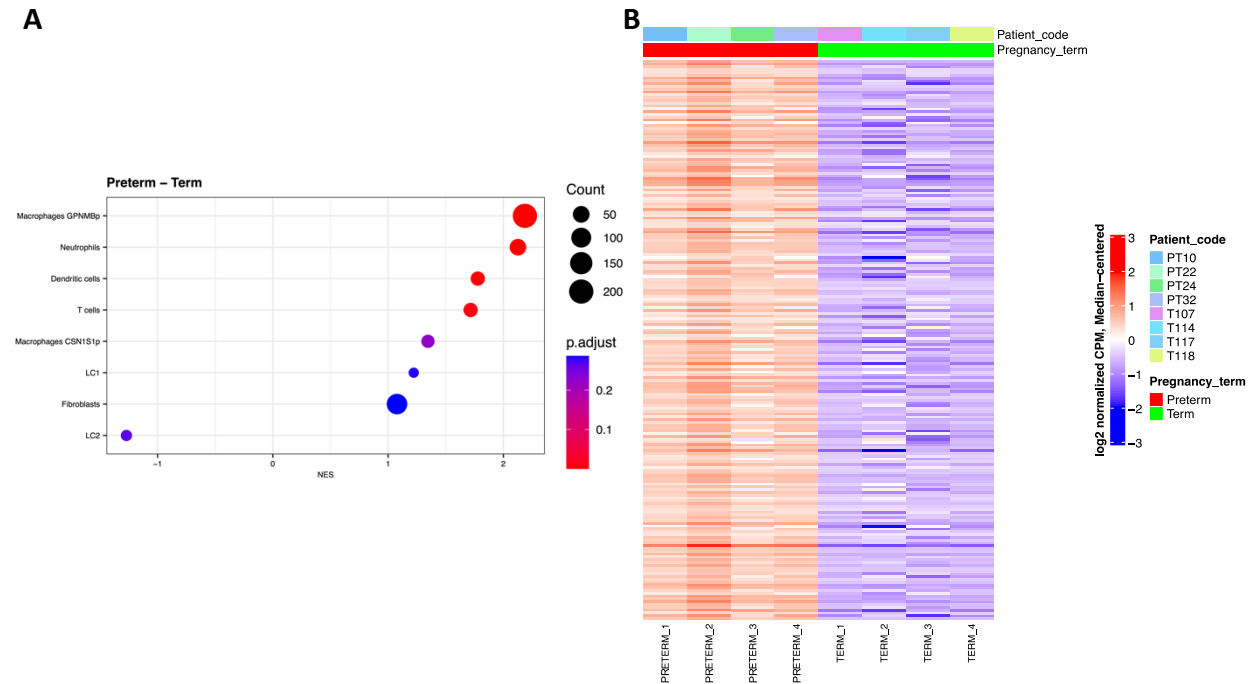


Figure 2.16. Single cell gene signatures in differentially expressed term and preterm HM EV mRNA. (A) Single cell sequencing signatures for GPNMB+ macrophages, neutrophils, dendritic cells, T cells, CSN1S1+ macrophages, lactocyte cluster 1 (LC1), fibroblasts, and lactocyte cluster 2 (LC2) in differentially expressed term and preterm HM EV mRNA. Higher expression in all but one single cell signatures is present for preterm HM EVs (NES >0), term HM EVs have a higher expression for LC2 signatures only. (B) Heatmap of core set of most upregulated genes in preterm HM EVs for GPNMB+ macrophage signatures. Genes with log fold-change >1 and percent distance of >0.5 were retained, TMM with RUVr k=5 normalization.

2.5 Discussion

In this study, we have quantitatively characterized EV cargo from term and preterm HM. We observed that preterm HM EVs had a higher number of proteins and mRNA related to immune system processes. Whereas we propose that term HM EVs upregulate additional metabolic

pathways. Analysis of biological processes from total protein and RNA abundance suggested a more diverse biological regulation by term HM EVs.

A recent study by Wang *et al.* characterized proteins in term and preterm HM EVs using iTRAQ labelling¹⁴⁴. Our study complements their findings by using LC-MS/MS protein identification with label-free analysis allowing for the identification of an increased number of peptides. We reported over 19,000 total peptides, which greatly exceeds the 719 peptides identified previously¹⁴⁴. In this study, the SWATH technique further facilitated the identification of lower abundance proteins^{223,224}. As such, the current findings provide a foundational basis for further functional studies into the unique proteins identified in term and preterm HM (**Table 2.1**, and **Supplementary file**). Freiría-Martínez *et al.* also reported proteomics analysis of term and preterm whole HM and EVs²²⁵. Between the two groups reporting differentially expressed proteins, both describe upregulation of lysozyme, and Wang *et al.* also report increased levels of LF, in preterm HM EVs^{144,225}. Although these proteins were present in our dataset, we did not detect significantly different expression levels. It is important to note that the previous studies had isolated HM EVs from colostrum, mature milk, or both, while we obtained transitional HM. In HM, most abundant proteins include LF and lysozyme¹⁵, which may also oversaturate the mass spectra and interfere in the identification of lower abundance proteins²²⁶.

A previous study showed upregulation of cathepsin D in the milk of mothers that delivered prematurely⁷⁰. Proteases in human milk are suggested to aid digestion in infants with an added role of influencing infant immune system^{70,227}. To our knowledge, presence of cathepsin B has not been previously reported in proteomic studies of HM EVs, even though it has been detected

among the top 20 most abundant transcripts in colostrum HM fat layer¹⁹. Using proteomic analysis, we were able to detect a significantly higher level of cathepsin B in term HM EVs, when compared to preterm samples. Additionally, in our mRNA data we were able to detect cathepsin B in both term and preterm HM EVs. However, there was no statistically significant differences in expression (**Supplementary file**). The availability of cathepsin B protein could support digestion in infants during feeding.

The most significantly upregulated protein in term HM EVs was SERPINE2, which is a member of the serpin family of proteins that inhibit serine proteases²²⁸. A previous study investigated anti-inflammatory effects in a premature infant intestine model, where EGF treatment upregulated several *serpine* genes, including SERPINE2²²⁹. Antiproteases from the serpin family are important in infant digestion²³⁰, and have been shown to regulate inflammatory processes²³¹. Heat shock protein 70 was also upregulated in term HM EVs and may provide intestinal protection in infants by supporting the intestinal barrier, as previously demonstrated in a rat pup model²³².

In preterm HM EVs, caspase 14 protease was significantly upregulated. Its main proposed function is to regulate epidermal barrier formation^{233–235}. In the context of a premature birth, the support of barrier formation and immune regulation could be, in part, attributed to caspase 14. Additional cell proliferation and differentiation could be promoted by fibroblast growth factor binding protein 1²³⁶, one of the most upregulated proteins we found in preterm HM EVs (**Table 2.1**).

Another highly upregulated protein was elastin microfibril interfacier 3 or EMILIN-3, which can act as a regulator of TGF β ²³⁷. Moreover, this protein is implicated in various infant inflammatory diseases and is an important protein for immune response regulation^{238,239}. Under conditions of cellular stress, promoting gut epithelial cell survival is another route of protection, which is increased following HM EV treatment¹⁴⁷. Epithelial-to-mesenchymal transition (EMT) may occur as a result of microbe-induced inflammation to facilitate gut repair^{149,150} and HM EVs have been shown to affect EMT, via their TGF β 2 cargo, in normal and cancerous breast epithelial cells¹⁴⁸. Whether these TGF β -dependent responses are regulated by additional EV carrier proteins, such as EMILIN-3, remains to be determined.

In HM EV mRNA, we noted further GA-specific differences. The gestational age-specific differences were similar to those seen on the protein level, with more immune-related enrichments for preterm when functional enrichments were analyzed in STRING. It is notable that while the FDR value was similar between the top 200 significantly differentially expressed mRNA in preterm HM EVs, the fold-change varied 1- to 5-fold. When comparing the top 20 differentially expressed genes, many of the significantly upregulated genes in preterm EVs were implicated in immune signaling – *BCL2*, *IFITM10*, *CXCR4*, *CFD*, *WAS*, *FERMT3*. The anti-apoptotic signaling of BCL2 is prevalent during lactation and mammary tissue remodeling²⁴⁰. The significant upregulation of BCL2 in preterm HM EVs may represent the stage of gland development at the time of premature birth. For infants, increased presence of complement factor D (CFD) in preterm milk may help support the incomplete complement functions presenting in premature infants⁴⁷. Similarly, CXCR4 is an important cell receptor expressed in immune cells to mitigate hematopoiesis²⁴¹ and may further support development of infant immune system,

specifically innate²⁴². Among the genes with a 2-fold increase in expression was *HLA-H*.

Transfer of antibodies to infants via HM is well established and essential for immune system development⁶⁴, however the role for HLA molecules is less clear. It has been suggested that HLA molecules may be important in regulating or establishing tolerance, but more work is needed²⁴³.

In term HM EVs, significant increases in expression of several metabolic related mRNAs were observed. *GSTM1* had a 12-fold increase, the highest of any other gene measured by several folds, while *GSTM3* had an over 2-fold increase. GSTMs are part of the glutathione transferase family of enzymes and implicated in detoxification processes, thus being potent antioxidants^{244,245}. Preterm HM EVs also contained significant increases in members of glutathione antioxidant defense system – *GSR* and *GSTT2B* with 1.4- and 4.8-fold increases, respectively. Since breastfed infants are more protected against development of many diseases^{85,246}, the abundant presence of antioxidant promoting factors in HM may contribute to the overall health of infant. Term HM EVs also had increased expression in mRNA implicated in cellular signaling, such as ras and rab-family of proteins (*RASL11B*, *RAB3C*, *RAB6B*), insulin-like growth factor-binding protein 5 (*IGFBP5*), and *DACT1*. Significant increases seen in *PDLIM1* in term EVs may promote infant gut epithelial cell migration and survival²⁴⁷, an effect previously seen *in vitro* following treatment with term and preterm HM EVs¹⁴⁴.

HM EVs are purified from the skim milk fraction, while the separation of HM fat and cells occurs in the top layer and pellet, respectively. In previous human milk mRNA studies, the fat and cellular portions have been subjected to comprehensive RNA sequencing^{19,30,31,115}.

Whenever specified in the studies, the sequencing data showed enrichment of casein and LA transcripts, which we did not see in our data and could further emphasize a more cellular signaling-related function for EVs versus nutrient for other milk fractions. The HM EV sequencing data also allows for the comparison between human milk cells and EVs. Whether or not the cells found in milk are secretors of EVs remains to be determined but clustering the corresponding transcriptomes provides insight.

Single cell sequencing of HM has previously revealed leukocyte epithelial cells throughout lactation, as well as immune cells such as macrophages, T cells and neutrophils, and stem cells^{31,32,115,248}. It has been hypothesized that stem cells from HM could survive digestion and have regenerative and developmental roles in the infant²⁹. In mother-infant dyads, gene expression patterns in HM cells, specifically the JAK/STAT pathway genes, associated to infant microbiome outcomes²⁴⁹.

When analyzing cellular signatures of HM EVs, both term and preterm EVs had immune cell signatures, though they were significantly higher in preterm EVs. The origin of HM EVs may explain the functional effects seen prior studies, especially when inflammatory regulation was examined¹⁵⁹. In our transcriptomic data, preterm mRNA was most significantly upregulated for gene signatures of GPNMB+ macrophages, generally attributed to M2 macrophages and an anti-inflammatory phenotype^{250,251}. Given the vulnerability of infants, especially premature infants, to gut inflammatory diseases such as necrotizing enterocolitis, the EV cargo may provide significant protection. It is especially notable that EVs themselves have been shown to survive digestion in simulated conditions^{126,173} and have tissue bioavailability following oral and

intravenous supplementation in mice¹³². In a functional study, term HM EVs were shown to regulate T cell activation and were proposed to allow development of a more immune tolerogenic phenotype¹⁵⁹. Prior analyses from mature HM EV proteins and surface markers have also indicated an immune, epithelial, and mesenchymal stem cell origin for the EVs^{167,252}. Given the overall enrichment of preterm HM EVs in immune-related protein, mRNA, and cell signatures, it remains to be seen whether preterm EVs promote immunoregulatory effects *in vitro* and *in vivo*.

Limitations of this work include the lower biological sample number, with milk from 12 mothers analyzed in total. However, collecting fresh milk was imperative for isolation of EVs, thus experimental analyses proceeded with fresh samples available at the time. While every effort was made to collect milk at the same lactation stage post birth, some variation between term and preterm was present, and could have influenced the composition of HM EV cargo (**Supplementary file – Donor information**). The interpretation of data is based on *in silico* analyses, which require *in vitro* and *in vivo* validation of the cargo differences, especially to allow confirmation of the more immunoregulatory profile of preterm HM EVs proposed here.

Characterizing the term and preterm HM EV proteome and mRNA could provide insight for future studies investigating possible milk deficiencies and potential supplementation of donor milk or formula. Whether premature infants should be preferentially supplemented with premature HM, or vice versa in term infants, might be an important consideration to ensure the best possible outcomes for all infants, especially fragile premature infants. Overall, our data has demonstrated consistent diversity between term and preterm HM EVs. Temporal effects of the

cargo may be of importance, allowing HM EVs to have an immediate effect upon uptake via proteins, and delayed effect via translation of mRNA. Exact functional effects and clinical relevance of the differences in GA-specific EV cargo remain to be elucidated.

2.6 Materials and Methods

Milk collection

HM from donors was collected according to ethics protocols at the University of Ottawa and Children's Hospital of Eastern Ontario (#H-03-20-5643). Once written consent was obtained, donors were asked to sterilize the breast with an antibacterial wipe and manually express their milk into a sterile collection tube. A total of 20mL of milk was collected from each anonymous donor: 6 term and 6 preterm. Cesarean birth, antibiotic use, and any active maternal genetic, immune, and chronic inflammatory disease resulted in donor exclusion. Mother's age and parity, infant sex, age, gestational age, and birth weight, when available, were recorded (**Supplementary file – Donor information**). HM was classified as term for GA of more than 37 weeks, and preterm for GA of less than 37 weeks¹⁹⁶. Following collection, HM was transported to the lab to commence EV isolation within 30 minutes.

Extracellular vesicle isolation

Prior literature on milk EV isolation from diverse species has established that differential and ultracentrifugation is appropriate to obtain a sample enriched in EVs^{142,143,216,253,254}. We have previously described an isolation method for HM EVs with an end goal of proteomics analysis²¹⁵. Briefly, collected milk was centrifuged at 4600 x g to remove fat, cells, and cell debris. The skimmed milk was then centrifuged at 20,000 x g to remove the remaining fat, and

pellet large apoptotic and mitochondrial vesicles. The supernatant was subjected to two rounds of ultracentrifugation at 100,000 x g. The pellet was resuspended in 400 μ L of sterile PBS and stored in -80°C in aliquots until further analysis.

Extracellular vesicle characterization

HM EV surface markers and size were characterized using the Exoview R100 instrument (Nanoview BioSciences, USA), following protocols previously published²⁵⁵. Briefly, EVs were incubated overnight on Exoview chips with immunocapture spots for CD81, CD63, CD9, and mIgG. Following incubation, the chips were washed three times with an incubation solution. The chips were stained with anti-CD9-AF488, CD63-AF647, and CD81-AF555 antibodies for 1 hour. After another three washes, the chips were imaged using the Exoview R100 instrument. The acquired images were analyzed for fluorescence and size utilizing the ExoScan 2.5.5 acquisition software. Graphs were prepared using Prism 9.

HM EVs were visualized using scanning electron microscopy. EVs were prepared by re-suspending in PBS, then pelleted at 100,000 x g for 1.5hrs, at 4°C. The EV pellet was fixed in 4% glutaraldehyde for 15 minutes, and subsequently washed twice with PBS for 10 minutes each. The pellet was resuspended in 10 μ L ddH₂O and placed on an EM silicon chip to air-dry, followed by transfer to a 96-well plate. The sample was dehydrated in ascending ethanol (40%, 60%, 80%, 96–98%) by pipetting ethanol down the side of the well thereby immersing the silicon chip. After ethanol was evaporated, the samples were left to dry at room temperature for 24hrs. The following day, silicon chips were mounted on a carbon stage by removing the

adhesive, and Au-coated. The samples were imaged on a JSM-7500F FESEM (JEOL) microscope (University of Ottawa Materials Characterization Core Facility).

Proteomics

The liquid chromatography coupled to tandem mass spectrometry (LC-MS/MS) data acquisitions were performed at PhenoSwitch Bioscience Inc. (Sherbrooke, QC, Canada), using a Sciex TripleTOF 6600 instrument (Sciex, Foster City, CA, USA). All LC-MS/MS equipment and settings were used as previously described²⁵⁶. In brief, six individual samples (30µg each) were analyzed in Sequential Window Acquisition of All Theoretical Mass Spectra (SWATH) acquisition mode, with a 60-minute LC gradient. Analyst TF 1.8 software (Sciex) was used for instrument control, data processing, and acquisition.

To analyze the MS data, we employed a hybrid strategy based on a previously described proteomics pipeline²⁵⁶. Firstly, we used MSConvert to convert the file format from WIFF to mzML²⁵⁷. Then, we utilized proteomics analysis tools (MSFragger, Philosopher, EasyPQP) from the FragPipe GUI (v.17.1; <https://fragpipe.nesvilab.org/>) to search the human proteome (UP000005640, www.uniprot.org) and build preliminary libraries at 5% FDR (false discovery rate)^{258,259}. Next, we retrieved protein IDs from these libraries and inputted them into the ID mapping tool from UniProt.org (www.uniprot.org/id-mapping) to generate a FASTA file of protein targets. Finally, we employed this FASTA file to perform a "library-free search" with methionine oxidation set as variable modification and MBR (match between runs) enabled in DIA-NN (GUI; v.1.8), applying a more stringent 1% FDR to ensure increased confidence in the identifications and quantifications of peptides and proteins²⁶⁰.

For differential expression analysis, the tsv file generated by DIA-NN was curated and directly imported into R. All analyses were performed using the pOmics R package (github.com/nicohttmann/pOmics). Further analysis only considered proteins that were quantified in at least 50% of the samples and imputation was performed using a shifted Gaussian distribution (shift = 1.8 standard deviations (SD), width = 0.3 SD) to account for missing protein MaxLFQ intensities. The composition of the identified proteins was compared with all human proteins to identify over-represented Gene Ontology (GO) cellular components^{261,262}. To identify differentially abundant proteins between term and preterm groups, pairwise Student's t-tests were conducted. Due to the limited sample size, p-values were not corrected. Proteins were considered significantly changed based on a threshold of $p < 0.05$ and an absolute \log_2 fold-change > 0.5 . Based on the sets of significantly up- and downregulated proteins, functional enrichment analysis (over-representation analysis) was performed using GO biological process parameters. Further functional annotations were done using STRING (<https://www.string-db.org>) and PANTHER (<http://www.pantherdb.org/>) databases according to respective presets.

RNA sequencing and analysis

RNA from HM EVs was extracted using Qiagen miRNeasy kit (Qiagen, Germany) coupled with a phenol-chloroform precipitation step. RNA quality was assessed using LibQC (McGill Sequencing Facility). Total RNA from term and preterm HM EV samples (n=4, each group) was sequenced at the McGill Sequencing Facility (Montreal, Canada). RNA libraries were prepared using NEBNextUltra II Directional RNA kit, and sequenced using Illumina NovaSeq 6000. Nf-core rnaseq nextflow pipeline was employed with default settings^{263,264}. The reads were aligned

to the GRCh38 reference genome using STAR²⁶⁵. Reads aligning to exons were counted using Subread featureCounts, and counts were summarized over genes²⁶⁶.

Differential expression was analyzed using edgeR with a library size correction by the Trimmed Mean of M-values (TMM) algorithm. To remove unwanted variation, RUVseq method was employed, using two algorithms – RUVs and RUVr, with values of the “k” factor from 1 to 5^{267,268}. Implementing RUVr or RUVs with increasing values of k improved the clustering of samples, and RUVr k=5 was chosen for further downstream analysis based on sample clustering by PCA and p-value distribution histograms. Gene set enrichment analysis (GSEA) was further performed in R/Bioconductor using the clusterProfiler and msigdb packages^{269–271}. The gene sets used were limited to the MSigDB groups "Hallmark", C2, C3, C5, and C7. Only sets containing between 10 and 1000 genes were surveyed as a cut-off independent method to identify significantly enriched gene sets.

2.7 Acknowledgements

We would like to thank Dr. Yun Liu from the uOttawa Materials Characterization Core Facility for technical support; Dr. Leif Anderson, Dr. Ray Eby and Nanoview Biosciences for surface marker characterization; Prof. Maxim Berezovski at the uOttawa John L. Holmes Mass Spectrometry Facility for guidance on proteomics analysis; and Dr. Senthilkumar Kailasam at the Canadian Centre for Computational Genomics for assistance with RNA sequencing. Additional thanks to the support staff at CHEO Research Institute, especially NICU project lead coordinator Chantal Horth, and research assistants Rebecca Grimwood, Denise Campuzano for patient recruitment, sample collection, and Samira Chamaa for administrative support. The

funding for this project was provided by the Canadian Institutes of Health Research grant (PJT 162423) to J-F.B., E.F., and I.A.

2.8 Data availability

Supplementary data are available from the publisher.

Chapter 3. Characterization of term and preterm human milk extracellular vesicle microRNAs

Manuscript 2: Vahkal, B., Altosaar, I., Hoang, H.D., Alain, T., Barisani, D., Côté, M., Beaulieu, J.F. and Ferretti, E., 2024. Shielding against necrotizing enterocolitis: Insights from gestational-age-specific profiling of human milk extracellular vesicle microRNAs. *Scientific Reports*. Under review. March 24th. ID: dd76c97e-f682-4743-8dd8-f7433ad6396b.

3.1 Preface

Since the field is limited in miR characterization of HM EVs from colostrum and transitional lactational stages, I sought to compare GA-specific changes in the latter. Given the potential importance of milk-derived miRs in mitigating NEC risk, highly conserved and abundant term and preterm HM EV miRs were compared against NEC tissue sequencing datasets to postulate mechanistic explanations for the risk reduction. This work builds upon previous findings in the previous chapter where GA-specific cargo enrichments were found. Here, similarity among the most abundant miRs is evident, suggesting an underlying conservation of HM miRs irrespective of GA and lactational stage.

The data presented in this publication were analyzed by me and co-authors, with specific support in sequencing data interpretation by Dr. Tommy Alain, Dr. Huy-Dung Hoang, and Dr. Donatella Barisani. The manuscript text and figures were prepared by me in collaboration with all co-authors.

Shielding against necrotizing enterocolitis: Insights from gestational-age-specific profiling of human milk extracellular vesicle microRNAs

Brett Vahkal¹⁻³, Illimar Altosaar^{1#}, Huy-Dung Hoang^{1,4}, Tommy Alain^{1,2,4}, Donatella Barisani⁵,
Marceline Côté¹⁻³, Jean-François Beaulieu^{6*}, Emanuela Ferretti^{4,7*}

¹University of Ottawa, Department of Biochemistry, Microbiology and Immunology, Ottawa, ON, K1H 8M5, Canada

²Ottawa Centre for Infection, Immunity, and Inflammation, Ottawa, ON, K1H 8M5, Canada

³Ottawa Institute of Systems Biology, Ottawa, ON K1H 8M5, Canada

⁴Children's Hospital of Eastern Ontario Research Institute, Ottawa, ON, K1H 8L1, Canada

⁵School of Medicine and Surgery, University of Milano Bicocca, Monza, MI, 20900, Italy

⁶Université de Sherbrooke, Department of Immunology and Cell Biology, Sherbrooke, QC, J1H 5N4, Canada

⁷Children's Hospital of Eastern Ontario, Department of Pediatrics, Division of Neonatology, Ottawa, ON, K1H 8L1, Canada

#Current address: Proteins Easy Research Centre, Kemptville Campus Education and Community Centre, North Grenville, ON, K0G1J0, Canada

**Co-corresponding authors*

3.2 Abstract

The composition of human milk (HM), a vital source of nutrition for infants, is influenced by gestational age (GA). Premature infants have increased susceptibility to necrotizing enterocolitis (NEC), a severe gut inflammatory disease. Although HM feeding offers protection against NEC,

the underlying biological mechanisms remain elusive. Here, HM extracellular vesicles (EVs) and their microRNA (miR) cargo were characterized in GA-specific cohorts. A total of 969 and 905 miRs were identified in term and preterm HM EVs, respectively. Comparison with previously described colostrum and mature HM revealed conservation of abundant miRs across lactation stages, where the miR abundance differed based on 3' or 5' sequence. Expression analysis identified 12 significantly different miRs between term and preterm HM EVs, with similar functional enrichments in metabolism and immune-related pathways. Analysis of selected miRs, including miRs downregulated in NEC, revealed enrichments in cell differentiation, inflammation modulation, and epithelial integrity maintenance, aligning with the functional enrichments for total HM EV miRs, which may overall shield against NEC-associated dysregulation. These findings underscore fundamental gestational-age-specific associations observed in HM EV miRs. Understanding the interplay between HM EV miRs and neonatal health could guide the development of specialized therapeutics that mitigate the risk of NEC in premature infants.

3.3 Introduction

Human milk (HM) provides essential nutrition to infants¹⁰. A prevailing challenge in HM research includes the variation in milk composition, which can be influenced by gestational age (GA)^{5,17,202,220,272}. Infants born prematurely are vulnerable to life-threatening gut inflammatory diseases, such as necrotizing enterocolitis (NEC)^{95,273,274}. While HM feeding has been shown to decrease the risk of developing NEC^{45,193}, the exact biological mechanisms underlying this protection are unknown. Part of the protection could be conveyed by HM extracellular vesicles

(EVs)^{84,85,151,163,169,275}, which may withstand digestion to carry immunomodulating microRNAs (miRs) to the infant intestine^{126,133,173}.

Changes in human milk composition have been identified across lactation stages among colostrum (up to 4 days after birth), transitional (5 days to two weeks after birth), and mature (>1 month after birth) milk^{5,220}. The distinct patterns also encompass milk miRs, suggesting a role in development and gastrointestinal maturation^{175,176}. Previous studies have demonstrated that miRs are differentially expressed in colostrum, transitional or mature milk^{276,277}, and that the highly expressed HM miRs are immune-related^{127,171,183}. Differences in miR composition have also been detected in term versus preterm HM EV samples, wherein the preterm group expressed a larger number of regulatory miRs¹⁷³. For example, miR-148a was found to be higher in preterm HM¹⁷¹ and could affect fetal colon cell proliferation, and epithelial-mesenchymal transition¹⁴⁶. EVs could also impact processes in the intestinal mucosa. In a mouse model, treatment with miR-depleted bovine milk EVs resulted in elevated intestinal inflammation and expression of chemokine CXCL9²⁷⁸, indicating that milk EVs could also modulate innate immunity and inflammation. Notably, miRs involved in small intestine goblet cell differentiation, modulation of inflammation, and epithelial integrity maintenance are under-expressed in human NEC intestinal tissue in comparison to healthy control tissue²⁷⁹. The miRs previously identified in HM EVs have many of these functional enrichments and may explain how HM feeding conveys protection in infants, especially against the development of NEC¹⁶⁹.

MiRs regulate gene expression post-transcriptionally via mRNA decay and translation suppression²⁸⁰, with potential differences depending on whether mRNAs contain miR binding

sites in the 3' or 5' end of the untranslated region (UTR)²⁸¹. To exert a high degree of post-transcriptional regulation, different miRNAs have overlapping mRNA targets to increase the likelihood of repression^{282,283}. Milk miRNAs are largely conserved among different mammalian species, indicating the importance of delivering the miRNAs to offspring for developmental regulation²⁰⁷. The identity and abundance of milk miRNAs originating from either the 3' or 5' arm of their miR precursor, and the relative overlap of their target mRNAs are still largely unknown, especially in the context of a stringent patient cohort.

To unravel the constellation of miRNAs contained within HM EVs that may exert significant functional effects on infant health and development, HM samples were collected from GA-specific cohorts following term or preterm infant birth. EV-contained miRNAs were isolated from HM of mothers in a transitional lactation stage. Using high throughput RNA sequencing, 969 and 905 miRNAs were identified in term and preterm HM EVs, respectively. The most abundant miRNAs were previously detected in colostrum or mature HM, while our alignment added specificity of 3' or 5' miR sequences with relative abundance to total miR pool. Differential expression analysis resulted in 12 significantly different miRNAs between term and preterm HM EVs. Strongest evidence for functional enrichments included pathways related to metabolism and immune system, with a larger number of miR targets predicted for term HM. To investigate the potential of HM EV miRNAs to modulate NEC, the abundance of select miRNAs that are significantly downregulated in NEC intestinal tissue was measured. In silico analysis revealed that proposed targets of the NEC-related miRNAs include several immune-related genes and pathways. In previous HM analyses^{127,171,173,208,284,285} and our HM EV data, the selected miR-141-3p, miR-200a-3p and 5p, and miR-375-3p were among the highly abundant miRNAs. We discovered that

irrespective of a term or preterm birth, the HM EV-contained miRs were enriched in a conserved panoply of protective immune- and signaling-related pathways. The downstream effects in infants could ensure the adaptation of the newborn's gastrointestinal tract to the extra-uterine environment and prevent inflammatory dysregulation present in NEC.

3.4 Results

1. Sequencing results and miR characterization

To investigate GA-specific miRs in HM, EVs were first isolated from term and preterm HM, followed by extraction of EV-contained nucleic acids, in a workflow that has been previously described for the corresponding samples with an end-goal of RNA sequencing²⁷². Following an RNA quality check, HM EV-contained miRs were subjected to high throughput small RNA sequencing to quantify the miR abundance. A total of 969 and 905 miRs were identified in term and preterm HM EVs, respectively (**Figure 3.1A** and **Supplementary data A**). The majority of the miRs were shared, while the number of unique miRs were 162 in term EVs, and 98 in preterm EVs (**Figure 3.1B**).

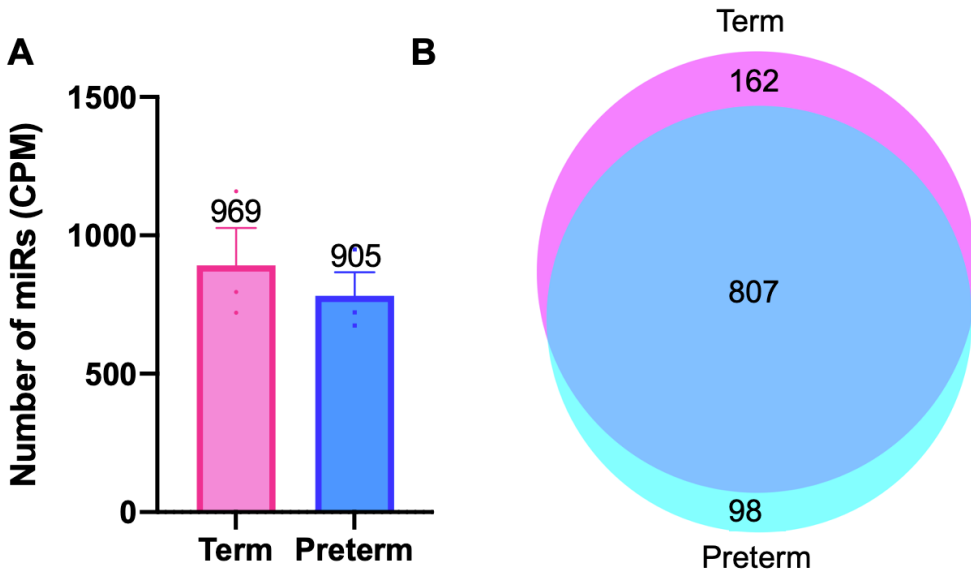


Figure 3.1. Human milk extracellular vesicle miR sequencing results. (A) Total microRNAs (miRs) identified in term and preterm HM EVs following RNA sequencing. Average $n=3$ for each preterm and term. (B) Venn diagram of the common and unique miRs present in two or more biological replicates.

In the top 20 most abundant miRs detected in each group, the majority overlapped between the two groups (**Figure 3.2** and **Supplementary data B**), including the top three most abundant – miR-148a-3p, let-7f-5p and miR-141-3p. The abundance of the top three miRs was significantly higher when compared to the next top 100 miRs in both term and preterm human milk EVs (**Figure 3.3A**).

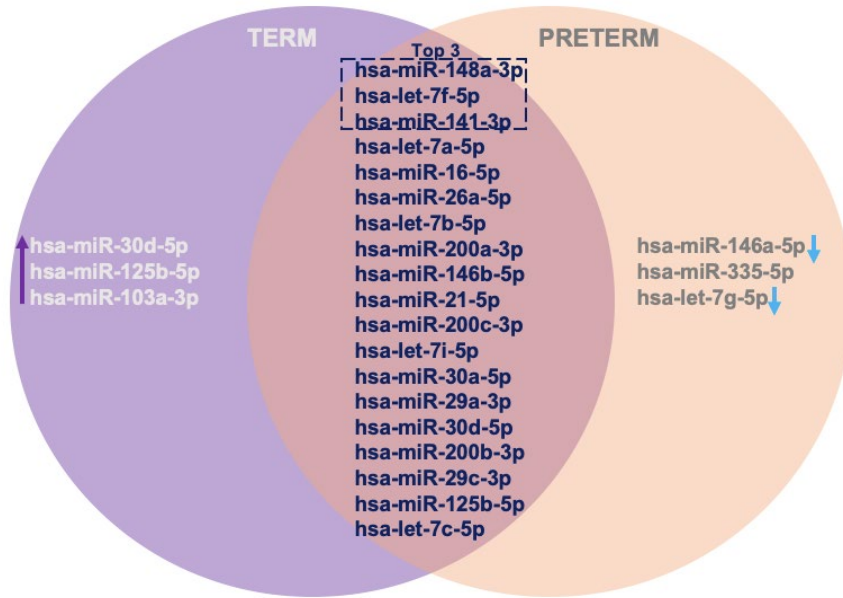


Figure 3.2. Top 20 most abundant miRNAs in term and preterm HM EVs. Majority of miRNAs are shared between the two conditions. Among the most abundant miRNAs, no significant changes in expression were seen. MiRNAs marked with purple arrow denote upregulation in term HM EVs; miRNAs marked with blue arrows denote downregulation in term HM EVs, p -value = ns.

2. MiR target prediction and functional characterization

The miRabel target prediction tool was used to predict targets and affected pathways for the top three most abundant miRNAs. Overall, an average of over 1000 target genes were predicted for each miR (**Supplementary data C**). Target genes with a miRabel significance score of $<0.05^{286,287}$ were further subjected to pathway analysis using KEGG database. In total, over 300 pathways were predicted, with the majority of those shared among the three miRNAs (**Supplementary data D**). Several pathways in the immune system were enriched, including T-cell receptor, Th17 cell differentiation, IL-17 and TNF signaling, bacterial invasion and infection. Pathways in signaling and cell proliferation regulation, such as Wnt, JAK-STAT, Ras, MAPK, PI3K-Akt, were also present (**Supplementary data D** and **Figure 3.3B**). The highest number of target genes was

identified in metabolic pathways, while the highest enrichment scores were for TGFβ and FoxO signaling pathways (Figure 3.3B).

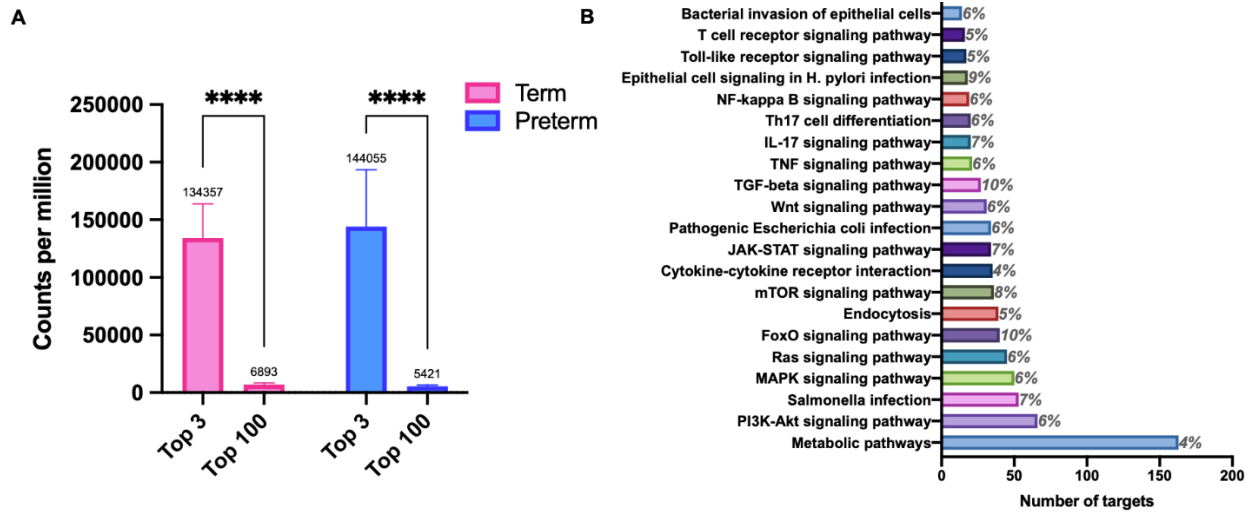


Figure 3.3. Abundance and functional prediction of top 3 miRs - hsa-miR-148a-3p, hsa-let-7f-5p and hsa-miR-141-3p in human milk EVs. (A) Average abundance of top three miRs was significantly higher than the next top 100 miRs detected in either term or preterm HM EVs. ******** $p < 0.001$; $n = 3$ and 100, respectively; two-way ANOVA with Sidak's multiple comparisons. **(B)** Predicted KEGG pathways targeted by top 3 miRs. Select immune and signaling-related pathways that were identified in all three miRs with a total target number > 10 were plotted. Target genes with a significance score of < 0.05 were included in pathway analysis with annotated value representing the enrichment percentage. Pathway with the highest number of target genes was related to metabolism.

To expand functional analysis, the 20 most abundant miRs in term and preterm HM EVs were further analyzed. For improved visualization of the relatively large number of predicted targets, miRNet was utilized. A total of 2532 target mRNA were predicted, with distinct clustering of miRs based on their shared targets (Figure 3.4A and Supplementary data E). Several miRs segregated based on their higher number of shared targets in comparison to other miRs. MiR-16-5p, let-7b-5p, and miR-335-5p had the highest number of interactions among the targets of the

top 20 miRs, indicated by positioning of the node and target mRNAs in the interactome plot (**Figure 3.4A**).

For prediction of enriched biological functions, the top four miRs by degree score (miR-16-5p, let-7b-5p, miR-335-5p, and miR-30a-5p), and two most abundant miRs in the sequencing pool (miR-148a-3p and miR-141-3p) were further compared. Following KEGG enrichment analysis, miR-16-5p, let-7b-5p, and miR-335-5p shared significant enrichments in Jak-STAT and insulin signaling pathways. TGF β pathway was significantly enriched in miR-335-5p and miR-148a-5p, with gene hits against 11 and 5 mRNAs in the pathway, respectively (**Figure 3.4B** and **Supplementary data E**). MAPK signaling pathway was significantly enriched for miR-355-5p only, but miR-16-5p and let-7b-5p had the highest number of target mRNA in the pathway (**Figure 3.4B**). Additional significantly enriched pathways from more than one miR included Wnt for miR-16-5p and miR-148a-3p, *E. coli* infection for miR-16-5p and let-7b-5p, chemokine signaling for miR-355-5p and miR-148a-3p, and apoptosis for miR-30a-5p and miR-148a-3p.

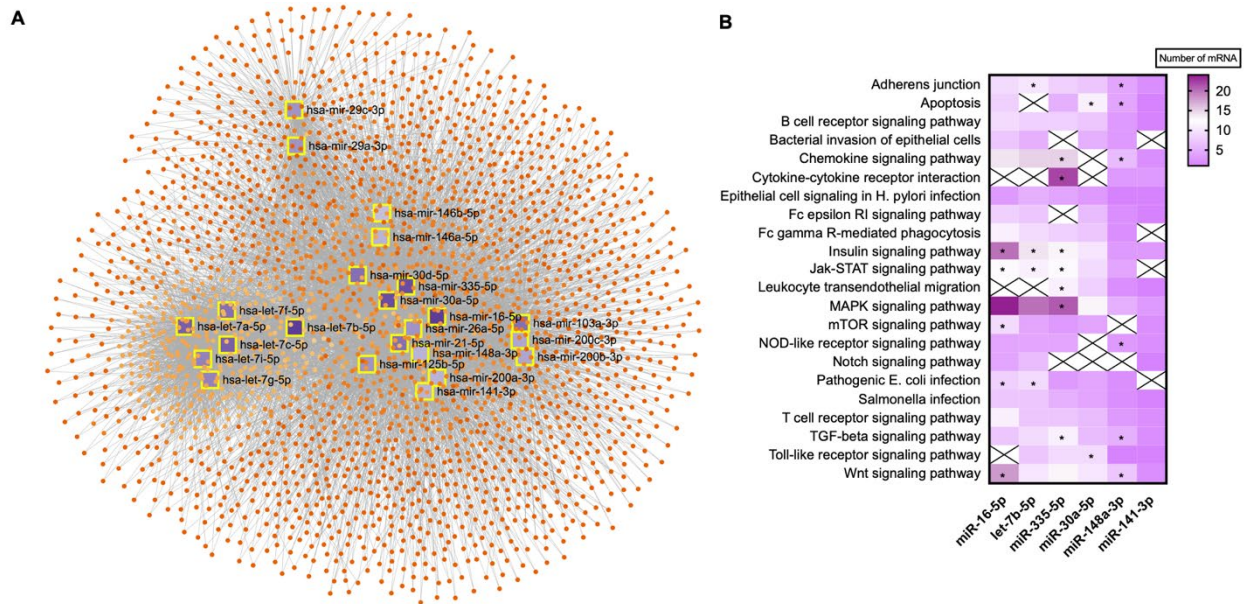


Figure 3.4. Targets and functional prediction of top 20 term and preterm human milk EVs. (A) Total of 2532 target mRNA were identified. miRNAs clustered based on their common targets. Number of total targets (degree) indicated by ascending purple fill of highlighted squares. mRNAs – orange circles. Degree constraint >2. (B) KEGG enrichment analysis of select miR targets. Top 4 miRNAs in degree score (miR-16-5p, let-7b-5p, miR-335-5p, and miR-30a-5p), and top 2 miRNAs from sequencing abundance (miR-148a-3p and miR-141-3p) were plotted. Select enriched pathways were chosen with a gradient representing number of allocated target mRNA, *p-value ≤0.05. miRNet analysis.

3. Gestational age-based miR differences

Next, differential expression of miRNAs was explored in term versus preterm samples. A total of 12 differentially expressed miRNAs was identified, of which six miRNAs were significantly up- and downregulated in term HM EVs (Table 3.1 and Figure 3.5A).

Table 3.1. Significant differentially expressed term or preterm HM EV miRs with log 2-fold change and adjusted p-value. Positive log 2-fold change indicates miR upregulation in term HM EVs.

miR	Log 2-fold change	Adjusted p-value
hsa-miR-409-3p	3.29	0.05
hsa-miR-381-3p	2.72	0.03
hsa-miR-31-5p	2.54	0.01
hsa-miR-708-5p	2.48	0.05
hsa-miR-383-5p	2.06	0.03
hsa-miR-382-5p	1.37	0.04
hsa-miR-33b-3p	-2.04	0.02
hsa-miR-122b-3p	-2.03	0.02
hsa-miR-100-3p	-1.99	0.03
hsa-miR-122-5p	-1.95	0.02
hsa-miR-1268a	-1.88	0.03
hsa-miR-1268b	-1.87	0.03

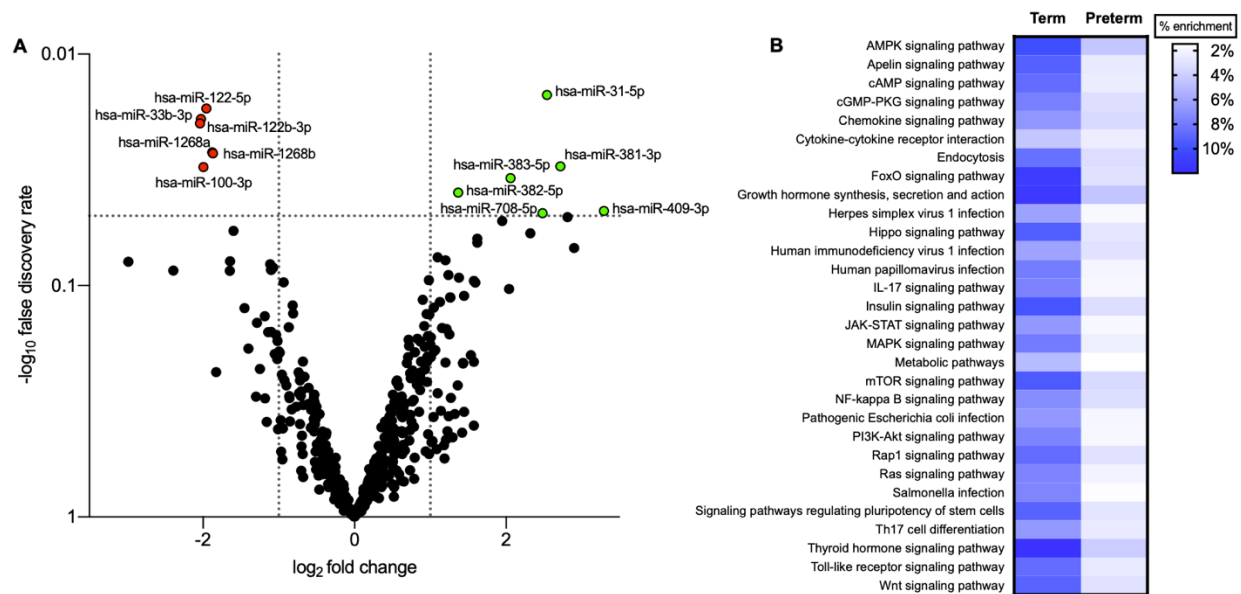


Figure 3.5. Differential expression analysis and functional enrichment of term and preterm human milk EV miRs. (A) Volcano plot of differentially expressed miRs. Twelve significant differentially expressed miRs are labeled ($p < 0.05$, $\log_2 FC < +/-1$), term versus preterm HM EV miRs, $n=3$. (B) KEGG target pathway prediction for significantly ($p < 0.05$) upregulated miRs in term and preterm HM EVs. Select immune and signaling-related pathways that were identified for both term and preterm HM EV miRs were plotted.

Notably, the significantly up- or downregulated miRs did not appear among the top 100 most abundant miRs for either condition (**Supplementary data A and F**). The significant differentially expressed miRs were subjected to target prediction and pathway analysis using miRabel. Upregulated miRs from term and preterm EVs had many common affected pathways, though the number of identified target genes and enrichment score for each pathway was lower in preterm (**Supplementary data F and Figure 3.5B**). Functionally, a variety of pathways were identified, with the strongest evidence for metabolic pathways as well as signaling pathways relevant to immune signaling, metabolic signaling and cell proliferation. Overall, term and preterm EV miR target genes shared several predicted pathways. Based on the differential expression analysis, term HM EVs appear to harbor RNA species with more abundant target genes when shared pathways are compared between the two GA groups (**Figure 3.5B**).

Individual lists of all miRs from term and preterm HM EVs were submitted to miRNet for total target prediction analysis. After filtering with a degree score of one, 11860 and 14593 target mRNAs were retained for term and preterm HM EV miRs, respectively. To include a higher potential of biologically relevant targets, a further constraint was applied with degree score of 20, which reduced the number of targets to 1856 for term and 1733 for preterm HM EV miRs. In the total pool of identified targets, term had 205 and preterm had 84 unique mRNA targets (**Supplementary data G**). When functional enrichments of unique mRNA in each group were compared, term had enrichments in nuclear related protein activity. A predicted target, β -catenin (CTNNB1), which is a key player in the Wnt signaling pathway²⁸⁸, displayed multiple interactions within the 205 unique mRNAs. 111 of the predicted mRNAs were phosphoproteins

and as such, had enrichments in signaling pathways. 38 out of 205 unique mRNAs were zinc-fingers, many implicated in transcriptional regulation (**Supplementary data G**).

Unique mRNA targets from preterm HM EV miRs had no significant functional enrichments. 52 out of 84 mRNAs categorized to phosphoproteins and 41 were nucleus related, indicating abundance of unique mRNA related to signaling and transcriptional regulation. Several of the miR target mRNAs were predicted to interact (**Supplementary data G**).

4. HM EVs contain miRs that are dysregulated in NEC intestinal tissue

Prior studies have indicated therapeutic potential for milk-derived miRs in colon epithelial cells and necrotizing enterocolitis models^{146,289}. To characterize GA-specific miRs sequenced here in a clinical context, we explored the overlap of significantly downregulated miRs in NEC-diagnosed infant intestinal tissue, and the abundance of those miRs in HM. Ng *et al.* reported differentially expressed miRs in NEC intestinal tissue versus surgical controls, with nine miRs significantly decreased in NEC tissue by 0.07-0.31 fold: miR-375, miR-203, miR-200b-5p, miR-194-3p, miR-200a, miR-215, miR-31, miR-192-3p and miR-141²⁷⁹. To investigate the presence of those miRs in HM, data was collated from select miR sequencing studies, when publicly available (**Table 3.2**). All significantly downregulated NEC miRs have been previously detected in several fractions of HM – cells, lipids, whey, and EVs, with miR-141, miR-200a, miR-200b, and miR-375 present among the top 10-100 most abundant miRs sequenced to date^{173,174,290,291}.

Table 3.2. Presence of select miRs in prior sequencing studies of human milk cells, lipids, or EVs. MiRs that were significantly downregulated in necrotizing enterocolitis were selected for screening.

NEC related miR	HM cells	Mature HM lipids	Mature HM lipids	Colostrum HM lipids	HM EVs
hsa-miR-141-3p	Y*#	Y*#	Y#	Y#	Y#
hsa-miR-141-5p	Y*	Y	N	Y	Y
hsa-miR-192-3p	Y*	Y*	N*	N	Y
hsa-miR-200a-3p	Y*#	Y*#	Y	Y#	Y#
hsa-miR-200a-5p	Y*#	Y*#	Y	Y	Y
hsa-miR-200b-5p	Y*#	Y*#	Y	Y	Y
hsa-miR-203a-3p	Y*	Y*	Y	Y	Y
hsa-miR-215-5p	Y*	Y*	N	Y	Y
hsa-miR-31-5p	Y*	Y*	N	Y	Y
hsa-miR-375-3p	Y*#	Y*#	Y*	Y#	Y*#
<i>Study reference #</i>	290	290	174	291	173

Y* - Yes, but without 3p or 5p specificity marked

N* - No, but present in 192-5p

- present in top 10-100 most abundant miRs

Many of the highly abundant miRs in HM have previously been reported without 3' or 5' specificity. Our sequencing data indicates significant abundance differences, with most 5' miR counts being absent or very low when compared to the 3' sequence. The opposite was detected for miR-31 and miR-192, where the 5' sequence was more abundant, and for miR-215, where the 3' miR was not identified in our sequencing results (**Supplementary data A**). Three miRs had the highest abundance among the NEC-relevant miRs – miR-375-3p, miR-200a-3p, and miR-141-3p (**Figure 3.6**). Term-specific differences were detected for miR-31-5p only, indicating an overall high degree of HM EV miR conservation among the NEC-relevant miRs (**Figure 3.6**).

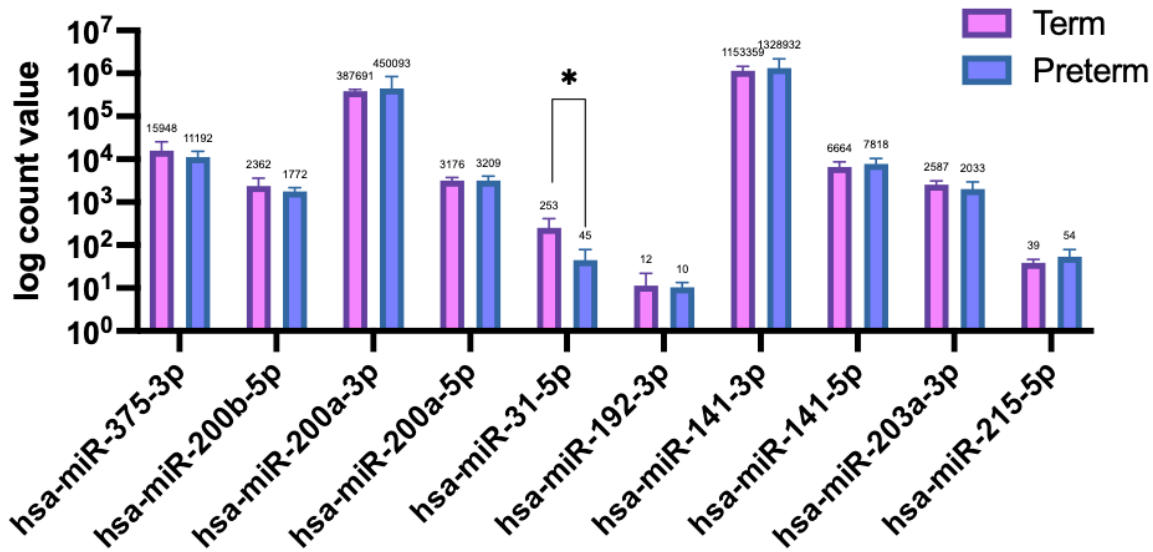


Figure 3.6. Abundance of candidate miRNAs in human milk EVs that are significantly downregulated in necrotizing enterocolitis. Differences in abundance were identified depending on 3' or 5' miR sequence for miR-200a, miR-141, and miR-215 for which the 3' miR was not identified in our sequencing. MiR-31-5p was significantly more abundant in term HM EVs. Top of error bar - average abundance value of three biological replicates, * $p < 0.04$, miRDeep2 analysis.

The three highly abundant miRNAs were selected for further target prediction and functional enrichment analysis. Mir-200a-3p and miR-141-3p had the most shared targets, while miR-375 had the largest number of targets (**Figure 3.7A**). Given the high abundance of the three miRNAs in HM, the immune-related mRNA targets shared by all three were further analyzed for functional enrichments. Leukocyte chemotaxis, cytokine production, mediation of immune response, regulation of programmed cell death, and metabolic process were among the significant functionally enriched pathways (**Figure 3.7B**).

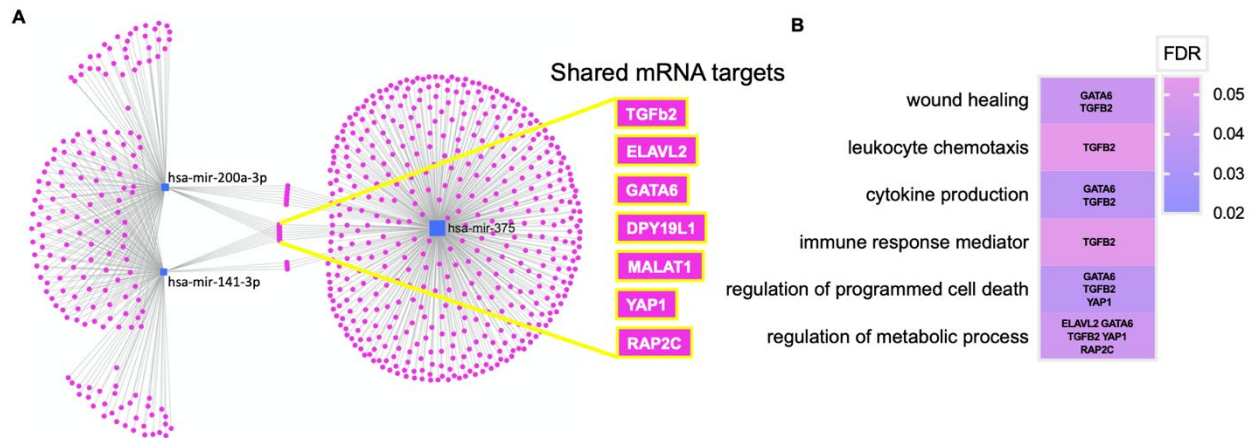


Figure 3.7. Targets and functional prediction of miRs significantly downregulated in necrotizing enterocolitis with high abundance in human milk EVs. (A) Three miRs with a total of predicted targets of 647 mRNA, of which seven were shared. miR-375 had the highest number of predicted target mRNA, indicated by size of blue rectangular box. Degree constraint >2. (B) Biological enrichment analysis of select miR targets. Select enriched biological processes were chosen with a gradient representing false discovery rate (FDR) ≤ 0.05 ; miRNet analysis.

We performed a comparative analysis with NEC-candidate miR targets and mRNAs that were significantly differentially expressed in NEC intestinal tissue, to assess potential overlap between genes. From Tremblay *et al.*, 382 genes that were significantly increased (fold-change >1) in NEC human tissue were selected along with predicted target genes for significantly downregulated miRs identified in NEC tissue^{279,292}. Between the two gene sets, 32 mRNAs were shared (**Figure 3.8A** and **Supplementary data H**), though not found to be significant (p value = 0.454). Out of the common mRNA, JAK2 and CCR5 had the highest significance among the differentially expressed genes in NEC. The predicted target for miR-375 was JAK2, and miR-203a-3p for CCR5 (**Figure 3.8A**).

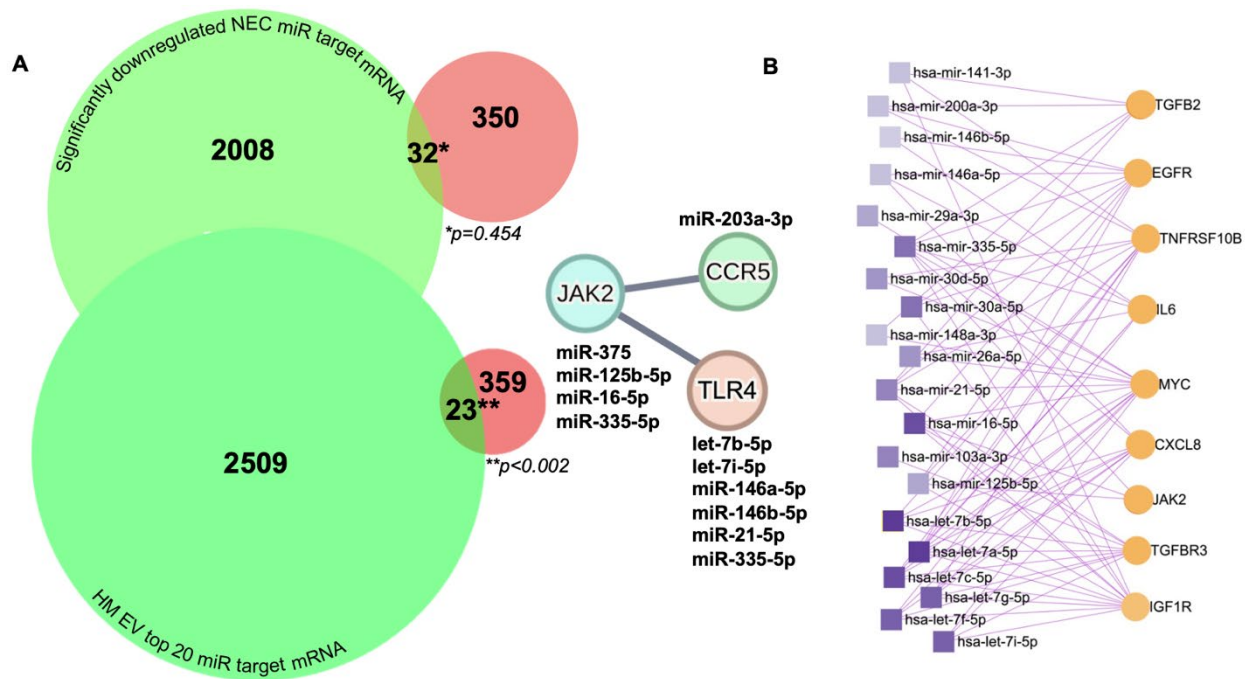


Figure 3.8. MiR target analysis of dysregulated mRNA in necrotizing enterocolitis intestinal tissue. (A) Significantly downregulated miRs in necrotizing enterocolitis (NEC) target 2034 mRNA (top green circle), and top 20 term and preterm HM EV miRs target 2532 mRNA (bottom green circle). Of the total mRNA targets, 32 and 23 overlap with significantly upregulated genes in NEC intestinal tissue (red circle), respectively. Common miR targets – JAK2, CCR5 and TLR4, formed high confidence interactions enriched in cytokine signaling (JAK2-CCR5) or leukocyte activation (JAK2-TLR4), STRING analysis, confidence score >0.7. (B) Select mRNA targets of top 20 most abundant miRs in human milk EVs. Targets include differentially expressed genes in NEC (JAK2, IL6, TGF, EGF, TNFRSF, CXCL, IGF) and signaling protein MYC, the highest targeted mRNA by total HM EV miR pool. MiRNet, degree constraint >2.

To investigate the targets of the most abundant HM EV miRs in the context of differentially expressed NEC mRNAs, the two gene sets were again compared to assess overlap (Supplementary data E and H). A total of 23 mRNAs were shared between the two groups with statistical significance when compared to the sequenced gene pool (p-value <0.002) (Figure 3.8A). While CCR5 was not among the predicted targets for the shared mRNA, JAK2 and toll-

like receptor 4 (TLR4) were targeted by several HM EV top 20 miRs: miR-125b-5p, miR-16-5p, miR-335-5p; and let-7b-5p, let-7i-5p, miR-146a-5p, miR-146b-5p, miR-21-5p, miR-335-5p, respectively (**Figure 3.8A**). Analysis of all the shared mRNA targets in STRING revealed that JAK2 formed high confidence interactions with both CCR5 and TLR4 that included significantly ($p < 0.05$) enriched pathways or biological processes in the immune system (**Figure 3.8A** and **Supplementary data H**).

A constraint was further added to the list of top 20 HM EV miR targets to visualize mRNAs that are differentially expressed in NEC intestinal tissue – JAK, IL6, TGF, EGF, TNFRSF, CXCL8, and IGF1. Also included was the gene most targeted by top 20 miRs – MYC, targeted by 14 out of the 20 most abundant miRs. The NEC relevant mRNAs were also multi-targeted by several miRs: 5 for TGF β 2, 9 for EGFR and TNFRSF10B, 3 for JAK2, 7 for IL-6, IL-6R, and CXCL8, 12 for IGF1R, 9 for TGFBR3 (**Figure 3.8B**). These findings reveal a miR interaction network predominantly targeting immune system-related genes, highlighting the potential effect of HM EV miRs in modulating NEC dysregulation.

3.5 Discussion

In this study, over 900 EV-contained miRs were identified from a cohort of mothers exclusively in a transitional lactation stage who delivered either term or preterm infants. The miRs had a high degree of conservation, with majority of the top 20 miRs identified in both groups. The abundance of miR-148a-3p, let-7f-5p and miR-141-3p significantly eclipsed the following top 100 miRs in both term and preterm EVs. The similarity of term and preterm miR profiles was demonstrated by differential expression analysis, where only 12 significant differentially

expressed miRs were found in both groups with overlapping functional enrichments in metabolic, immune, and signaling related pathways. While the 12 miRs were significantly up- or downregulated, the individual miR abundance was low when compared to the whole miR pool. When the miR targets between term and preterm EVs were compared, many of the mRNAs overlapped or were predicted to interact in conserved functional pathways, indicating that miRs could downregulate targets in a pathway in tandem or even concomitantly. Since the most abundant HM EV miRs are also conserved between species²⁰⁷, the likelihood of a retained biological effect for EV-contained miRs is increased for the significantly enriched biological processes and pathways identified in our analyses.

We have previously shown GA-specific differences in transitional HM EV protein and mRNA cargo, including in their corresponding functional enrichments, which may be due to differences in cellular origin for term and preterm HM EVs²⁷². Here we report a limited variation in the miR cargo targets and functional enrichments, but further investigation may elucidate whether distinct effects emerge depending on cell activation status or biological state.

It is notable that in both term and preterm HM EV miRs, the 3' or 5' miR abundance varied, especially in the 20 most abundant miRs. For example, while miR-141-3p was one of the most abundant miRs in HM EVs, its 5' counterpart was over 100-fold less abundant. Conversely, for miR-146b-5p, the abundance differed by 10-fold with the 3p sequence, with both miRs having either high or medium abundance when compared against the total miR pool (**Supplementary data A**). Though the biological relevance and functional implications of the strand-specific

differences remain to be elucidated, the information could be valuable for future therapeutic avenues to understand milk miR stability and functionality^{293–295}.

The most abundant miRs identified in transitional HM in this study, such as miR-148a-3p and let-7f-5p, have been previously found in HM EVs from varying lactation stages^{126,155,173,179,184,205}, and drastic differences in individual HM miR abundances have been reported¹⁷³. Following functional enrichment analysis of the top miR-148a-3p, let-7f-5p and miR-141-3p reported here, highest number targets were predicted to impact metabolic pathways. However, many signaling pathways were also implicated, including insulin signaling, which in the intestine, could be related to inflammation and immune response as recently demonstrated in a mouse model of inflammatory bowel disease (IBD)²⁹⁶. Relevant to intestinal maturation, significant enrichments in Wnt, mTOR, Ras, MAPK, and PI3K-Akt signaling pathways may impact intestinal cell proliferation and differentiation^{297–300}.

Several immune-related pathways were also functionally enriched, including bacterial infection, Th17-cell signaling, and innate immune system processes (TLR-responses). Most significantly impacted pathways involved TGF β , important for intestinal repair and anti-inflammatory processes in infants^{47,301}, and FOXO-signaling, which regulates development of regulatory T cells^{302,303}. The identification of TGF β -signaling enrichment by miRs was notable given the abundance of the cytokine in HM³⁰¹ and may point to an intricate feedback loop within the HM components. Development and regulation of these pathways are essential for all infants regardless of gestational age, though the dysregulation marked in gastrointestinal diseases is more associated with prematurity³⁰¹.

Given that HM EVs are proposed to survive digestion and could interact with intestinal epithelial and immune cells^{126,173}, we explored the role that miRs may play in the protection provided by HM feeding against NEC^{10,45,273,304}. Of the nine significantly decreased miRs in NEC intestinal tissue – miR-375, miR-203, miR-200b-5p, miR-194-3p, miR-200a, miR-215, miR-31, miR-192-3p and miR-141²⁷⁹, the majority were present and highly abundant in our data, and when queried against prior HM miR sequencing studies, they were also present at high levels in HM lipids, cells, and EVs^{173,174,290,291}. Circulating levels of miR-375 were affected by NEC diagnosis, indicating that as the disease develops, the miR expression is downregulated³⁰⁵. Reduced levels of miR-375 and miR-31 have also been reported in other intestinal disorders, such as IBD or celiac disease^{306,307}, which are characterized by their effects on inflammation and altered immune response. This suggests that the downstream effects of these reduced miRs may have profound impacts on inflammatory regulation in infants and lead to different diseases.

Although a limited number of samples were analyzed, it is interesting to note that miR-31-5p was significantly downregulated in preterm HM. An upregulation in miR-146a-3p and 5p, although not significant ($p < 0.07$ and 0.9 , respectively, **Supplementary data F**) was also detected. This variation may be important in intestinal maturation, which is especially vital for premature infants, and could be affected by miR-31 through the activation of Wnt pathway³⁰⁸, and by miR-146a, which has been implicated in epithelial regeneration through inflammasome control^{309–313}.

Relevant for premature infants and NEC pathogenesis, many of the HM EV-derived miRs characterized here bioinformatically, have been investigated in intestinal inflammation^{155,309,314,315}. The lack of milk EV-derived miR-200a-3p could lead to increased intestinal inflammation and upregulation of CXCL9 chemokine²⁷⁸, while miR-375-3p has been shown to downregulate inflammation in epithelial cells³¹⁶, and its consumption in milk may protect infants from developing allergies³¹⁷. MiR-141 inhibits both inflammation and necroptosis in intestinal epithelial cells, the former via TLR4 regulation^{318,319}. The most abundant miR-148-3p could promote M1 macrophage polarization and inhibit inflammation and protect tight junctions in intestinal epithelial cells via NF- κ B regulation^{155,314}. Through regulation of TLR4/NF- κ B, let-7d-5p has also been proposed to regulate experimental NEC in rats³²⁰. With TLR and NF- κ B being among significantly enriched pathways in our analyses (**Figures 3.3-3.5**), the most abundant miRs in HM EVs could jointly influence pathways relevant for NEC pathogenesis.

To explore the implications of miR-mRNA targeting, the previously identified 382 significantly upregulated genes in NEC intestinal tissue were compared with gene targets of significantly downregulated NEC miRs²⁹². Milk miRs could prevent or attenuate the dysregulation of the NEC-relevant mRNA, as the predicted multi-miR targets JAK2, IL6, TGF, EGF, TNFRSF, CXCL, and IGF1 overlap with NEC gene signatures.

Functional enrichment analysis of the three most abundant HM EV miRs – miR-200a-3p, miR-375, and miR-141-3p indicated that they may target pathways in leukocyte chemotaxis and cytokine production among others, with cytokine storm being a hallmark of NEC^{95,238}. IL-17

upregulation by Th17 cells is a proposed biomarker of NEC in neonates and has been suggested to exacerbate disease severity^{100,321}. HM EVs have been previously shown to modulate CD4+ T cell activation¹⁵⁹ and in our data, both IL-17 and Th17 related pathways were predicted to be significantly impacted by the three most abundant miRs (**Figure 3.3B**), but were also overall functionally enriched in the total EV-contained miRs (**Figure 3.5B** and **Supplementary data**).

Though a few studies have observed attenuation or prevention of severe intestinal inflammation following HM EV treatment, attributing this effect to a collection of, or individual miRs is a challenge. In this study, we found that regardless of the GA-status of the mother, miR targets were enriched in similar functional processes and pathways highly relevant to NEC. As a result of these bioinformatics analyses, we propose that in both term and preterm HM EVs, most abundant miRs could concomitantly affect pathogenesis of NEC and potentially shield against other inflammatory diseases. In healthy infants, the presence of the immunomodulatory miRs may support cell differentiation, including that of immune cells, and regulate immune response to microbiota. While HM contains abundant miRs, delivery to the intestinal lumen may be restricted to EV-contained miRs, thereby setting the stage for prevention of intestinal diseases. With premature infants especially at risk of severe and devastating intestinal diseases, the importance of EV-contained miR supplementation²⁸⁹ requires further investigation.

3.6 Materials and Methods

Milk collection and extracellular vesicle isolation

We have previously collected and characterized term and preterm HM EV samples discussed in this study²⁷². All HM samples in this study were collected from donors in accordance with ethics

protocols at the University of Ottawa, The Ottawa Hospital, and the Children's Hospital of Eastern Ontario, with Research Ethics Board approval (#H-03-20-5643). Donor exclusion criteria included caesarean birth, antibiotic use, and active maternal genetic, immune, and chronic inflammatory diseases. After obtaining written consent, 20 mL of milk was manually expressed by mothers into sterile tubes. The collected HM was classified as term (GA > 37 weeks) or preterm (GA < 37 weeks) from a total of six mothers (**Table 3.3**).

Table 3.3. Human milk donor information. Characteristics of mothers' milk donated within two weeks of term or preterm birth, n=3, each group. GA – gestational age at birth.

Donor #	Infant GA	Term (T) or preterm (PT)	Infant age (days)	Infant sex	Donor age (years)	Donor parity
107	39 weeks, 1 day	T	9	F	34	2
114	38 weeks, 1 day	T	6	M	33	1
117	40 weeks	T	11	F	34	0
10	34 weeks, 4 days	PT	9	M	36	0
24	24 weeks, 3 days	PT	14	M	22	0
32	29 weeks	PT	9	M	26	5

Fresh HM was transported to the lab within 30 minutes for EV isolation. The isolation method included differential and ultracentrifugation to remove milk fat, cells, and other contaminants. EVs were characterized for surface markers and size using the Exoview R100 instrument, and scanning electron microscopy was performed for morphology analysis²⁷².

miR sequencing and analysis

For RNA extraction, miRs were obtained using Qiagen miRNeasy kit (Qiagen, Germany) and RNA quality was assessed as formerly described²⁷². The miRs from term and preterm HM EV samples (n=3 for each group), were sequenced and analyzed at the McGill Genome Centre

(Montreal, Canada). MiR libraries were prepared with QIAseq miRNA Library Kit (Qiagen, Germany), and sequenced on Illumina NovaSeq 6000 with a sequence length distribution of 101bp and an approximate depth of 18-23 million reads per sample. To quantitatively identify miRs, including novel miRs, a Nextflow workflow tool of nf-core/smrnaseq small RNA sequencing analysis pipeline was utilized (version 2.1.0, last accessed December 13th, 2022)²⁶³.

Briefly, adapter sequences were trimmed and reads aligned to mature and hairpin miRs using Bowtie (version 1.3.1, last accessed December 13th, 2022). To obtain miR counts and perform sample clustering, SAMtools was utilized (version 1.15.1, last accessed December 13th, 2022). Reads were mapped against the human reference genome (GRCh38) followed by discovery of novel and known miR using miRDeep2 (version 1.3, last accessed December 13th, 2022). The miR counts were transformed to counts per million (CPM) and differential expression analysis was performed using edgeR³²²⁻³²⁴. Statistically significant and differentially expressed miRs were defined as log fold change $\geq 1/-1$, with a false discovery rate (FDR) value of < 0.05 .

The miR target predictions and functional enrichments were performed using publicly available tools: miRNet (<https://mirnet.ca/>, last accessed October 26th, 2023) and miRabel (<http://bioinfo.univ-rouen.fr/mirabel/>, last accessed February 16th, 2023)^{287,325}. For miRNet, filtering by degree scores between 2-50 was utilized to constrain the number of shared mRNA targeted by miRs. The predicted miR targets in miRabel were ranked by score to account for multi-database identification and experimental validation of targets. Following filtering and ranking, functional characterization was performed using KEGG or biological process enrichment analysis within the miRNet and miRabel framework. In miRNet, functional

enrichments were exported with corresponding statistical p-value. In miRabel, all functional enrichments were filtered to include those with an FDR of <0.05. Further functional characterization and enrichment of proposed miR targets were performed by using STRING database following default settings, unless otherwise described (last accessed January 16th, 2024)³²⁶. Additional graphing used GraphPad Prism 9 software (California, USA).

To assess overlap between sets of miR target mRNA, BioVenn web application was used to visualize proportional distribution of shared targets³²⁷, and an overlapstats package was used to calculate significance of shared targets (http://nemates.org/MA/progs/overlap_stats.html, last accessed January 16th, 2024).

3.7 Acknowledgements

We would like to thank Dr. Senthilkumar Kailasam at the Canadian Centre for Computational Genomics for assistance with small RNA sequencing. We are grateful to the support staff at The Ottawa Hospital, Monarch Centre, and Centretown Community Health Centre. Special appreciation goes to the team at the CHEO Research Institute, particularly NICU project lead coordinator Chantal Horth, along with research assistants Rebecca Grimwood and Denise Campuzano, for their invaluable contributions to patient recruitment and sample collection. This research was funded by the Canadian Institutes of Health Research: grant number PJT 162423 to J-F.B., E.F., and I.A.

3.8 Data availability

Supplementary data are available from the publisher.

Chapter 4. Effect of gestational-age specific extracellular vesicles on inflammation in intestinal and immune cells

Manuscript 3: Vahkal, B., Altosaar, I., Ariana, A., Jabbour, J., Pantieras, F., Daniel, R., Tremblay, E., Sad, S., Beaulieu, J.F., Côté, M., and Ferretti, E., 2024. Human milk extracellular vesicles modulate inflammation and cell survival in intestinal and immune cells. *Pediatric Research*. In press. ID: PR-2024-1001.

4.1 Preface

To gain insight into GA-based effects of HM EVs in cell culture, immune and intestinal epithelial cells were utilized in this study. This work follows the findings of the second manuscript, by connecting the effect of abundant miRs, their target genes and enriched pathways, to immune and cell death-related signaling. Here, differential regulation of cytokine expression and secretion was measured for term and preterm HM EVs, highlighting the unique responses of HM to newborn's GA.

This manuscript contains collaborative work between laboratories and authors. All the experimental data were analyzed and graphed by me. The HM was processed by me, Josie Jabbour, and Falia Pantieras. Imaging assistance was provided by Redaet Daniel. Intestinal epithelial cell treatments were performed by Dr. Tremblay in Dr. Beaulieu's laboratory at the University of Sherbrooke. Primary macrophage and THP-1 cell experiments were performed by me with support from Dr. Ariana and Dr. Sad. I wrote the original draft of the manuscript, with input from all co-authors.

Human milk extracellular vesicles modulate inflammation and cell survival in intestinal and immune cells

Brett Vahkal¹⁻², Illimar Altosaar¹, Ardeshir Ariana¹⁻², Josie Jabbour¹, Falia Pantieras¹, Redaet Daniel¹⁻², Éric Tremblay³, Subash Sad¹⁻², Jean-François Beaulieu^{3*}, Marceline Côté^{1-2*}, Emanuela Ferretti^{4*}

¹University of Ottawa, Department of Biochemistry, Microbiology and Immunology, Ottawa, ON, K1H 8M5, Canada

²Ottawa Centre for Infection, Immunity, and Inflammation, Ottawa, ON, K1H 8M5, Canada

³Université de Sherbrooke, Department of Immunology and Cell Biology, Sherbrooke, QC, J1H 5N4, Canada

⁴Children's Hospital of Eastern Ontario, Department of Pediatrics, Division of Neonatology, Ottawa, ON, K1H 8L1, Canada

*Co-corresponding authors

4.2 Abstract

Human milk contains extracellular vesicles (EVs) that carry bioactive molecules such as microRNA, to the newborn intestine. The downstream effects of EV cargo on signaling and immune modulation may shield neonates against inflammatory diseases, including necrotizing enterocolitis. Premature infants are especially at risk, while human milk-feeding may offer protection. The effect of gestational-age specific term and preterm EVs from transitional human milk was characterized on human intestinal epithelial cells (HIECs and Caco-2), primary macrophages, and THP-1 monocytes. We hypothesized that term and preterm EVs differentially influence immune-related cytokines and cell death. We found that preterm EVs were enriched in

CD14 surface marker, while both term and preterm EVs increased epidermal growth factor secretion. Following inflammatory stimuli, only term EVs inhibited secretion of IL-6 in HIECs, and reduced expression of pro-inflammatory cytokine IL-1 β in macrophages. Term and preterm EVs inhibited secretion of IL-1 β and reduced inflammasome related cell death. We proposed that human milk EVs regulate immune-related signaling via their conserved microRNA cargo, which could promote tolerance and a homeostatic immune response. These findings provide basis for further studies into potential therapeutic supplementation with EVs in vulnerable newborn populations by considering functional, gestational age-specific effects.

4.3 Introduction

Human milk (HM) feeding has been shown to safeguard against infant inflammatory gut diseases, including necrotizing enterocolitis (NEC), which disproportionately affects premature neonates¹⁰. The mechanisms underlying this protection remain poorly understood⁴⁵. The vulnerability of neonates to NEC is partially due to an inefficient response to T-cell-dependent antigens, weak Th1 and antibody responses, and an impaired innate immunity. As a result, neonates have a high mortality rate under increased pathogen exposure⁶⁰. HM-contained extracellular vesicles (EVs) have been proposed as potential protective shields. Recent studies in immune cells have indicated a crucial role for HM EVs in immunoregulation^{137,159}.

In a previous study, CD4⁺ T cell activation was inhibited in response to treatment with HM EVs¹⁵⁹. This transient suppression may be crucial for preventing excessive immune activation, thus promoting tolerance to foreign antigens¹⁵⁹. In a separate study, macrophages were shown to take up milk EVs and could have altered growth and proliferation as a result of treatment²².

In neonates, macrophages are present in mid-gestation^{328,329} and may contribute to the cytokine storm commonly seen in NEC^{95,238}. Neonatal sepsis and NEC are characterized by infiltrating macrophages and secretion of inflammatory cytokines^{330,331}. A dose-dependent increase in pro-inflammatory cytokine expression was recently demonstrated in porcine macrophages following treatment with goat milk EVs³³², while protection against inflammation was seen in murine macrophages stimulated with bovine milk EVs¹³⁷. Additional findings of HM EVs being bioavailable, and bovine milk EVs restoring epithelial and immune cell barriers in the intestine of C57BL/6J mice¹³⁷, support the prospect of HM EVs regulating immune responses in breastfed neonates.

While controlling cytokine responses is important for the newborn's immune system, regulation of immune cell activation and death is also critical. Overwhelming sepsis, both a risk factor and a potential critical endpoint for NEC⁹⁵, may be mediated by pyroptosis, a programmed cell death mechanism that is induced by activation of the inflammasome³³³. The inflammasome-induced pyroptotic cell death is partially responsible for maintaining intestinal microbial homeostasis and is tightly controlled. In response to danger signals, such as pathogenic bacteria and its outer membrane component lipopolysaccharide, pro-inflammatory cytokine IL-1 β , along with other cytokines, is upregulated in both antigen-presenting and epithelial barrier cells³³⁴. While multiple inflammasome blocking strategies have been trialed in animal models, inhibition of IL-1 β and IL-18, two markers of pyroptosis, have conferred protection against sepsis^{334,335}.

The timing of infant's birth at term (>37 weeks of gestation) or preterm (<37 weeks of gestation)¹⁹⁶ may influence the composition of mother's milk and EV cargo within^{171,201,336}. The

composition of mothers' milk can vary further based on the stage of lactation, which can be divided into colostrum, expressed within the first 72 hours post-birth; transitional milk, which is secreted within the first two weeks and up to one month post-birth; and mature milk, which is expressed from one month post-birth⁵. We, and others, have reported significant differences in the HM protein, lipid, and microRNA (miR) levels^{144,173,191,225,272}, while preterm HM EVs have been found to have a greater impact on cell proliferation and migration in intestinal injury compared to term EVs¹⁴⁴. However, only a limited number of studies have investigated the effects of gestational age-specific EV preparations on human immune cells or animal models of NEC, and characterized the miRs or proteins contained within these EVs^{144,173}, highlighting the need for further research in the context of intestinal inflammation.

To investigate the potential for gestational-age specific transitional HM EVs to regulate immune response, the impact on cytokine expression, secretion, and cell death were characterized. We hypothesized that the inflammatory response in human gut epithelial cells, primary macrophages, and in a leukemia monocytic cell line, THP-1 cells, differs following pre-treatment with term or preterm HM EVs. First, surface markers of term and preterm EVs were characterized. Then, cells were treated with HM EVs prior to inflammatory activation with heat-killed bacteria, or a low dose of LPS. We measured differential regulation of several key cytokines, while both term and preterm HM EVs reduced secretion of IL-1 β in macrophages. We proposed HM EV miR cargo as an effector, wherein the most abundant miRs were conserved between donors. These findings could have implications for improved nutrient supplementation for vulnerable neonates as well as support the development of novel therapeutic interventions for intestinal inflammatory diseases.

4.4 Results

1. HM donor characteristics

Transitional HM from a total of 45 donors was collected and processed for EV isolation. An overview of the HM donor and infant characteristics can be found in Table S1. Per gestational age, 23 HM samples were obtained following preterm birth, and 22 following term birth. The infants' gestational ages ranged from 23 to 41 weeks. In the total cohort, mothers gave birth to 28 (57.1%) male infants, while 21 (42.86%) were female. Four donors with twin births included both male and female infants, while three of the four twin births were preterm. The age of the HM donors ranged from 22 to 44 years, with a median age of 30 years (**Table S1**).

2. HM EVs are enriched in immune-related surface markers

Following isolation, EVs were first characterized based on surface expression of canonical EV markers CD9, CD63, and CD81 using super-resolution imaging (**Figure 4.1**). As expected, majority of the vesicles were triple positive for CD9, CD63, and CD81 surface expression (**Figure 4.1C and G**). We have previously measured an enrichment in immune cell markers for preterm HM EVs, wherein CD14 was present in our proteomics analyses²⁵, thus CD14 surface expression was also explored on both term and preterm EVs (**Figure 4.1A-C and E-G**). CD14 was detected in 848 out of 3261 vesicles in term HM EVs (**Figure 4.1C**), and 942 out of 2841 vesicles in preterm EVs (**Figure 4.1G**). Two term and three preterm HM EVs were single positive for CD14, indicating limited background signal and further confirming the presence of CD14 alongside CD9, CD63 and CD81 surface markers (**Figure 4.1C and G**). Following particle size analysis to measure the size distribution of the EVs, the mean diameters for term

and preterm HM EVs were 188nm and 161nm, respectively (**Figure 4.1D and H**).

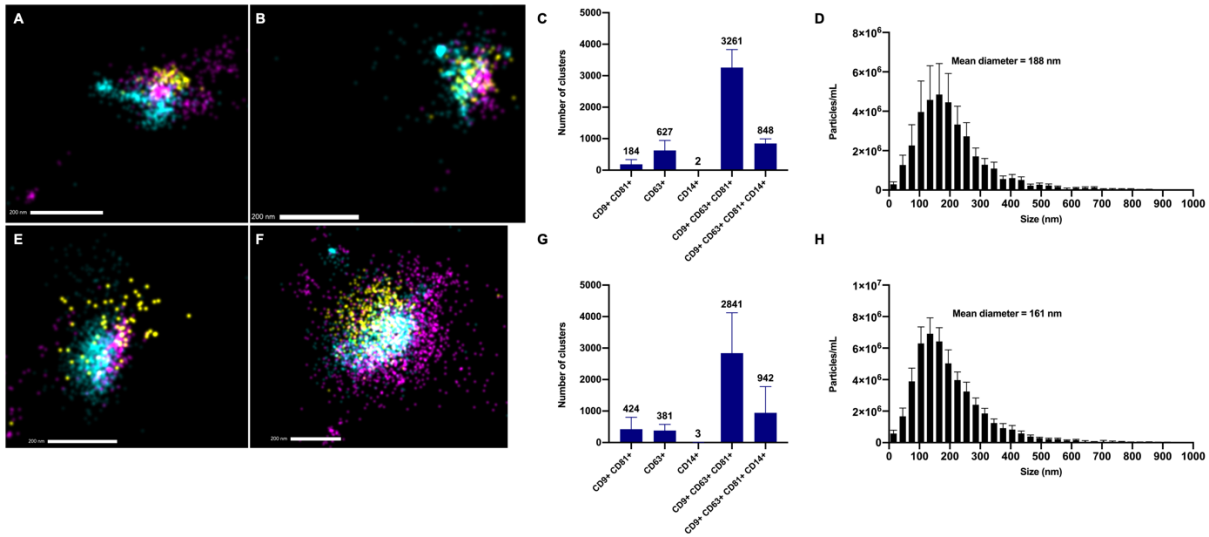


Figure 4.1. Characterization and super-resolution imaging of CD9, CD63, CD81, and CD14 HM EV surface markers. Term (A-C) and preterm (E-G) HM EVs are positive for CD14 (yellow); in addition to canonical EV markers CD63 (cyan), 81 and 9 (purple). The positive fluorescence signal per cluster of EVs did not differ significantly between term (C) and preterm (G) EVs. $n=2$, term and preterm HM EVs. Histograms represent average from three fields of view per sample. (D and H) Particle size distribution measured using Zetaview. The mean EV diameter was 188 nm for term (D) and 161 nm (H) for preterm HM EVs, $n=8$.

We subsequently evaluated the CD14⁺ signal on term and preterm EVs, in a surface marker panel. Surface marker analysis was performed on term and preterm HM EVs using Miltenyi MACSPlex Exosome Kit, which measured fluorescence intensity of 37 surface epitopes using flow cytometry. Term and preterm EVs clustered together based on detectable surface markers (**Figure 4.2A**). Besides the canonical EV markers CD9, CD63 and CD81, term or preterm HM EVs were positive for ROR1, HLA-DR, DP,DQ, HLA-ABC, CD326, CD146, CD133/1, CD105, CD86, CD45, CD44, CD40, CD29, CD24, CD14 and CD4 (**Figure 4.2B**). A statistically significant difference between term and preterm samples was measured for CD14 only, where

preterm had higher levels of CD14. No other significant differences among surface marker levels were detected.

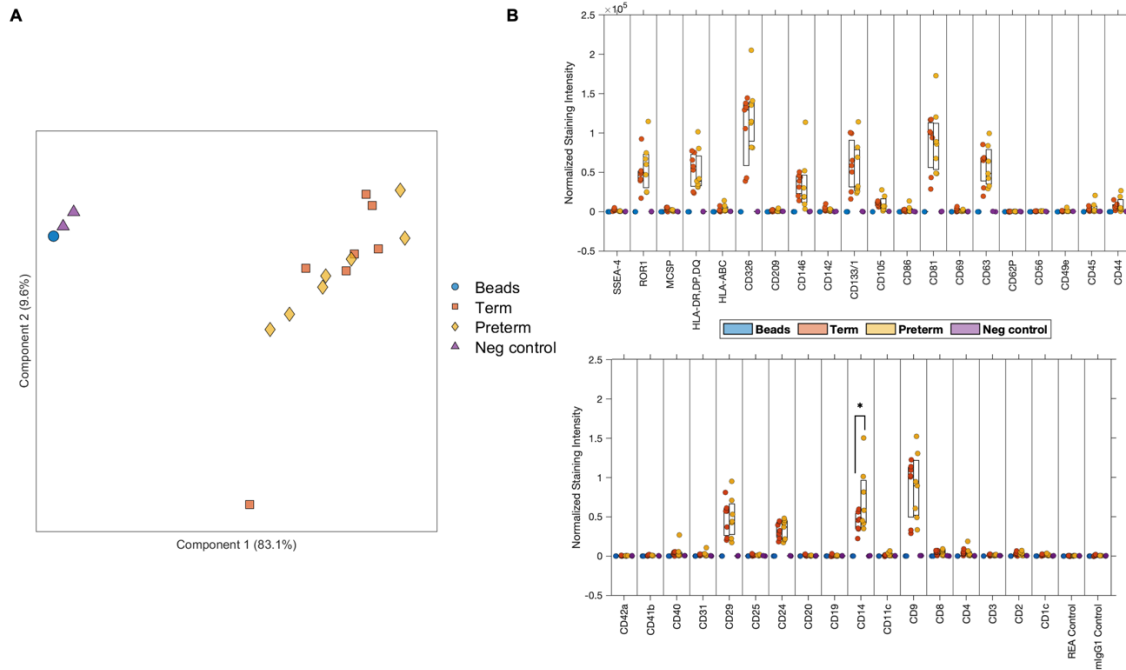


Figure 4.2. HM EV surface marker characterization. (A) Clustering of term and preterm HM EVs using principal component analysis ($n=7$), negative control, and capture beads only control ($n=2$). (B) Following background normalization, HM EVs expressed surface markers ROR1, HLA-DR,DP,DQ, HLA-ABC, CD326, CD146, CD133/1, CD105, CD86, CD45, CD44, CD40, CD29, CD24, CD14, and CD4, in addition to canonical EV markers CD9, 63 and 81. $n=2-7$, $*p<0.04$, Welch's t -test.

3. HM EVs induce protective signals and regulate inflammatory cytokines in human intestinal epithelial cells

Confluent Caco-2 cell culture was used to model infant intestinal epithelium since Caco-2 cells 20-days post differentiation exhibit similar morphological and functional characteristics to human mid-gestation small intestinal villus enterocytes³³⁷⁻³³⁹. When cells were treated with term

HM EVs for 24 hours, Caco-2 cell viability was increased at treatment concentrations of 20µg/mL and 40µg/mL. Statistical analysis using two-way ANOVA found an overall significant difference in viability across six and 24 hours ($DF_{1,13}$; $F=28.09$; $p<0.04$), and when combined with treatment ($DF_{2,13}$; $F=6.458$, $p<0.01$), wherein post-hoc analysis revealed that treatment with 20µg/mL of EVs significantly increased cell viability when compared to control at 24 hours (**Figure 4.3A**).

To further investigate if a protective effect of HM EVs on intestinal cells was induced, epidermal growth factor (EGF) levels in cell media were measured. Treatment of Caco-2 cells with term or preterm HM EVs significantly increased levels of EGF, regardless of inflammatory activation with heat-killed bacteria (**Figure 4.3B**). Treatment with term HM EVs resulted in significantly higher EGF levels when compared to preterm HM EVs.

Since CD14 is proposed to facilitate homeostatic immune response in infants³⁴⁰, and Caco-2 cells have been shown to express CD14, as well as release and take up soluble CD14 (sCD14)^{341,342}, we sought to characterize CD14 levels in response to term or preterm HM EV treatment. Caco-2 surface expression of CD14 was analysed using flow cytometry. Surface expression of CD14 was elevated following both term and preterm HM EV treatment, but significantly increased by preterm HM EVs (**Figure 4.3C**). When soluble CD14 levels were measured in cell media, both

term and preterm HM EVs significantly increased secretion of sCD14 regardless of inflammatory activation by heat-killed bacteria (**Figure 4.3D**).

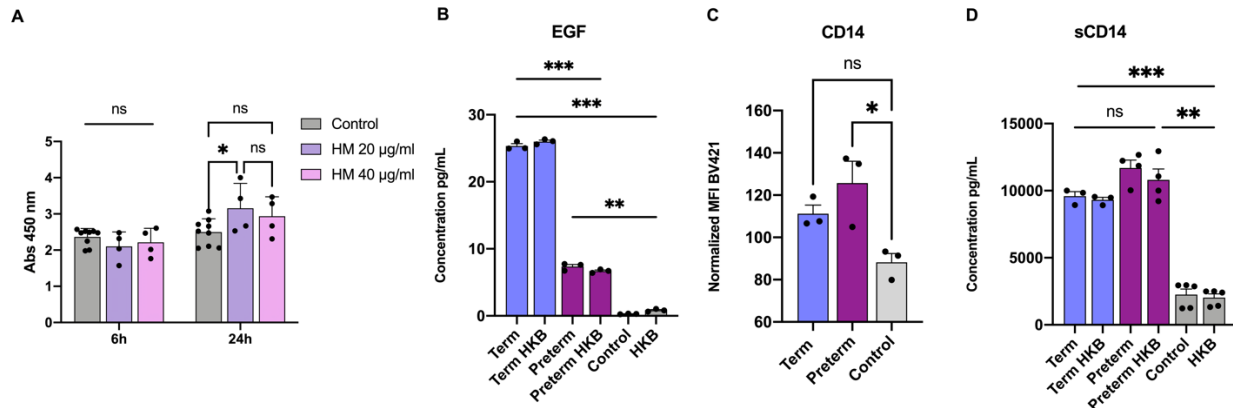


Figure 4.3. Effects of HM EVs on Caco-2 intestinal cells. (A) Cell viability following treatment with term HM EVs, or media only control for 6 or 24 hours. Viability measured with XTT assay - absorbance (450nm), $n=4-9$, $*p<0.04$, two-way ANOVA with Tukey's test, two replicate experiments. (B) EGF levels in cell media following inflammatory activation with heat-killed bacteria (HKB, 10^9 HKU) on cells treated for 22h with term or preterm HM EVs ($20\mu\text{g/ml}$), or media only control. Regardless of inflammatory activation with HKB, both term and preterm HM EVs significantly increased levels of EGF. Term HM EVs resulted in significantly higher levels when compared to preterm, $n=3$. (C) CD14 surface expression normalized to HKB treatment, median fluorescence intensity (MFI) of BV421, $n=3$, $ns: p=0.09$. Plot is representative of two replicate experiments. (D) Soluble CD14 levels in media were significantly increased by term and preterm HM EVs, regardless of inflammatory activation with HKB, $n=3-4$. $***p<0.001$, $**p<0.01$, $*p<0.04$, ns =non-significant, one-way ANOVA.

To investigate inflammatory markers on intestinal epithelial cells, a normal non-transformed cell line, human intestinal epithelial cells (HIECs), were used for further experiments. HIECs are normal embryonic human intestinal cells³³⁸, which have been used to study endocytosis of HM EVs and miR cargo^{126,173}, and inflammatory response³⁴³⁻³⁴⁵.

Following inflammatory activation with heat-killed bacteria, pre-conditioning with term and preterm HM EVs reduced expression of IL-8 and TNF α (**Figure 4.4C and F**). Term HM EVs decreased expression of IL-1 β , while increasing IL-6 expression. Conversely, preterm HM EVs increased IL-1 β mRNA transcripts, but had no significant effect on IL-6 expression (**Figure 4.4A-B**). TGF β 2 and IL-10 expression was not significantly affected by either treatment (**Figure 4.4D-E**). JAK2 expression was significantly reduced following term HM EV treatment alone. Following addition of heat-killed bacteria, both term and preterm HM EVs decreased JAK2 expression (**Figure 4.4G**).

On the protein level, secretion of IL-6 and IL-8 in response to term or preterm HM EVs had significant differences between the two gestational ages (**Figure 4.4H**). In the absence of heat-killed bacteria, term HM EVs had no effect on IL-6 levels in HIECs when compared to control, while preterm HM EVs significantly increased levels. When heat-killed bacteria were added, term HM EVs maintained IL-6 levels similar to control, while preterm HM EVs had no effect (**Figure 4.4H**).

Though HM EVs affected IL-8 expression, the cytokine secretion in HIEC media was unaffected. Notably, the biological variance among individual HM EV donors was high (**Figure 4.4I**). Overall, both term and preterm HM EVs modulated cytokines in HIECs, while only term samples downregulated IL-1 β expression and IL-6 secretion.

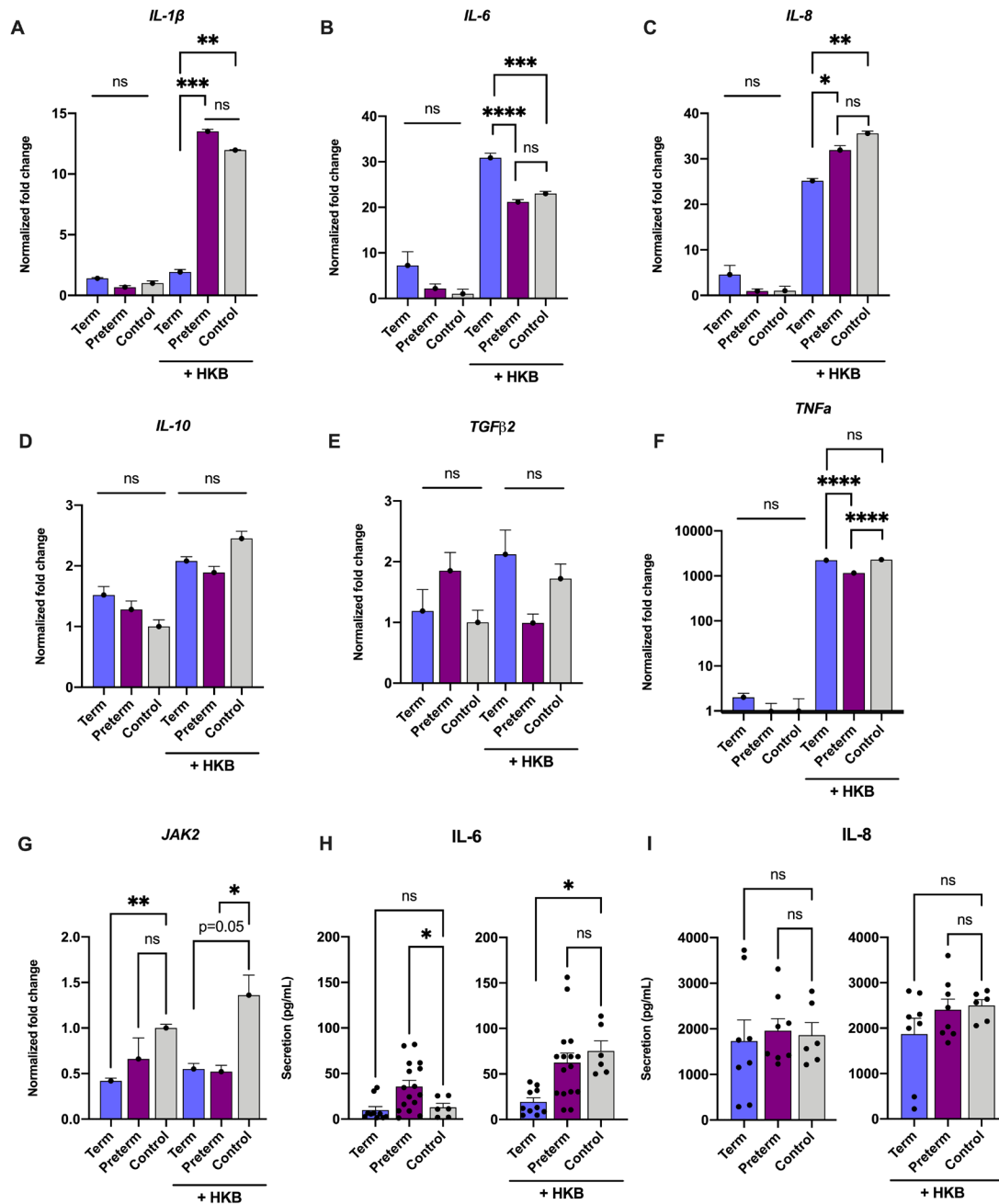


Figure 4.4. HM EVs regulate expression and secretion of cytokines and signaling proteins in human intestinal epithelial cells. Cells were treated with 20µg/mL term or preterm HM EVs, followed by inflammatory activation with heat-killed bacteria (HKB, 10⁹ CFU). **(A-G)** Gene expression relative to no treatment control of media only (y=1). **(H-I)** Secretion of IL-6 and IL-8 following treatment. n=6-16, in replicate experiments. ****p<0.0001, ***p<0.001, **p<0.01, *p<0.04, ns=non-significant, one-way ANOVA with multiple comparisons.

4. HM EVs downregulate inflammatory markers and cell death in human macrophages and monocytes

Prior to downstream analyses, HM EV uptake into THP-1 macrophages was visualized to determine a sufficient timeframe for EV uptake. HM EVs were taken up as early as two hours post-treatment when visualized with live cell imaging over the course of four hours (**Figure S1A**). Using confocal imaging, 6.5 hours post-treatment, EVs were taken up into endosomal and lysosomal compartments overlapping concomitantly with dextran on the intracellular periphery (**Figure S1B-E**).

To test the effect of HM EVs on inflammatory regulation in immune cells, macrophages were pretreated with term or preterm HM EVs alone or followed by LPS for inflammatory activation. Treatment with LPS increased the expression of IL-1 β , IL-6, IL-8, IL-18, and TNF α between two to 2000-fold in the macrophages (**Figure 4.5**). In the presence of LPS, both term and preterm HM EVs significantly reduced the expression of IL-6, IL-18, and TGF β 2 (**Figure 4.5B, D-E**). Preterm HM EVs upregulated expression of IL-1 β and IL-8, while expression of the cytokines was significantly inhibited by term HM EVs (**Figure 4.5A and C**). Expression of TNF α was significantly increased by both term and preterm HM EVs, when compared to control (**Figure 4.5F**). In the absence of LPS, IL-6 expression was upregulated by term HM EVs, and IL-8 expression was significantly increased by preterm HM EVs (**Figure 4.5B-C**). JAK2 expression was not significantly altered in control conditions, whereas following addition of LPS, both term and preterm HM EVs significantly reduced expression (**Figure 4.5G**). In a

cytometric bead array, secretion of IL-6, IL-8, IL-10 and TNF α was not significantly altered by HM EV pre-treatment (**Figure S2**).

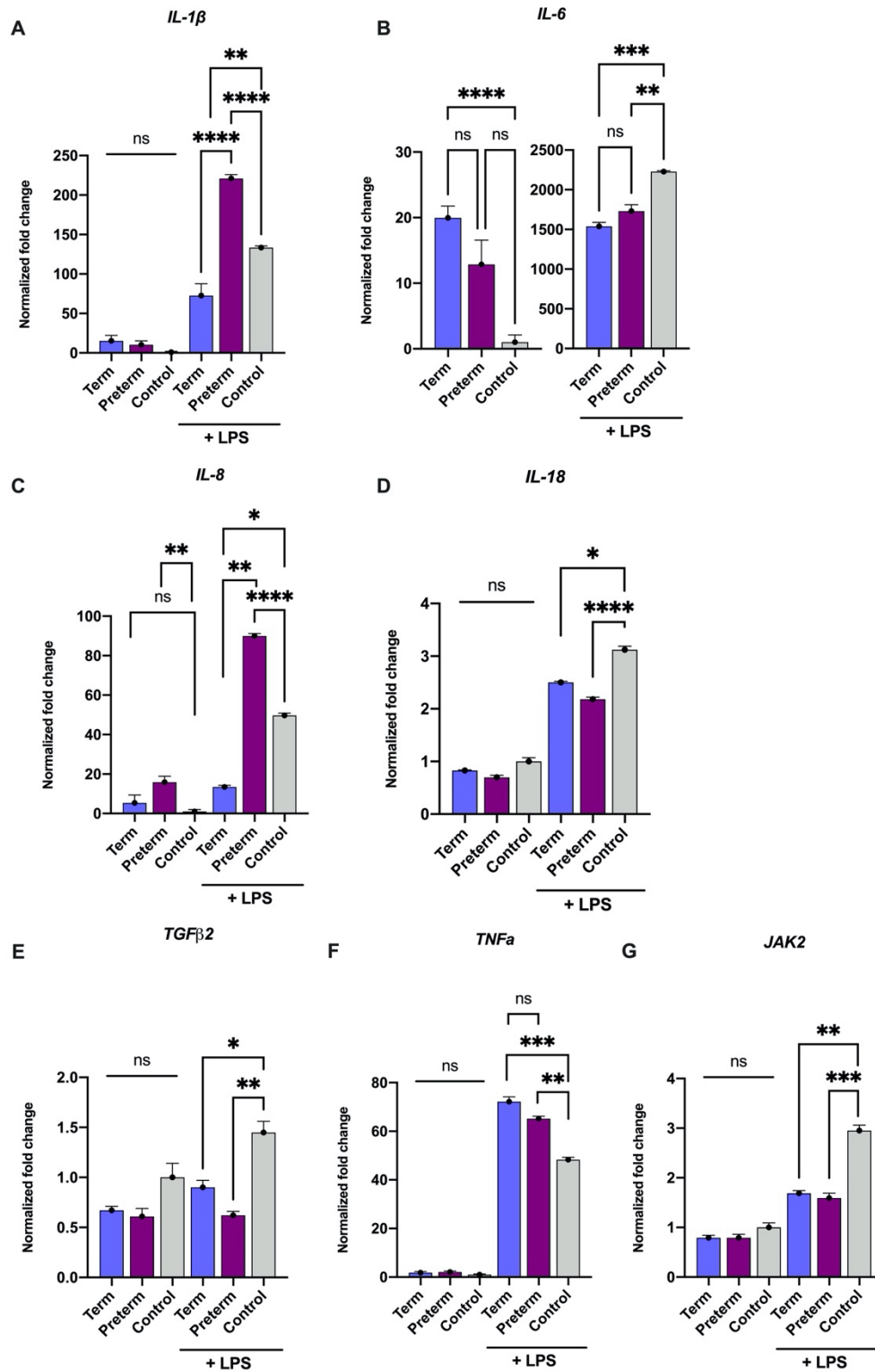


Figure 4.5. HM EVs regulate expression of cytokines and signaling proteins in macrophages. Cells were pre-treated with 40 μ g/mL term or preterm HM EVs, followed by inflammatory

*activation with LPS (1ng/mL). Gene expression relative to no treatment control of media only ($y=1$), $n=4-9$, in replicate experiments. **** $p<0.0001$, *** $p<0.001$, ** $p<0.01$, * $p<0.04$, ns=non-significant, one-way ANOVA with multiple comparisons..*

After measuring significant up-and down-regulation of IL-1 β expression, we measured secretion levels using ELISA. Following both term and preterm EV treatment and inflammatory activation, IL-1 β secretion was significantly decreased (**Figure 4.6A**). Macrophages can secrete IL-1 β via a pattern recognition receptor known as NLRP3 (NOD-like receptor (NLR) family pyrin domain-containing 3), which leads to inflammasome activation³³³. Since HM EVs regulated IL-1 β expression and secretion, we explored whether the expression of proteins of the inflammasome complex were affected. Following treatment, gene expression of the inflammasome-associated AIM-2, Caspase-1, and Gasdermin D were generally unaffected by both term and preterm HM EVs, while NLRP3 expression was significantly increased. Notably, preterm HM EVs increased expression of NLRP3 more than term HM EVs (**Figure 4.6B**).

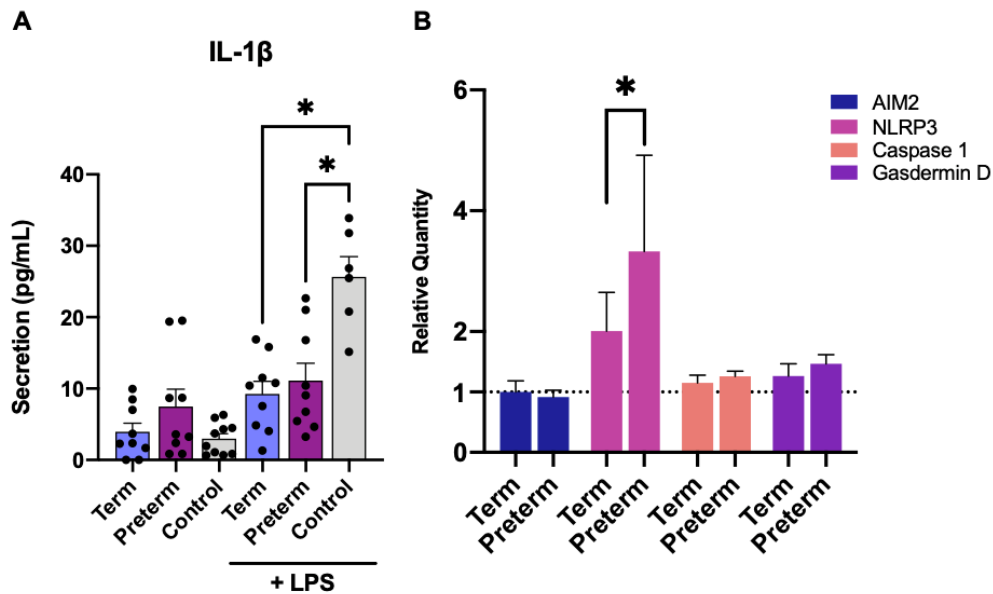


Figure 4.6. Term and preterm HM EVs regulate inflammasome in macrophages. (A) Secretion of inflammasome marker IL-1 β was measured using ELISA in human PBMC-derived macrophages after pre-conditioning with 40 μ g/mL preterm or term HM EVs for six hours, then inflammatory activation with LPS (1ng/mL) for two hours, or media only control. $n=6-9$, replicate experiments. $*p<0.04$, one-way ANOVA. **(B)** Expression of NLRP3 inflammasome related genes NLRP3, AIM-2, Caspase 1, and Gasdermin D. Gene expression relative to LPS treatment. Gene expression below line at $y=1$ on graph represents downregulation of expression. Treatment with both term and preterm EVs had limited effect on expression when compared to control for all genes except NLRP3. NLRP3 expression was significantly increased by preterm HM EVs when compared to term. $n=3$, $*p<0.04$, one-way ANOVA with multiple comparisons.

Following effects on IL-1 β and IL-18, both markers of the inflammasome, we sought to indirectly measure the effect of HM EVs on inflammasome-induced cell death. For an established and mechanistic analysis of inflammation in immune cells, the THP-1 human leukemia monocytic cell line was used³⁴⁶. We followed a previously published method for priming THP-1 monocytes with LPS, followed by pyroptosis-induction using nigericin³⁴⁷. We found that while HM EVs induced low levels of cell death when compared to media alone

(**Figure 4.7A**), they also significantly inhibited death induced by LPS and nigericin (**Figure 4.7B**). Since we observed large biological variability in the HM EVs' ability to attenuate cell death, we compared control and treated-groups for individual HM EV donor responses. Several samples that elicited an initial cell death response in the absence of inflammatory stimuli, also inhibited large-scale cell death when later treated with LPS and nigericin, suggesting the presence of a tolerogenic response. This effect was seen following treatment with both term and preterm HM EVs (**Figure 4.7C-D**).

To gain insight into the HM EV cargo, by delineating which components may exert the cellular effects, we used Ingenuity Pathway Analysis (IPA, Qiagen) to investigate downstream targets of HM EV miRs. The most abundant term and preterm HM EV miRs, sequenced previously (**Table S3**), were predicted to directly target the IL-1 family, including IL-1 β and IL-18, Gasdermin D, as well as members upstream of the inflammasome pathway: TLR4, MYD88, and NEK7³⁴⁸ (**Figure 4.7E, Figure S3, Table S4**). Relevant for classical apoptotic cell death³⁴⁹, HM EV miRs were also predicted to target Caspase-3 and -9, BCL-2, BAX, and BAK (**Table S4**). However, only term HM EVs exhibited protective effects in THP-1 monocytes against etoposide-induced apoptosis (**Figure 4.7F**).

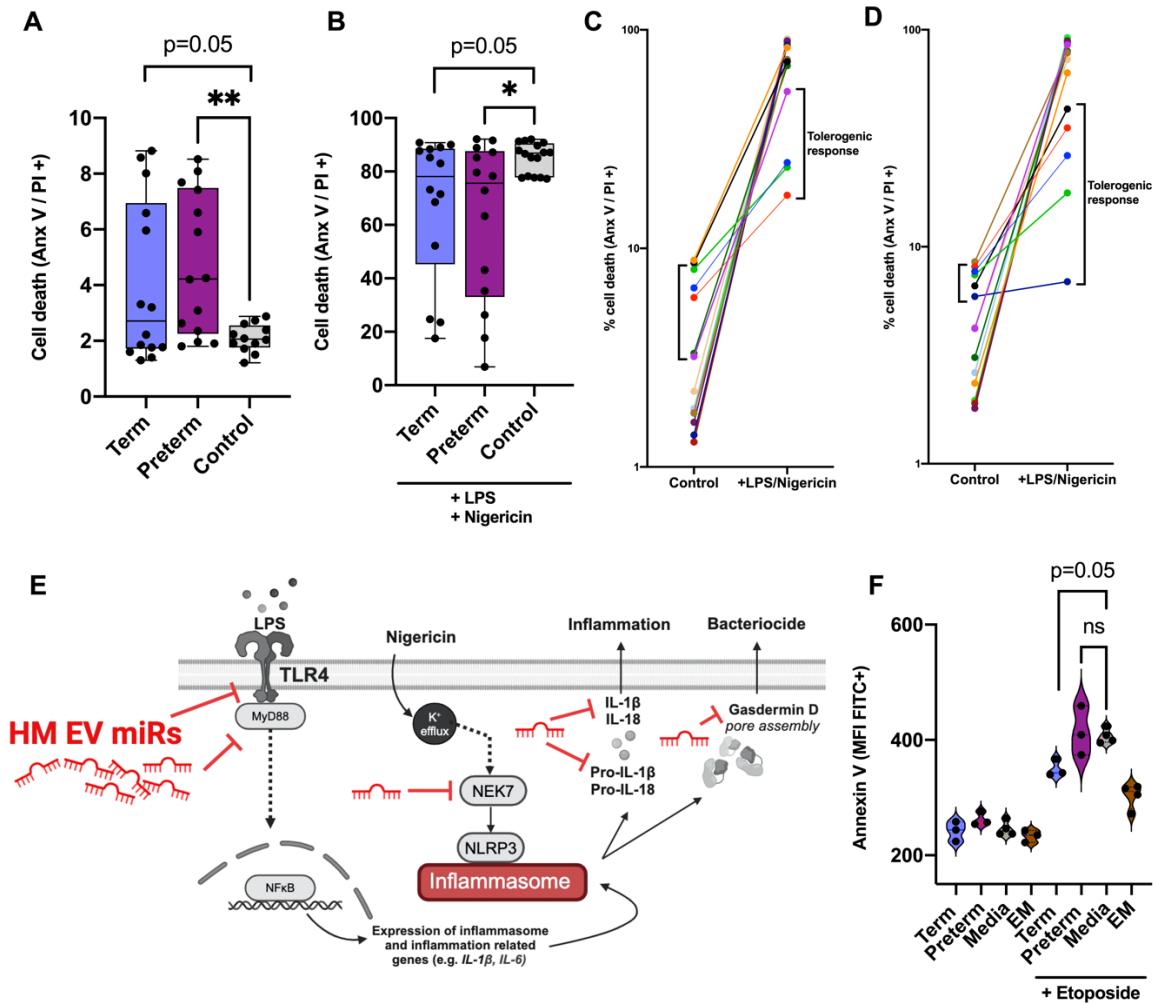


Figure 4.7. HM EVs regulate cell death in THP-1 monocytes. Cells were treated with 40µg/mL term or preterm human milk EVs for 6 hours, followed by inflammatory activation with 1ng/mL LPS for two hours, and 10µg/mL nigericin for 1 hour. Cell death was measured in THP-1 cells treated with (A) term or preterm HM EVs, or media only control; (B) term or preterm HM EVs with LPS and nigericin, or LPS and nigericin alone. Protection against nigericin and LPS induced pyroptotic cell death was measured by flow cytometry of annexin V and propidium iodide signal. n=10-16, four replicate experiments. Tolerogenic response was present in THP-1 cells treated with either term (C) or preterm (D) HM EVs. Tolerogenic response was proposed for biological replicates that increased cell death in control samples but protected against pyroptotic cell death following inflammatory activation, indicated in brackets. (E) HM EV miRs predicted targets TLR4, MYD88, and NEK7 could result in downregulation of programmed cell

death via upstream inhibition of inflammasome pathway. **(F)** Term, but not preterm HM EVs, reduced apoptosis. THP-1 monocytes were treated with 40µg/mL term or preterm human milk EVs for 6 hours, followed by etoposide (30µM) for 4 hours, with or without an emricasan (EM, 10µM) pre-treatment for 30 minutes, or media only control. Geometric mean of fluorescence intensity (FITC) was plotted, n=3. **p<0.01, *p<0.04, ns=non-significant, one-way ANOVA with multiple comparisons.

4.5 Discussion

We found that both term and preterm HM EVs were enriched in epithelial (CD326)³⁵⁰, immune (HLA, CD24, CD14)^{351–353}, and stem (CD133, CD29)^{354,355} cell-related surface markers (**Figure 4.2**). Gestational-age based differences were detected for CD14, a modulator of toll-like receptor 2 and 4 signaling³⁵⁶, which was more abundant on the surface of preterm HM EVs. In Caco-2 cells, treatment with term and preterm HM EVs upregulated CD14 surface expression, while secretion of soluble CD14 was increased following exposure to term and preterm HM EVs (**Figure 4.3C-D**). Through cell surface activation and secretion, both CD14 receptor and its soluble form promote immune tolerance, and potentially contributing to the development of gut-microbiota homeostasis^{64,357}.

EVs from mature term HM have been shown to be enriched in CD14 when compared to matched serum EVs, with CD326 and CD24 being the most abundant surface markers²⁵². In transitional HM EVs characterized here, CD326 was also among the most abundant. We did not detect CD3 positive vesicles, which have been previously measured on mature HM EVs²⁵². These differences could reflect changes in the EV-secreting cellular architecture as lactation progresses. Breast milk could contain higher concentrations of epithelial and immune cells^{30–32,115}. Here,

increased CD14 levels on preterm HM EVs may indicate that immune cells are a major EV source. This finding is consistent with our previous work, which showed that preterm HM EVs have RNA signatures indicative of more abundant immune cell origins²⁷².

In vulnerable infants with an immature intestine, the equipoise of intestinal epithelium and gut resident macrophages is paramount. Milk-derived EVs have been proposed to influence immune cells associated with oral and gut mucosa^{137,159}, while support of epithelial cell function is critical to maintain intestinal homeostasis. EGF is present in HM and important in promoting the intestinal barrier³⁵⁸. Term and preterm HM EVs significantly increased EGF levels (**Figure 4.3B**), which could support the proliferation and differentiation of intestinal epithelial cells, and act as an anti-inflammatory mediator in the developing human intestine²²⁹. We have previously identified abundant epidermal growth factor receptor kinase substrate 8-like protein 2 (EPS8), a regulator of EGFR signaling³⁵⁹, from proteomics analysis of both term and preterm HM EVs cargo²⁷². EGFR may provide protection against NEC, supported by earlier research, where treatment with HM reduced TLR4 signaling and inhibited apoptosis via EGFR signaling¹¹².

When investigating cytokine levels in the inflammatory response of human intestinal epithelial cells and PBMC-derived macrophages, term and preterm HM EVs had differential effects on the expression of cytokines IL-6, IL-8, and TNF α , influenced further by the cell type. For IL-6, epithelial cells showed an increase in expression in response to term HM EVs, with no significant change for preterm HM EVs (**Figure 4.4**). We observed that in PBMC-derived macrophages, both HM EVs reduced expression (**Figure 4.5**). In the intestine, IL-6 may have protective effects by supporting homeostasis by induction of cell proliferation, survival, and

maintenance of crypt stem cells³⁶⁰. Conversely, in macrophages, secretion of IL-6 indicates polarization to an inflammatory M1 phenotype, which is associated with NEC^{361,362}.

Opposite expression patterns were seen for pro-inflammatory cytokines IL-8 and TNF α , with increases in macrophages (**Figure 4.5**), but decreases in HIECs (**Figure 4.4**). Preterm HM EVs were not able to attenuate IL-8 expression in HIECs, and increased it in macrophages, while term HM EVs significantly reduced its expression. Preterm neonates are more vulnerable to inflammatory diseases, and their immune system is still developing. In this context, preterm human milk EVs may play a role in boosting the immune system, preparing it to respond to potential infections and inflammation. By increasing IL-8 expression, preterm HM EVs may help recruit neutrophils to the site of inflammation, promoting a robust immune response, and enhancing the elimination of pathogens³⁶³.

Remarkably, regardless of cell type, term HM EVs downregulated IL-1 β expression (**Figure 4.4 and 5**), while both term and preterm significantly reduced their secretion (**Figure 4.6A**). The decrease in LPS-associated cytokines, including IL-1 β , following treatment with mature HM EVs has also recently been shown^{160,161}. Further evidence from mouse studies using bovine milk-derived EVs also indicate significant decreases in IL-1 β ^{137,364}. Taken together with our results, the downregulation of IL-1 β appears to be conserved between different cell types – intestinal epithelial cells and macrophages tested here, and irrespective of lactation stage, or gestational age. IL-1 β and IL-18 are potent pro-inflammatory cytokines that can promote polarization of T cells to an inflammatory phenotype³⁶⁵. HM EVs ability to reduce cytokine levels in macrophages may support a more balanced and homeostatic immune response, aligning with previous findings in T cells¹⁵⁹.

HM EVs protect against the development of NEC, which may be via inhibition of necroptosis, attributed partly to HM oligosaccharides¹⁰⁶. We showed that term transitional HM EVs downregulated apoptosis in monocytes (**Figure 4.7F**), and in earlier studies, cell death was reduced in intestinal epithelial cells in response to HM EV treatment^{147,151}. Here, EVs that increased cell death in the absence of LPS and nigericin, had an overall protective effect once pyroptosis was induced. This may indicate the promotion of tolerance to gut microbiota. While we saw a HM EV-dependent decrease in programmed cell death following treatment with inflammasome and pyroptosis inducer nigericin (**Figure 4.7**), we measured a limited effect on Gasdermin D expression and an increase in NLRP3 expression (**Figure 4.6B**). The selective regulation of the inflammasome components by term and preterm HM EVs may reflect a homeostatic regulation of the host immune response. The reduction in inflammatory cell death by HM EVs may support immune barrier function, allowing the macrophages to be retained, and to release Gasdermin D fragments thereby exerting cytotoxic effects on bacteria³³⁴. Gasdermin D release from immune and intestinal epithelial cells has been shown to limit bacterial loads, specifically in the context of *Salmonella* infection³⁶⁶. It could also stimulate goblet cells to secrete mucus, thus maintaining gut homeostasis³⁶⁷.

MiRs, such as miR-146a-5p and miR-148a, have been proposed to play a role in intestinal epithelium integrity and inflammasome regulation, which may be relevant in NEC-related signaling^{137,309,310}. Since biological variation in the abundance of miRs carried by HM EVs may influence their efficacy, we focused on the miRs that have been found to be most abundant. Based on our prior miR sequencing (**Table S3**), we propose that the downregulation of inflammatory cytokines and programmed cell death could be attributed to abundant miRs common to both term and preterm HM EVs, which also include miRs that are significantly

downregulated in NEC²⁷⁹. HM EV miRs were predicted to directly target IL-1 and IL-18, gasdermin D, and upstream regulators of the inflammasome – NEK7, MYD88, and TLR4 (**Figure 4.7E**).

For modulating the expression of cytokines, term and preterm miRs were enriched for targets in the JAK-STAT pathway. Indeed, following HM EV treatment, JAK2 expression was significantly downregulated in both macrophages and HIECs in the presence of inflammatory signals induced by LPS or heat-killed bacteria. JAK2 is also significantly upregulated in NEC intestinal tissue²⁹². MYD88 has been shown to activate JAK2 and STAT signaling, thereby miRs targeting both MYD88 and JAK2 may result in the downregulation of several key inflammatory genes, most notably, IL-6 and IL-1 β ³⁶⁸. Thus, much of the cellular signaling and inflammatory response may be multi-targeted by HM EV miR cargo, with the abundant miRs conserved between HM donors (**Table S4**).

We observed large biological variability in the effects of HM EVs on cultured cells, indicating the need for large-scale studies. Nonetheless, our results suggest that supplementation with EVs from transitional HM may drive a tolerogenic immune response. Whether HM feeding itself, even when supplemented with a higher concentration of EVs, can overcome bacterial infection, cytokine storm, and sepsis, remains to be elucidated. Since colostrum and transitional HM have been shown to contain a higher number of immunoregulatory proteins, miRs and EVs^{17,85,220,272}, supplementation strategies may have increased efficacy if derived from HM of those lactational stages. Interestingly, we found that only term HM EVs, not preterm, reduced IL-6 secretion in intestinal epithelial cells, attenuated expression of IL-1 β and IL-8, and decreased apoptosis. Thus, term HM EV supplementation may also provide more effective protection for premature neonates, especially in their first few weeks of life, and could be preferential in compromised

infants to prevent dysregulation of inflammatory signaling. Overall, these results shed further light on the bioactive components of transitional milk and could provide basis for both term and preterm HM EV supplementation in a clinical setting to investigate direct protection against NEC in targeted patient populations^{83,289}.

4.6 Materials and Methods

Ethics

HM was obtained from donors following ethics approval by the University of Ottawa, The Ottawa Hospital, and the Children's Hospital of Eastern Ontario (Research Ethics Board approval #H-03-20-5643). Donors were excluded if they had delivered via caesarean section, used antibiotics, or had active maternal genetic, immune, or chronic inflammatory diseases. Upon receiving written consent, donors sterilised their breast with an antibacterial wipe, followed by manual expression of 20mL of milk into sterile containers. The HM samples were collected from 45 donors, and further categorized based on gestational age (GA) as either term (GA > 37 weeks) or preterm (GA < 37 weeks) (**Table S1**).

Isolation of EVs

To obtain an EV-enriched pellet from freshly collected HM, we followed previously characterized protocols utilizing differential and ultracentrifugation^{142,143,215,216,253,254}. HM was centrifuged twice at 4600×g for 30 minutes within 30 minutes of milk collection, to separate fat, cells, and cell debris. To reduce remaining fat content and remove larger apoptotic vesicles, the skimmed milk was then centrifuged at 20,000×g for 30 minutes at 4°C. The supernatant was carefully removed and ultracentrifuged twice at 100,000×g for 1.5 hours at 4°C using a Beckman

Coulter ultracentrifuge (Optima XPN-100 or Optima L-100 XP, Beckman Coulter) with a fixed angle rotor (Type 70 Ti, k factor: 216, Beckman Coulter). The EV-enriched pellet was resuspended in 400 μ L of sterile phosphate-buffered saline (PBS) in aliquots and stored at -80°C until further analyses.

Super-resolution microscopy

EVs were immunolabeled and visualized using the EV Profiler Kit (ONI, Cat. No. EV-MAN-1.0) through direct stochastic optical reconstruction microscopy (dSTORM). Sample preparation and imaging were performed by Oxford Nanoimaging (ONI). Briefly, EVs were immobilized on microfluidic chips, followed by sample preparation according to kit instructions. The antibodies used included CD9/81-CF647 (kit, excitation/emission: 642/662nm), CD63-CF568 (kit, excitation/emission: 562/583nm), and CD14-BV421 (Cat No. 563743, BD Biosciences, excitation/emission: 405/421nm). dSTORM imaging buffer was added prior to image acquisition. Imaging was conducted on the Nanoimager S Mark III microscope (ONI, United Kingdom) with 30ms exposure. Surface markers were imaged with 640nm, 561nm, and 405nm lasers at power settings of 30%, 50%, and 100% respectively, capturing 1,000 frames per channel with an illumination angle of 47° . For subpopulation analyses of EVs expressing one, two, or three markers, ONI's CODI online platform (<https://alto.codi.bio>) was utilized. This included density-based clustering analysis with drift correction and filtering to assess each vesicle.

Nanoparticle tracking analysis

Extracellular vesicles were characterized using nanoparticle tracking analysis (NTA) on a ZetaView PMX110 instrument (Particle Metrix, Germany). Samples were diluted in PBS and analyzed after calibration with 105 and 500nm-sized polystyrene beads. The instrument was set for 85 sensitivity, 30 frames per second, and 100 shutter speed. ZetaView software was used to analyze the samples at 11 camera positions, and a system temperature of approximately 21°C.

Surface marker analysis

Term and preterm EVs were prepared for the overnight protocol following manufacturer's instructions (MACSPlex Exosome Kit, Cat. No. 130-108-813, Miltenyi Biotec, Bergisch Gladbach, Germany). Briefly, 10µg/mL of EVs, 120µL of capture beads, or negative control buffer, were incubated with 15µL MACSPlex EV Capture Beads in low protein binding tubes. The next day, 500µL of MACSPlex Buffer was added to each tube and centrifuged at room temperature at 3000×g for 5 minutes. Detection cocktail (CD9, CD63, CD81) was added to each tube and incubated at room temperature for one hour. After washing, the samples were resuspended in a final volume of 150µL. Samples were immediately analyzed on LSR Fortessa (BD Biosciences, San Jose, CA) following set-up instructions provided by MACSPlex Exosome Kit protocol. Following acquisition, samples were first gated using FlowJo software, version 10 (BD Biosciences) following kit instructions and a previously published protocol³⁶⁹. Then further analyzed using MPAPASS software, whereby fluorescence intensity was normalized to background, as formerly described^{369,370}.

To detect changes in Caco-2 CD14 surface expression, confluent cells were stained with anti-CD14 (BV421-conjugated, Cat. No. 563743, BD Biosciences), or unstained controls, and

acquired on LSR Fortessa by gating on single cell populations based on forward and side scatter profile.

Cell culture

Intestinal epithelial cell lines Caco-2/15 and HIECs were cultured following established protocols³³⁷. Briefly, the cells were cultured at 37°C, 5% CO₂-95% air, in Dulbecco's modified Eagle's medium (DMEM) supplemented with 10% fetal bovine serum (Gibco, Thermo Fisher Scientific, Waltham, MA). Caco-2 cells were grown to confluence for enterocytic differentiation, achieved 25 to 30 days post-seeding, which has been previously described³⁷¹. Prior to the start of the treatments, cell culture dishes were matched for cell density, standardized previously. The density of Caco-2 cells was 750,000, and 300,000 for HIECs, per 35mm dish³⁷¹⁻³⁷³. Both Caco-2 and HIECs were treated with term or preterm HM EVs (20µg/mL) for 22 hours, followed by heat-killed bacteria (*Escherichia coli* and *Salmonella typhimurium*) at a concentration of 10⁹ CFU/mL for two hours.

Human peripheral blood mononuclear cells (PBMCs) isolation was performed using SepMate™ tubes (Cat. No. 85450, STEMCELL Technologies, Vancouver, Canada) and a density gradient centrifugation method with Lymphoprep™ (Cat. No. 07801, STEMCELL Technologies), following the manufacturer's protocol. Monocytes were then isolated from PBMCs using negative selection with EasySep™ Human Monocyte Isolation Kit (STEMCELL Technologies). Briefly, the PBMCs were diluted to a concentration of 5 × 10⁷ cells/ml. The cells were then incubated with 50µl/ml antibody isolation cocktail. Following addition of 50µl of magnetic beads, cells were placed in a magnet for 10 minutes to capture non-monocyte populations.

Monocytes isolated in the supernatant were counted and 10^7 cells were added into a polystyrene petri dish (100 mm x 15 mm) pre-coated with recombinant human M-CSF (Cat. No. 216-MC, R&D Systems) to a final concentration of 10ng/mL. The cells were then cultured in RPMI medium supplemented with 10% FBS (10 mL total volume per dish) for a period of 6 days at 37°C in a humidified atmosphere containing 5% CO₂ to promote macrophage differentiation. On day six, once fully differentiated, 1.5×10^5 macrophages per well were seeded in 48-well plates and treated with term or preterm HM EVs (40µg/mL) for six hours, followed by LPS treatment (1ng/mL) for two hours.

THP-1 monocytes were obtained from ATCC (TIB-202™) and cultured in RPMI 1640 medium containing 10% FBS, 50 µg/mL gentamicin, and 1% β-mercaptoethanol. For microscopy, THP-1 cells were differentiated to macrophages by treatment with 50ng/mL phorbol 12-myristate 13-acetate (PMA) for a duration of 72 hours. Following differentiation, the cells were washed with phosphate-buffered saline (PBS) to remove residual PMA and cultured for an additional 24 hours in PMA-free RPMI 1640 medium supplemented with 10% FBS. Cell death was induced following previously established protocols. First, THP-1 monocytes were treated with term or preterm HM EVs (40µg/mL) for six hours. To induce pyroptosis³⁴⁷, cells were treated with LPS (1ng/mL, Cat. No. L4524, MilliporeSigma, Burlington, MA) for two hours, followed by nigericin (10µg/mL, Cat. No. N7143-5MG, MilliporeSigma, Burlington, MA) for one hour. For apoptosis³⁷⁴, cells were treated with either emricasan (10µM, Cat. No. S7775, Selleck Chemicals, Houston, TX) for 30 minutes, followed by etoposide (30µM), or etoposide alone for 3.5 hours.

Cell viability

For a viability assay of Caco-2 cells, 300,000 cells per well were seeded in 6-well plates and grown to confluence over four days. Then, 20 or 40 μ g/mL of HM EVs were added to cells. Cell viability was measured after 6- or 24-hour incubation using XTT Cell Proliferation Assay Kit (Cat. No. 10010200, Cayman Chemical, Ann Arbor, MI). Briefly, XTT reagent was thawed at room temperature. Then, equal amounts of reagents were mixed and 20 μ L of total reagent was added per well in the dark. Following a two-hour incubation, absorbance at 450nm was measured using Synergy H1 Multi-Mode Plate Reader (BioTek, Winooski, VT).

To assess the viability of THP-1 monocytes at the endpoint of all treatments, cells were stained for Annexin V and propidium iodide (Annexin V-FITC Apoptosis Staining/Detection Kit, Cat. No. ab14085, Abcam), according to kit protocol. The percentage of dead or alive cells was measured immediately using flow cytometry on BD Fortessa, followed by gating using FlowJo. Data from a total of 10,000 cells per sample that were acquired.

Microscopy

1x10³ macrophages per well were seeded in untreated μ -Slide 8 Well plates (Cat. No. 80826, Ibidi, Germany) prior to treatment with 20 μ g/mL of DiR-labeled HM EVs or DiR-PBS background control. Briefly, 5 μ L of XenoLight® DiR (Cat. No. 125964, Perkin Elmer, Waltham, MA) was added to 40 μ L of EVs, and diluted to a final volume of 1mL with PBS. Control samples included dye in PBS alone. EVs and negative control were stained for 40 minutes at room temperature on a rotating spinner, then ultra-centrifuged at 100,000 \times g for 30 minutes to pellet vesicles. Prior to macrophage treatments, stained EVs and negative control

were resuspended in 40 μ L of PBS. To visualize cellular compartments, macrophages were further treated with 10kDa dextran (FITC, 0.5mg/mL, Cat. No. D1820, Invitrogen, Waltham, MA) for one hour, and wheat germ agglutinin (WGA, AF350, 50 μ g/mL, Cat. No. W11263, Thermo Fisher Scientific, Waltham, MA) for 30 minutes. Following treatment, cells were washed twice with cold PBS before proceeding to live-cell imaging or fixed in 4% PFA for confocal imaging. Live cell imaging was done on a Quorum Spinning Disk with a 63X objective (1.4 NA). Fixed cell imaging was done on a Zeiss LSM 880 with a 63X objective (1.4 NA). Image processing and background correction was performed using ImageJ.

RNA extraction and quantitative real-time PCR (qPCR) analysis

At the end point of intestinal cell and macrophage treatments RNA was extracted using Qiagen RNeasy mini kit (Cat. No. 74104, Qiagen, Germany), following manufacturer's instructions, and stored at -80°C. cDNA was synthesized from 200-500ng of total RNA using iScript™ cDNA Synthesis Kit (Bio-Rad, Hercules, CA) in a final reaction volume of 40 μ l. Following synthesis, the cDNA was diluted to 10ng RNA/ μ l and stored at -20°C. qPCR was performed using SsoAdvanced Universal SYBR Green Master Mix (Bio-Rad) in a total reaction volume of 10 μ l. CFX Connect thermocycler (Bio-Rad) was used for amplification of the target genes by a standard cycling protocol with an annealing/extension temperature of 60°C. Gene expression across different treatments was analyzed using the comparative threshold cycle (Ct) $\Delta\Delta$ Ct method reported previously^{375,376}. Reference genes *RPL0*, *PPIA*, and *B2M* were used for normalization based on published primer sequences, which have been shown to exhibit stable expression across epithelial or immune cells. All primer sequences are listed in Table S2.

Cytokine secretion

The cell culture supernatants were collected following completion of treatments on intestinal cells and macrophages, and stored at -80°C until analysis. Cell media was analyzed using ELISA for secretion of EGF, sCD14, IL-6, IL-8, or IL-1 β at the end point of treatments. To determine secretion concentration, the 'Quantikine human' (R&D Systems, Minneapolis, MN) ELISA assay kits were used for individual cytokines. Delta (450-570nm) absorbance was measured using Synergy H1 Multi-Mode Plate Reader (BioTek). For primary macrophages, Human Inflammatory Cytokine Cytometric Bead Array (Cat. No. 551811, BD Biosciences) was used following manufacturer's protocol. Data was acquired using LTR Fortessa (BD Biosciences) based on manufacturer's set-up template. Standard curves and analyte concentrations were determined using BD CellQuest Pro software (BD Biosciences).

Bioinformatics analyses

List of miRs with the highest abundance common to term and preterm HM EVs with their corresponding abundance values (counts per million, CPM) were uploaded for Ingenuity Pathway Analysis (IPA, Qiagen). For analysis of miR targets, cut-off filters included experimental and high confidence predictions only. The predicted target genes were filtered to include targeted pathways related to apoptosis, inflammasomes, JAK/STAT signaling, MAPK signaling, Toll-like receptor cascades, necroptosis, pyroptosis, and other signaling pathways involved in immune responses, cell death, and disease processes. Input data and exact filtering parameters are listed in the supplementary materials (Table S3 and Figure S3).

Statistical analyses

Statistical analyses were conducted using GraphPad Prism 9 software (Version 9.0.0, GraphPad, San Diego, CA). Results were presented as mean \pm SEM. Welch's t-test was employed to compare two groups when comparing surface marker expression levels. When comparing three or more groups, a one-way analysis of variance (ANOVA) was performed. Multiple comparison tests were used post-hoc to identify specific group differences following a significant ANOVA result. Tukey's test was performed to compare every possible pair of means, while a Dunnett's test was used to compare each group mean to a designated control mean. The Brown-Forsythe test was used to assess the assumption of equal variances prior to performing ANOVA. To compare cell viability at six and 24 hours, two-way ANOVA analysis was performed. Statistical significance was defined as $p \leq 0.05$.

4.7 Acknowledgements

We gratefully acknowledge the support of the staff at The Ottawa Hospital, Monarch Centre, and Centretown Community Health Centre. For their contributions to patient enrolment and sample collection, we would like to thank Chantal Horth, NICU project lead coordinator, and research assistants Rebecca Grimwood and Denise Campuzano, at the CHEO Research Institute. Special thanks to Alison Fujii (Oxford Nanoimaging) for her expertise in sample preparation and super-resolution imaging. We are thankful to Dr. Ryan Reshke and Dr. Derrick Gibbings (University of Ottawa) for generously providing microscopy reagents and technical training. Additional thank you to Dr. Tommy Alain and Aida Said for assistance with IPA. We extend our sincere appreciation to Dr. Vera Tang and Dr. Joshua Welsh for their assistance with flow cytometry and MPAPass surface marker analysis. We also thank the uOttawa Flow Cytometry and Virometry core as well as the uOttawa CBIA core (RRID: SCR_021845), funded by the University of

Ottawa, Ottawa, Natural Sciences and engineering Research Council of Canada, and the Canada Foundation for Innovation. We are grateful to Dr. Alicia Vilorio-Petit and Dr. Mathieu Lavallée-Adam for their advice and improvements to the manuscript. B.V. is thankful for partial support from Estonian University of Life Sciences. Figures depicting pathways were drawn using BioRender.

4.8 Data availability

Supplementary data are available from the publisher.

Chapter 5. General discussion

EVs in preterm milk differ from term in three key molecular signatures: 1) higher abundance of immune-related proteins and mRNA; 2) enrichment in gene signatures and surface markers pointing to immune cell origin; and 3) decreased ability to attenuate inflammatory markers in intestinal and immune cells. Despite the changes, notable similarities with term HM EVs include conservation of abundant miRs, and ability to downregulate pyroptosis and IL-1 β secretion.

In Chapters 2 and 3, GA-based differences in EV-cargo were elucidated. On the protein and mRNA level, the cargo contrasted between term and preterm with increased signalling and metabolism enrichments in the former, and immune-related functions for the latter. The abundance of metabolism related cargo in term HM EVs suggests more support for substantial anti-oxidative processes, which are vital to counteract the negative effects of a newborn's immune response in the face of bacterial colonization³⁷⁷. The comparative decrease in these factors in preterm EVs may be insufficient to support preterm neonates with increased inflammation who consume mother's milk within two weeks of birth.

In contrast, the abundant miRs were overall conserved between the two groups. The diversity of the total targets, both up and downregulating in the same or related pathways makes the case for a dynamic regulation within HM components themselves, perhaps giving EVs the ability to respond to a variety of biological conditions in distinct cell types. It also suggests that miRs are the major bioactive modulators of HM EVs, given their conservation in milk across gestational ages, lactation stages, and even species that differ from humans²⁰⁷.

The findings from all experimental chapters presented in this thesis have important implications for HM EVs in the context of NEC and innate immune responses, including mitigation via toll-like receptors or TLRs. An array of TLRs are expressed on cardiac myocytes, mesenchymal stem cells, epithelial cells, and several neuronal cells, which can carry out important functions in the respiratory and cardiovascular systems, influence GI signaling, and regulate the central nervous system in newborns⁵⁶. TLRs 1, 2, and 6 were identified among the proteomic cargo of HM EVs. In the mRNA cargo, both term and preterm EVs contained TLR4 transcripts, while TLR9 was uniquely present in preterm EVs. Though the abundance of the TLR mRNA was low, with number of transcripts per million between 10 to 25, given their presence alongside dozens of interacting proteins and mRNA, TLR-signaling was still among the enriched pathways in HM EVs.

Conversely, a major predicted target of EV-contained miRs, including the most abundant miR-148a-3p and miR-141-3p, was the TLR4 receptor as well as many of its downstream signaling partners. It has been postulated that signaling ligands present in HM can also lead to upregulation of miR-146b, miR-223, and let-7i following feeding, which decrease expression of TLR4 in the gut of mice³⁷⁸. It is therefore possible that the corresponding milk EV-contained miRs can target TLR4 and related signaling more expediently and help prevent dysregulation in NEC.

In Chapter 4, differential regulation of inflammatory markers in cell culture by term and preterm HM EVs was observed. In macrophages under inflammatory conditions, IL-1 β secretion, which could be induced by TLR4³⁷⁹, was curtailed following treatment with both EVs, while IL-6 secretion was inhibited by term HM EVs only. However, I did not measure TLR expression or

activation directly, though in a separate study in intestinal organoids, EVs from all lactational stages reduced TLR4 expression¹⁶³. It is notable that Zonneveld and colleagues showed that mature HM EVs do not suppress the activation of TLRs 2 and 4 in the presence of LPS, while significant inhibition was seen for TLRs 3 and 9¹⁵⁹. But, the study was conducted in a human embryonic kidney reporter cell line, with modified gene expression affecting pathways that may intersect with TLR signaling such as cell death, cell proliferation, metabolism, and secretion³⁸⁰.

The enrichment of immunomodulatory proteins and mRNA in preterm milk EVs may be essential in supporting the immune system of premature infants. In the context of acute and chronic stages of NEC⁹⁴, the initial intestinal damage in the acute stages may be regulated by HM components, while the chronic pro-inflammatory cascade could be unstoppable with non-therapeutic levels of HM bioactive molecules. Data from Chapter 4 suggest that preterm HM EVs are unable to decrease IL-6 levels in response to inflammatory stimuli and can upregulate expression of pro-inflammatory IL-8 in epithelial cells. The elevation of both cytokines may initially allow for defense against pathogens, but sustained increases may be damaging. The EVs were characterized from HM within the first two weeks of birth, wherein these GA-based immunomodulatory differences may dissipate once lactation reaches the mature stage. Since the persistence and clearance of HM EV-derived cargo is not fully established, these initial changes may be protective.

Mitigation of inflammatory cell death could have substantial impacts in regulating a newborn's response to infection^{94,381}. Cell death controlled by the inflammasome signaling is prevalent in macrophages and causes pore-formation as a vector of disease control via subsequent release of

intracellular cytokines and Gasdermins^{365,382}. This can also counterpoise to sepsis by supporting a cytokine storm during bacterial infection^{334,366,382}. The conserved inhibition of IL-1 β release, IL-18 expression, and cell death by both term and preterm EVs point to a retained mitigative action regardless of GA.

Several conflicting cargo-effects within the EVs or with HM were postulated in this thesis. Both inhibition and promotion of TLR signaling was predicted. This included increases measured for its co-effector CD14, especially by preterm HM EVs. Signaling via the CD14/TLR4 complex is also upregulated in neonatal sepsis⁵⁶. In addition to sCD14, the cytokine TGF- β is abundant in HM, which can improve intestinal permeability and have anti-inflammatory effects⁶³. However, overexpression of TGF- β 1 could promote fibrosis, which can have a negative outcome for necrotizing enterocolitis patients³⁸³. EV-cargo contained TGF- β antagonist EMILIN-3, and numerous miRs were predicted to directly target TGF- β with additional targets in its associated pathway. Term EV mRNA cargo contained enriched processes corresponding to immune signaling, including IL-1, which was downregulated in our cell culture experiments pointing instead to inhibitory targeting via the miR cargo. It may be that HM can both induce and inhibit pathways and processes following uptake to dynamically respond to the health status of a newborn, and on a cellular level, the biological activation and presence of signaling proteins in intestinal or immune cells.

This adaptive regulation has been established for HM, but the results presented here suggest further enabling by the HM EV cargo. The access of HM EVs to various cell types can also be affected by the health status of the newborn. In disease states, the EVs have increased access to

gut-associated immune cells¹³⁷, wherein the selective inhibition of abundant immune signaling proteins expressed in these cells may be beneficial. The abundance of certain HM cargo may influence infant outcomes, as an increase in cytotoxic CD8⁺ T cells from HM has been associated with infant inflammatory diseases and early intestinal damage, while lower levels can be protective³⁸. In this perspective, higher concentrations of immunoregulatory proteins in preterm HM EVs may tip the scales to inflammation in preterm newborns.

5.1 Limitations

An advantage of the work presented in this thesis is the conserved timing of milk expression within two weeks of birth and sample preparation that allows direct comparisons between term and preterm HM EV cargo and the biological effects in cell culture. However, more information could be obtained from the proteomics and sequencing data. Since the majority of HM EV samples characterized with proteomics and RNA sequencing were not fully used in cell culture studies, the hypothesis of cargo action remains as such. To mitigate this, the data was compared to previous milk studies across lactational stages to proceed with the most likely conserved candidates, such as miR-141-3p, miR-148a-3p, and let-7 for target predictions. Optimizing a machine learning approach could allow broader predictions of effect by integrating information on donor characteristics and the detected EV cargo combined with results from human intestinal and immune cell experiments.

For a mechanistic explanation of cargo action, the effects of term and preterm HM EVs on the individual components of inflammasome signaling should be characterized. The postulated miR targets TLR4, Myd88, Gasdermin D, and Caspase 11 activity can be measured via Western blot.

On an individual miR level, validation of predicted targets in inflammasome signaling would be beneficial. To measure the major predicted miR targets postulated in Chapter 4, synthetic miR mimics and inhibitors could be used in macrophages to validate and measure effects on target protein levels following induction of pyroptosis. To allow for translation of HM EVs from bench to bedside, the overall protection by GA-based EVs against pyroptotic cell death in intestinal epithelial and immune cells should be further characterized in an animal model.

Given the crucial role of inflammasome-induced cell death in NEC and sepsis, the ability of HM EVs to reverse the signaling following a high concentration of inflammatory stimuli should be trialed. Experiments conducted in Chapter 4 used the minimum EV concentration to observe a biological effect (40 μ g/mL), but the inclusion of high-dose EVs may be more effective. Since large variability was present between HM EVs of different donors, future studies should include larger cohorts in analysis to better identify conserved patterns. While the biological variability following treatments in cell culture may have resulted from inherent cargo variability and abundance in each donor, it may also be due to our experimental approach. The quantity of EV treatment was based on the total protein quantity, which can vary between vesicles. The field is largely inconsistent between using total protein quantity versus particles per mL to determine the amount of EVs for treatment³⁸⁴⁻³⁸⁶. Since we proposed miRs as a main effector, it is possible that the amount present in each vesicle differs, and that difference may not be correlated to the variation in protein quantity. Therefore, the uneven distribution of biological material may have inadvertently occurred during our cell culture treatments and contributed to the biological variability measured.

An additional limitation in this EV-based project is the use of differential and ultracentrifugation for EV isolation. While this isolation technique has been widely used in HM EV studies^{142,146,151,156,163,172,191,205,387,388}, the persistence of contaminant particles and proteins in the EV-enriched fraction has been demonstrated in recent years. In a heterogenous biofluid such as milk, casein micelles are most prevalent³⁸⁹⁻³⁹¹. Any contaminants should have limited effects on RNA sequencing, as majority of RNA species are transferred in EVs and the RNA isolation procedure removes interfering fat and proteins, however, the impact on protein cargo was detected. In our proteomics data, caseins, and the most abundant HM proteins, such as lysozyme, lactoferrin, were measured. Since EV preparations were used to treat cells, it is possible that the potential contaminants carried over during treatments and impacted intracellular signaling. These technical obstacles in milk EV research emphasize the need to improve isolation and purification strategies, while also maintaining the structural integrity, biological activity, and heterogeneity of the EV population³⁹¹.

5.2 Future directions

Since characterization of the HM EV cargo is a crucial stepping stone for therapeutic approaches, it will be important to quantify the amount of EVs delivered per feed to newborns, including the quantity of total and individual miRs transported. Successful supplementation strategies will also be dependent on the ability of EVs to escape lysosomal degradation. It may be that majority of EVs consumed during breastfeeding are destined for lysosomal degradation with differences in the clearance rate depending on the newborn's health status. For example, in bacterial infection that accompanies NEC, the infiltration of lysosome-rich macrophages in the

intestine may lead to increased degradation of EVs, thereby reducing the cargo activity^{116,140}. In such cases, increasing the doses of milk-miRs may be clinically relevant.

The incorporation of EVs in infant therapeutics is a promising avenue. To date, the majority of clinical trials optimize stem cell-derived EVs for potential treatment of pulmonary³⁹², neurological, and other inflammatory diseases^{393,394}. For efficient drug delivery, milk-derived EVs have been proposed over synthetic carriers due to reduction in allergic responses^{395,396}. Based on pre-clinical testing, milk EVs could be purposed as a treatment against intestinal inflammatory diseases in newborns and older infants³⁹⁷. However, the availability of fresh milk for EV isolation has resulted in much of the research field focusing on bovine milk for such supplementation strategies and to improve current formula and fortifier products³⁹⁸. In characterizing HM EVs, production of the abundant proteins and miRs could be a sustainable avenue which is evidenced by the emergence of synthetic milk start-up companies, such as BIOMILQ^{399,400}.

Premature infants in the NICU are provided with mother's milk as a main nutrient source in the first weeks of life whenever possible. This milk can be supported by addition of pasteurized donor milk or human milk-based fortifier products, which are nearly always derived from mature milk months post-birth⁴⁰¹. Still, premature infants have a higher incidence of intestinal disease and increased generalized inflammatory processes. Given the findings of this thesis, term milk from transitional lactational stage may be preferential for feeding of premature infants in their first few weeks of life due to its increased antioxidative and signaling contents, fewer immunomodulatory proteins and RNA, and ability to decrease immune responses in cell culture.

In this thesis, I sought to contribute to the field by continued characterization of term and preterm HM EVs, which is crucial for our understanding of their diverse roles in neonatal health and disease, especially in developing therapeutics for vulnerable preterm neonates^{83,289}. The advancement in milk EV characterization from different biological conditions could benefit translational and clinical research. Thus, the future impact of HM EVs relies on utilizing the EVs, and the ability to translate the bioactive molecules into effective clinical treatments, which can benefit all infants, but especially the most fragile premature population.

References

1. Colleluori, G., Perugini, J., Barbatelli, G. & Cinti, S. Mammary gland adipocytes in lactation cycle, obesity and breast cancer. *Rev. Endocr. Metab. Disord.* **22**, 241–255 (2021).
2. Kobayashi, K. Culture models to investigate mechanisms of milk production and blood-milk barrier in mammary epithelial cells: a review and a protocol. *J. Mammary Gland Biol. Neoplasia* **28**, 8 (2023).
3. Hannan, F. M., Elajnaf, T., Vandenberg, L. N., Kennedy, S. H. & Thakker, R. V. Hormonal regulation of mammary gland development and lactation. *Nat. Rev. Endocrinol.* **19**, 46–61 (2023).
4. Lawrence, R. A. Biochemistry of Human Milk. in *Breastfeeding* (eds. Lawrence, R. A. & Lawrence, R. M. B. T.-B. (Ninth E.)) 93–144 (Elsevier, 2022).
5. Ballard, O. & Morrow, A. L. Human milk composition. *Pediatr. Clin. North Am.* **60**, 49–74 (2013).
6. Gabrielli, O. *et al.* Preterm milk oligosaccharides during the first month of lactation. *Pediatrics* **128**, e1520-31 (2011).
7. Kent, J. C. *et al.* Longitudinal changes in breastfeeding patterns from 1 to 6 months of lactation. *Breastfeed. Med.* **8**, 401–407 (2013).
8. Cabinian, A. *et al.* Transfer of maternal immune cells by breastfeeding: Maternal cytotoxic T lymphocytes present in breast milk localize in the Peyer's patches of the nursed infant. *PLoS One* **11**, e0156762 (2016).
9. LeMaster, C. *et al.* The cellular and immunological dynamics of early and transitional human milk. *Commun. Biol.* **6**, 539 (2023).
10. Underwood, M. A. Human milk for the premature infant. *Pediatr. Clin. North Am.* **60**, 189–207 (2013).
11. Dallas, D. C. *et al.* Endogenous human milk peptide release is greater after preterm birth than term birth. *J. Nutr.* **145**, 425–433 (2015).
12. Anderson, G. H. The effect of prematurity on milk composition and its physiological basis. *Fed. Proc.* **43**, 2438–2442 (1984).
13. Parker, L. A. *et al.* Measures of lactation outcomes in women delivering preterm infants. *Nurs. Res.* **70**, 193–199 (2021).

14. Wang, C., Qiao, X., Gao, Z., Jiang, L. & Mu, Z. Advancement on milk fat globule membrane: Separation, identification, and functional properties. *Front. Nutr.* **8**, 807284 (2021).
15. Donovan, S. M. Human milk proteins: Composition and physiological significance. in *Nestlé Nutrition Institute Workshop Series* vol. 90 93–101 (2019).
16. Deeth, H. & Bansal, N. Whey Proteins: An Overview. in (eds. Deeth, H. C. & Bansal, N. B. T.-W. P.) 1–50 (Academic Press, 2019).
17. Trend, S. *et al.* Levels of innate immune factors in preterm and term mothers' breast milk during the 1st month postpartum. *Br. J. Nutr.* **115**, 1178–1193 (2016).
18. Maningat, P. D. *et al.* Gene expression in the human mammary epithelium during lactation: the milk fat globule transcriptome. *Physiol. Genomics* **37**, 12–22 (2009).
19. Lemay, D. G. *et al.* RNA sequencing of the human milk fat layer transcriptome reveals distinct gene expression profiles at three stages of lactation. *PLoS One* **8**, e67531 (2013).
20. Yan, X. *et al.* LncRNA and mRNA profiles of human milk-derived exosomes and their possible roles in protecting against necrotizing enterocolitis. *Food Funct.* **13**, 12953–12965 (2022).
21. Izumi, H. *et al.* Bovine milk contains microRNA and messenger RNA that are stable under degradative conditions. *J. Dairy Sci.* **95**, 4831–4841 (2012).
22. Izumi, H. *et al.* Bovine milk exosomes contain microRNA and mRNA and are taken up by human macrophages. *J. Dairy Sci.* **98**, 2920–2933 (2015).
23. Hård, A. L. *et al.* Review shows that donor milk does not promote the growth and development of preterm infants as well as maternal milk. *Acta Paediatr.* **108**, 998–1007 (2019).
24. Bokor, S., Koletzko, B. & Décsi, T. Systematic review of fatty acid composition of human milk from mothers of preterm compared to full-term infants. *Ann. Nutr. Metab.* **51**, 550–556 (2007).
25. Hylander, M. A., Strobino, D. M. & Dhanireddy, R. Human milk feedings and infection among very low birth weight infants. *Pediatrics* **102**, e38–e38 (1998).
26. Austin, S. *et al.* Human milk oligosaccharides in the milk of mothers delivering term Versus Preterm Infants. *Nutrients* **11**, 1282 (2019).
27. Gidrewicz, D. & Fenton, T. R. A systematic review and meta-analysis of the nutrient

- content of preterm and term breast milk. *BMC Pediatr.* **14**, (2014).
28. Bauer, J. & Gerstl, J. Longitudinal analysis of macronutrients and minerals in human milk produced by mothers of preterm infants. *Clin. Nutr.* **30**, 215–220 (2011).
 29. Ninkina, N. *et al.* Stem cells in human breast milk. *Hum. Cell* **32**, 223–230 (2019).
 30. Nyquist, S. K. *et al.* Cellular and transcriptional diversity over the course of human lactation. *Proc. Natl. Acad. Sci.* **119**, e2121720119 (2022).
 31. Twigger, A.-J. *et al.* Transcriptional changes in the mammary gland during lactation revealed by single cell sequencing of cells from human milk. *Nat. Commun.* **13**, 562 (2022).
 32. Martin Carli, J. F. *et al.* Single cell RNA sequencing of human milk-derived cells reveals sub-populations of mammary epithelial cells with molecular signatures of progenitor and mature states: a novel, non-invasive framework for investigating human lactation physiology. *J. Mammary Gland Biol. Neoplasia* **25**, 367–387 (2020).
 33. Aydın, M. Ş., Yiğit, E. N., Vatandaşlar, E., Erdoğan, E. & Öztürk, G. Transfer and integration of breast milk stem cells to the brain of suckling pups. *Sci. Rep.* **8**, 14289 (2018).
 34. Hassiotou, F. *et al.* Breastmilk stem cell transfer from mother to neonatal organs. *FASEB J.* **28**, 216.4 (2014).
 35. Carrillo-Lozano, E., Sebastián-Valles, F. & Knott-Torcal, C. Circulating microRNAs in breast milk and their potential impact on the infant. *Nutrients* **12**, (2020).
 36. Briere, C.-E., Jensen, T., McGrath, J. M., Young, E. E. & Finck, C. Stem-like cell characteristics from breast milk of mothers with preterm infants as compared to mothers with term infants. *Breastfeed. Med.* **12**, 174–179 (2017).
 37. Witkowska-Zimny, M. & Kaminska-El-Hassan, E. Cells of human breast milk. *Cell. Mol. Biol. Lett.* **22**, 11 (2017).
 38. Laouar, A. Maternal leukocytes and infant immune programming during breastfeeding. *Trends Immunol.* **41**, 225–239 (2020).
 39. Arvola, M. *et al.* Immunoglobulin-secreting cells of maternal origin can be detected in B cell-deficient mice. *Biol. Reprod.* **63**, 1817–1824 (2000).
 40. Dawson, C. A. *et al.* Tissue-resident ductal macrophages survey the mammary epithelium and facilitate tissue remodelling. *Nat. Cell Biol.* **22**, 546–558 (2020).

41. Cansever, D. *et al.* Lactation-associated macrophages exist in murine mammary tissue and human milk. *Nat. Immunol.* **24**, 1098–1109 (2023).
42. Trend, S. *et al.* Leukocyte populations in human preterm and term breast milk identified by multicolour flow cytometry. *PLoS One* **10**, e0135580 (2015).
43. Ames, S. R., Lotoski, L. C. & Azad, M. B. Comparing early life nutritional sources and human milk feeding practices: personalized and dynamic nutrition supports infant gut microbiome development and immune system maturation. *Gut Microbes* **15**, 2190305 (2023).
44. Luo, Y. *et al.* Milk-derived small extracellular vesicles promote bifidobacteria growth by accelerating carbohydrate metabolism. *LWT* **182**, 114866 (2023).
45. Sullivan, S. *et al.* An exclusively human milk-based diet is associated with a lower rate of necrotizing enterocolitis than a diet of human milk and bovine milk-based products. *J. Pediatr.* **156**, 562-567.e1 (2010).
46. Cheng, Y.-J. & Yeung, C.-Y. Recent advance in infant nutrition: Human milk oligosaccharides. *Pediatr. Neonatol.* (2021).
47. Cacho, N. T. & Lawrence, R. M. Innate immunity and breast milk. *Front. Immunol.* **8**, 584 (2017).
48. Belkaid, Y. & Hand, T. W. Role of the microbiota in immunity and inflammation. *Cell* **157**, 121–141 (2014).
49. McGreal, E. P., Hearne, K. & Spiller, O. B. Off to a slow start: Under-development of the complement system in term newborns is more substantial following premature birth. *Immunobiology* **217**, 176–186 (2012).
50. Filias, A. *et al.* Phagocytic ability of neutrophils and monocytes in neonates. *BMC Pediatr.* **11**, 29 (2011).
51. Nussbaum, C. *et al.* Neutrophil and endothelial adhesive function during human fetal ontogeny. *J. Leukoc. Biol.* **93**, 175–184 (2013).
52. Ivarsson, M. A. *et al.* Differentiation and functional regulation of human fetal NK cells. *J. Clin. Invest.* **123**, 3889–3901 (2013).
53. Lee, Y.-C. & Lin, S.-J. Neonatal natural killer cell function: relevance to antiviral immune defense. *Clin. Dev. Immunol.* **2013**, 427696 (2013).
54. Maheshwari, A. Innate immune memory in macrophages. *Newborn (Clarksville, Md.)* **2**,

- 60–79 (2023).
55. Salvo-Romero, E., Stokes, P. & Gareau, M. G. Microbiota-immune interactions: from gut to brain. *LymphoSign J.* **7**, 1–23 (2020).
 56. Dias, M. L., O'Connor, K. M., Dempsey, E. M., O'Halloran, K. D. & McDonald, F. B. Targeting the Toll-like receptor pathway as a therapeutic strategy for neonatal infection. *Am. J. Physiol. Integr. Comp. Physiol.* **321**, R879–R902 (2021).
 57. de Jong, E., Strunk, T., Burgner, D., Lavoie, P. M. & Currie, A. The phenotype and function of preterm infant monocytes: implications for susceptibility to infection. *J. Leukoc. Biol.* **102**, 645–656 (2017).
 58. Sadeghi, K. *et al.* Immaturity of infection control in preterm and term newborns is associated with impaired toll-like receptor signaling. *J. Infect. Dis.* **195**, 296–302 (2007).
 59. Förster-Waldl, E. *et al.* Monocyte toll-like receptor 4 expression and LPS-induced cytokine production increase during gestational aging. *Pediatr. Res.* **58**, 121–124 (2005).
 60. Simon, A. K., Hollander, G. A. & McMichael, A. Evolution of the immune system in humans from infancy to old age. *Proc. R. Soc. B Biol. Sci.* **282**, 20143085 (2015).
 61. Mezu-Ndubuisi, O. J. & Maheshwari, A. Role of macrophages in fetal development and perinatal disorders. *Pediatr. Res.* **90**, 513–523 (2021).
 62. Shen, C.-M., Lin, S.-C., Niu, D.-M. & Kou, Y. R. Development of monocyte Toll-like receptor 2 and Toll-like receptor 4 in preterm newborns during the first few months of life. *Pediatr. Res.* **73**, 685–691 (2013).
 63. Brenmoehl, J., Ohde, D., Wirthgen, E. & Hoeflich, A. Cytokines in milk and the role of TGF-beta. *Best Pract. Res. Clin. Endocrinol. Metab.* **32**, 47–56 (2018).
 64. Blais, D. R., Harrold, J. & Altosaar, I. Killing the messenger in the nick of time: persistence of breast milk sCD14 in the neonatal gastrointestinal tract. *Pediatr. Res.* **59**, 371–376 (2006).
 65. Downes, N. J. Consideration of the development of the gastrointestinal tract in the choice of species for regulatory juvenile studies. *Birth Defects Res.* **110**, 56–62 (2018).
 66. Demers-Mathieu, V., Nielsen, S. D., Underwood, M. A., Borghese, R. & Dallas, D. C. Changes in proteases, antiproteases, and bioactive proteins from mother's breast milk to the premature infant stomach. *J. Pediatr. Gastroenterol. Nutr.* **66**, 318–324 (2018).
 67. Chan, L. E., Beverly, R. L. & Dallas, D. C. The Enzymology of Human Milk BT - Agents

- of Change: Enzymes in Milk and Dairy Products. in (eds. Kelly, A. L. & Larsen, L. B.) 209–243 (Springer International Publishing, 2021).
68. Healy, D. B., Ryan, C. A., Ross, R. P., Stanton, C. & Dempsey, E. M. Clinical implications of preterm infant gut microbiome development. *Nat. Microbiol.* **7**, 22–33 (2022).
 69. Frazer, L. C. & Good, M. Intestinal epithelium in early life. *Mucosal Immunol.* **15**, 1181–1187 (2022).
 70. Demers-Mathieu, V., Nielsen, S. D., Underwood, M. A., Borghese, R. & Dallas, D. C. Analysis of milk from mothers who delivered prematurely reveals few changes in proteases and protease inhibitors across gestational age at birth and infant postnatal age. *J. Nutr.* **147**, 1152–1159 (2017).
 71. Olsen, W., Liang, N. & Dallas, D. C. Macrophage-immunomodulatory actions of bovine whey protein isolate, glycomacropeptide, and their in vitro and in vivo digests. *Nutrients* vol. 15 (2023).
 72. Lyu, Y., Kim, B. J., Patel, J. S., Dallas, D. C. & Chen, Y. Human milk protein-derived bioactive peptides from in vitro-digested colostrum exert antimicrobial activities against common neonatal pathogens. *Nutrients* vol. 16 (2024).
 73. Sanidad, K. Z. & Zeng, M. Y. Neonatal gut microbiome and immunity. *Curr. Opin. Microbiol.* **56**, 30–37 (2020).
 74. Gensollen, T., Iyer, S. S., Kasper, D. L. & Blumberg, R. S. How colonization by microbiota in early life shapes the immune system. *Science (80-.)*. **352**, 539–544 (2016).
 75. Tanaka, M. & Nakayama, J. Development of the gut microbiota in infancy and its impact on health in later life. *Allergol. Int.* **66**, 515–522 (2017).
 76. Eberl, G. Inducible lymphoid tissues in the adult gut: recapitulation of a fetal developmental pathway? *Nat. Rev. Immunol.* **5**, 413–420 (2005).
 77. Kurashima, Y., Tokuhara, D., Kamioka, M., Inagaki, Y. & Kiyono, H. Intrinsic control of surface immune and epithelial homeostasis by tissue-resident gut stromal cells. *Front. Immunol.* **10**, 1281 (2019).
 78. Maheshwari, A. *et al.* TGF- β 2 suppresses macrophage cytokine production and mucosal inflammatory responses in the developing intestine. *Gastroenterology* **140**, 242–253 (2011).

79. Koch, M. A. *et al.* Maternal IgG and IgA antibodies dampen mucosal T helper cell responses in early life. *Cell* **165**, 827–841 (2016).
80. Niewiesk, S. Maternal antibodies: clinical significance, mechanism of interference with immune responses, and possible vaccination strategies. *Front. Immunol.* **5**, 446 (2014).
81. Carr, L. E. *et al.* Role of human milk bioactives on infants' gut and immune health. *Front. Immunol.* **12**, (2021).
82. He, Y., He, Z., Leone, S. & Liu, S. Milk exosomes transfer oligosaccharides into macrophages to modulate immunity and attenuate adherent-invasive e. Coli (aiec) infection. *Nutrients* **13**, (2021).
83. Madden, J. W. Human breast milk exosomes may protect against necrotizing enterocolitis in preterm infants. *Pediatr. Res.* **90**, 244–245 (2021).
84. Galley, J. D. & Besner, G. E. The therapeutic potential of breast milk-derived extracellular vesicles. *Nutrients* **12**, 745 (2020).
85. O'Reilly, D. *et al.* Perspective: the role of human breast-milk extracellular vesicles in child health and disease. *Adv. Nutr.* **12**, 59–70 (2021).
86. Parker, M. G. *et al.* Promoting human milk and breastfeeding for the very low birth weight infant. *Pediatrics* **148**, e2021054272 (2021).
87. Hackam, D. J. & Sodhi, C. P. Bench to bedside — new insights into the pathogenesis of necrotizing enterocolitis. *Nat. Rev. Gastroenterol. Hepatol.* **19**, 468–479 (2022).
88. Waard, M. de *et al.* Time to Full Enteral Feeding for Very Low-Birth-Weight Infants Varies Markedly Among Hospitals Worldwide but May Not Be Associated With Incidence of Necrotizing Enterocolitis: The NEOMUNE-NeoNutriNet Cohort Study. *J. Parenter. Enter. Nutr.* **43**, 658–667 (2018).
89. Sisk, P. M., Lovelady, C. A., Dillard, R. G., Gruber, K. J. & O'Shea, T. M. Early Human Milk Feeding Is Associated With a Lower Risk of Necrotizing Enterocolitis in Very Low Birth Weight Infants. *J. Perinatol.* **27**, 428–433 (2007).
90. Battersby, C., Santhalingam, T., Costeloe, K. & Modi, N. Incidence of Neonatal Necrotising Enterocolitis in High-Income Countries: A Systematic Review. *Arch. Dis. Child. - Fetal Neonatal Ed.* **103**, F182–F189 (2018).
91. Shah, T. A. *et al.* Hospital and Neurodevelopmental Outcomes of Extremely Low-Birth-Weight Infants With Necrotizing Enterocolitis and Spontaneous Intestinal Perforation. *J.*

- Perinatol.* **32**, 552–558 (2011).
92. Gingle, J. G. & Butki, N. Necrotizing Enterocolitis. in (2024).
 93. Garg, P. M. *et al.* Hematological Predictors of Mortality in Neonates With Fulminant Necrotizing Enterocolitis. *J. Perinatol.* **41**, 1110–1121 (2021).
 94. Kanuri, S. H., Bagang, N., Ulucay, A. S. & Singh, G. P. Is intestinal cell death in necrotising enterocolitis assorted and multifarious? A special focus on risk factors and their pathogenic mechanisms. *Emj Gastroenterol.* (2023).
 95. Niño, D. F., Sodhi, C. P. & Hackam, D. J. Necrotizing enterocolitis: new insights into pathogenesis and mechanisms. *Nat. Rev. Gastroenterol. Hepatol.* **13**, 590–600 (2016).
 96. Leaphart, C. L. *et al.* A Critical Role for TLR4 in the Pathogenesis of Necrotizing Enterocolitis by Modulating Intestinal Injury and Repair. *J. Immunol.* **179**, 4808–4820 (2007).
 97. Richardson, W. M. *et al.* Nucleotide-Binding Oligomerization Domain-2 Inhibits Toll-Like Receptor-4 Signaling in the Intestinal Epithelium. *Gastroenterology* **139**, 904-917.e6 (2010).
 98. Sampath, V. *et al.* SIGIRR Genetic Variants in Premature Infants With Necrotizing Enterocolitis. *Pediatrics* **135**, e1530–e1534 (2015).
 99. Sodhi, C. P. *et al.* Toll-Like Receptor-4 Inhibits Enterocyte Proliferation via Impaired B-Catenin Signaling in Necrotizing Enterocolitis. *Gastroenterology* **138**, 185–196 (2010).
 100. Egan, C. E. *et al.* Toll-like receptor 4-mediated lymphocyte influx induces neonatal necrotizing enterocolitis. *J. Clin. Invest.* **126**, 495–508 (2016).
 101. Neal, M. D. *et al.* Toll-Like Receptor 4 Is Expressed on Intestinal Stem Cells and Regulates Their Proliferation and Apoptosis via the P53 Up-Regulated Modulator of Apoptosis. *J. Biol. Chem.* **287**, 37296–37308 (2012).
 102. Gribar, S. C. *et al.* Reciprocal Expression and Signaling of TLR4 and TLR9 in the Pathogenesis and Treatment of Necrotizing Enterocolitis. *J. Immunol.* **182**, 636–646 (2009).
 103. Furusawa, Y., Obata, Y. & Hase, K. Commensal microbiota regulates T cell fate decision in the gut. *Semin. Immunopathol.* **37**, 17–25 (2015).
 104. Shaw, A. *et al.* Premature Neonatal Gut Microbial Community Patterns Supporting an Epithelial TLR-mediated Pathway for Necrotizing Enterocolitis. *BMC Microbiol.* **21**,

- (2021).
105. Bertheloot, D., Latz, E. & Franklin, B. S. Necroptosis, pyroptosis and apoptosis: an intricate game of cell death. *Cell. Mol. Immunol.* **18**, 1106–1121 (2021).
 106. Werts, A. D. *et al.* A novel role for necroptosis in the pathogenesis of necrotizing enterocolitis. *Cell. Mol. Gastroenterol. Hepatol.* **9**, 403–423 (2020).
 107. Chi, C. *et al.* Effects of probiotics in preterm infants: A network meta-analysis. *Pediatrics* **147**, (2021).
 108. Chen, C.-C. & Walker, W. A. Probiotics and the mechanism of necrotizing enterocolitis. *Semin. Pediatr. Surg.* **22**, 94–100 (2013).
 109. Cuna, A. *et al.* NEC-like intestinal injury is ameliorated by *Lactobacillus rhamnosus* GG in parallel with SIGIRR and A20 induction in neonatal mice. *Pediatr. Res.* **88**, 546–555 (2020).
 110. Ganguli, K. *et al.* Probiotics prevent necrotizing enterocolitis by modulating enterocyte genes that regulate innate immune-mediated inflammation. *Am. J. Physiol. Gastrointest. Liver Physiol.* **304**, G132-41 (2013).
 111. Gomart, A., Vallée, A. & Lecarpentier, Y. Necrotizing Enterocolitis: LPS/TLR4-Induced Crosstalk Between Canonical TGF- β /Wnt/ β -Catenin Pathways and PPAR γ . *Front. Pediatr.* **9**, (2021).
 112. Good, M. *et al.* Breast milk protects against the development of necrotizing enterocolitis through inhibition of Toll-like receptor 4 in the intestinal epithelium via activation of the epidermal growth factor receptor. *Mucosal Immunol.* **8**, 1166–1179 (2015).
 113. Dellar, E. R., Hill, C., Melling, G. E., Carter, D. R. F. & Baena-Lopez, L. A. Unpacking extracellular vesicles: RNA cargo loading and function. *J. Extracell. Biol.* **1**, e40 (2022).
 114. Yates, A. G. *et al.* In sickness and in health: The functional role of extracellular vesicles in physiology and pathology in vivo: Part I: Health and Normal Physiology: Part I: Health and Normal Physiology. *J. Extracell. vesicles* **11**, e12151 (2022).
 115. Gleeson, J. P. *et al.* Profiling of mature-stage human breast milk cells identifies six unique lactocyte subpopulations. *Sci. Adv.* **8**, eabm6865 (2023).
 116. Arya, S. B., Collie, S. P. & Parent, C. A. The ins-and-outs of exosome biogenesis, secretion, and internalization. *Trends Cell Biol.* **34**, 90–108 (2024).
 117. Niel, G. van, D'Angelo, G. & Raposo, G. Shedding Light on the Cell Biology of

- Extracellular Vesicles. *Nat. Rev. Mol. Cell Biol.* **19**, 213–228 (2018).
118. Hessvik, N. P. & Llorente, A. Current knowledge on exosome biogenesis and release. *Cell. Mol. Life Sci.* **75**, 193–208 (2018).
 119. Jeppesen, D. K. *et al.* Reassessment of exosome composition. *Cell* **177**, 428–445.e18 (2019).
 120. Park, S. J. *et al.* Molecular Mechanisms of Biogenesis of Apoptotic Exosome-Like Vesicles and Their Roles as Damage-Associated Molecular Patterns. *Proc. Natl. Acad. Sci.* **115**, (2018).
 121. Tosar, J. P., Cayota, A. & Witwer, K. Exomeres and supermeres: Monolithic or diverse? *J. Extracell. Biol.* **1**, e45 (2022).
 122. Zhang, Q., Jeppesen, D. K., Higginbotham, J. N., Franklin, J. L. & Coffey, R. J. Comprehensive isolation of extracellular vesicles and nanoparticles. *Nat. Protoc.* **18**, 1462–1487 (2023).
 123. Larios, J., Mercier, V., Roux, A. & Grünberg, J. ALIX- And ESCRT-III–dependent Sorting of Tetraspanins to Exosomes. *J. Cell Biol.* **219**, (2020).
 124. Vietri, M., Radulovic, M. & Stenmark, H. The Many Functions of ESCRTs. *Nat. Rev. Mol. Cell Biol.* **21**, 25–42 (2019).
 125. O’Brien, K. P., Ughetto, S., Mahjoub, S., Nair, A. V & Breakefield, X. O. Uptake, Functionality, and Re-Release of Extracellular Vesicle-Encapsulated Cargo. *Cell Rep.* **39**, 110651 (2022).
 126. Liao, Y., Du, X., Li, J. & Lönnerdal, B. Human milk exosomes and their microRNAs survive digestion in vitro and are taken up by human intestinal cells. *Mol. Nutr. Food Res.* **61**, 1700082 (2017).
 127. Golan-Gerstl, R. *et al.* Characterization and biological function of milk-derived miRNAs. *Mol. Nutr. Food Res.* **61**, 1700009 (2017).
 128. Baier, S. R., Nguyen, C., Xie, F., Wood, J. R. & Zemleni, J. MicroRNAs are absorbed in biologically meaningful amounts from nutritionally relevant doses of cow milk and affect gene expression in peripheral blood mononuclear cells, HEK-293 kidney cell cultures, and mouse livers. *J. Nutr.* **144**, 1495–1500 (2014).
 129. Kusuma, R. J. *et al.* Human vascular endothelial cells transport foreign exosomes from cow’s milk by endocytosis. *Am. J. Physiol. - Cell Physiol.* **310**, C800–C807 (2016).

130. Lässer, C. *et al.* Human saliva, plasma and breast milk exosomes contain RNA: uptake by macrophages. *J. Transl. Med.* **9**, 9 (2011).
131. Wolf, T., Baier, S. R. & Zempleni, J. The intestinal transport of bovine milk exosomes Is mediated by endocytosis in human colon carcinoma caco-2 cells and rat small intestinal IEC-6 cells. *J. Nutr.* **145**, 2201–2206 (2015).
132. Manca, S. *et al.* Milk exosomes are bioavailable and distinct microRNA cargos have unique tissue distribution patterns. *Sci. Rep.* **8**, (2018).
133. Rani, P. *et al.* Milk miRNAs encapsulated in exosomes are stable to human digestion and permeable to intestinal barrier in vitro. *J. Funct. Foods* **34**, 431–439 (2017).
134. Zhou, F. *et al.* Small extracellular vesicles in milk cross the blood-brain barrier in murine cerebral cortex endothelial cells and promote dendritic complexity in the hippocampus and brain function in C57BL/6J mice. *Front. Nutr.* **9**, 838543 (2022).
135. Zempleni, J. Milk exosomes: beyond dietary microRNAs. *Genes Nutr.* **12**, 12 (2017).
136. Rani, P., Yenuganti, V. R., Shandilya, S., Onteru, S. K. & Singh, D. miRNAs: The hidden bioactive component of milk. *Trends Food Sci. Technol.* **65**, 94–102 (2017).
137. Tong, L. *et al.* Milk-derived extracellular vesicles protect intestinal barrier integrity in the gut-liver axis. *Sci. Adv.* **9**, eade5041 (2023).
138. Khanam, A., Ngu, A. & Zempleni, J. Bioavailability of orally administered small extracellular vesicles from bovine milk in C57BL/6J mice. *Int. J. Pharm.* **639**, 122974 (2023).
139. Imai, T. *et al.* Macrophage-dependent clearance of systemically administered B16BL6-derived exosomes from the blood circulation in mice. *J. Extracell. vesicles* **4**, 26238 (2015).
140. Ngu, A., Munir, J. & Zempleni, J. Milk-borne small extracellular vesicles: kinetics and mechanisms of transport, distribution, and elimination. *Extracell. vesicles Circ. nucleic acids* **4**, 339–346 (2023).
141. Viola, M. F. & Boeckxstaens, G. Intestinal resident macrophages: Multitaskers of the gut. *Neurogastroenterol. Motil.* **32**, e13843 (2020).
142. Admyre, C. *et al.* Exosomes with immune modulatory features are present in human breast milk. *J. Immunol.* **179**, 1969–78 (2007).
143. de la Torre Gomez, C., Goreham, R. V., Bech Serra, J. J., Nann, T. & Kussmann, M.

- “Exosomics”—A review of biophysics, biology and biochemistry of exosomes With a focus on human breast milk. *Front. Genet.* **9**, 92 (2018).
144. Wang, X. *et al.* Identification and peptidomic profiling of exosomes in preterm human milk: insights into necrotizing enterocolitis prevention. *Mol. Nutr. Food Res.* 1801247 (2019).
 145. Hock, A. *et al.* Breast milk-derived exosomes promote intestinal epithelial cell growth. *J. Pediatr. Surg.* **52**, 755–759 (2017).
 146. Reif, S., Elbaum Shiff, Y. & Golan-Gerstl, R. Milk-derived exosomes (MDEs) have a different biological effect on normal fetal colon epithelial cells compared to colon tumor cells in a miRNA-dependent manner. *J. Transl. Med.* **17**, (2019).
 147. Martin, C., Patel, M., Williams, S., Arora, H. & Sims, B. Human breast milk-derived exosomes attenuate cell death in intestinal epithelial cells. *Innate Immun.* **24**, 278–284 (2018).
 148. Qin, W. *et al.* Biology of human tumors exosomes in human breast milk promote EMT. *Clin Cancer Res* **22**, (2016).
 149. Kalluri, R. & Weinberg, R. A. The basics of epithelial-mesenchymal transition. *J. Clin. Invest.* **119**, 1420–1428 (2009).
 150. Hofman, P. & Vouret-Craviari, V. Microbes-induced EMT at the crossroad of inflammation and cancer. *Gut Microbes* **3**, 176–185 (2012).
 151. Pisano, C. *et al.* Human breast milk-derived extracellular vesicles in the protection against experimental necrotizing enterocolitis. *J. Pediatr. Surg.* **55**, 54–58 (2020).
 152. Hu, X. *et al.* Comparison and investigation of exosomes from human amniotic fluid stem cells and human breast milk in alleviating neonatal necrotizing enterocolitis. *Stem Cell Rev. Reports* **19**, 754–766 (2023).
 153. Reif, S. *et al.* Cow and human milk-derived exosomes ameliorate colitis in DSS murine model. *Nutrients* **12**, (2020).
 154. Miyake, H. *et al.* Human breast milk exosomes attenuate intestinal damage. *Pediatr. Surg. Int.* **36**, 155–163 (2020).
 155. Guo, M., Zhang, K. & Zhang, J. Human breast milk-derived exosomal miR-148a-3p protects against necrotizing enterocolitis by regulating p53 and Sirtuin 1. *Inflammation* **45**, 1254–1268 (2022).

156. He, S., Liu, G. & Zhu, X. Human breast milk-derived exosomes may help maintain intestinal epithelial barrier integrity. *Pediatr. Res.* **90**, 366–372 (2021).
157. Torrez Lamberti, M. F., Parker, L. A., Gonzalez, C. F. & Lorca, G. L. Pasteurization of human milk affects the miRNA cargo of EVs decreasing its immunomodulatory activity. *Sci. Rep.* **13**, 10057 (2023).
158. Karra, N., Van Herwijnen, M. J. C., Wauben, M. H. M., Swindle, E. J. & Morgan, H. Human milk extracellular vesicles preserve bronchial epithelial barrier integrity and reduce TLR3-induced inflammation in vitro. *J. Extracell. Biol.* **1**, e54 (2022).
159. Zonneveld, M. I. *et al.* Human milk extracellular vesicles target nodes in interconnected signalling pathways that enhance oral epithelial barrier function and dampen immune responses. *J. Extracell. Vesicles* **10**, e12071 (2021).
160. Cho, Y.-E. *et al.* Human breast milk EVs mitigate endothelial dysfunction: Preliminary study. *bioRxiv* 2024.05.20.594769 (2024).
161. Ascanius, S. R., Hansen, M. S., Ostefeld, M. S. & Rasmussen, J. T. Milk-derived extracellular vesicles suppress inflammatory cytokine expression and nuclear factor- κ B activation in lipopolysaccharide-stimulated macrophages. *Dairy* vol. 2 165–178 (2021).
162. Azaryan, E. *et al.* Effect of HM-Exos on the migration and inflammatory response of LPS-exposed dental pulp stem cells. *BMC Oral Health* **23**, 95 (2023).
163. Gao, R. *et al.* A comparison of exosomes derived from different periods breast milk on protecting against intestinal organoid injury. *Pediatr. Surg. Int.* **35**, 1363–1368 (2019).
164. Wang, L. *et al.* Human breast milk-derived exosomes protect against intestinal ischemia and reperfusion injury in neonatal rats. *J. Pediatr. Surg.* **57**, 1264–1268 (2022).
165. Melnik, B. C., John, S. & Schmitz, G. Milk: an exosomal microRNA transmitter promoting thymic regulatory T cell maturation preventing the development of atopy? *J. Transl. Med.* **12**, 43 (2014).
166. Yang, M. *et al.* Comparative proteomic analysis of milk-derived exosomes in human and bovine colostrum and mature milk samples by iTRAQ-coupled LC-MS/MS. *Food Res. Int.* **92**, 17–25 (2017).
167. Van Herwijnen, M. J. C. *et al.* Comprehensive proteomic analysis of human milk-derived extracellular vesicles unveils a novel functional proteome distinct from other milk components. *Mol. Cell. Proteomics* **15**, 3412–3423 (2016).

168. Larssen, P. *et al.* Tracing cellular origin of human exosomes using multiplex proximity extension assays. *Mol. Cell. Proteomics* **16**, 502–511 (2017).
169. Chen, W. *et al.* The emerging role of exosomes in the pathogenesis, prognosis and treatment of necrotizing enterocolitis. *Am. J. Transl. Res.* **12**, 7020–7033 (2020).
170. Civra, A. *et al.* Human colostrum and derived extracellular vesicles prevent infection by human rotavirus and respiratory syncytial virus in vitro. *J. Hum. Lact.* **37**, 122–134 (2021).
171. Shiff, Y. E. *et al.* MiRNA-320a is less expressed and miRNA-148a more expressed in preterm human milk compared to term human milk. *J. Funct. Foods* **57**, 68–74 (2019).
172. Ma, L. *et al.* Human breast milk exosomal miRNAs are influenced by premature delivery and affect neurodevelopment. *Mol. Nutr. Food Res.* **68**, 2300113 (2024).
173. Kahn, S. *et al.* Exosomal microRNAs in milk from mothers delivering preterm infants survive in vitro digestion and are taken up by human intestinal cells. *Mol. Nutr. Food Res.* **62**, 1701050 (2018).
174. Carney, M. C. *et al.* Metabolism-related microRNAs in maternal breast milk are influenced by premature delivery. *Pediatr. Res.* **82**, 226–236 (2017).
175. Floris, I. *et al.* MiRNA analysis by quantitative PCR in preterm human breast milk reveals daily fluctuations of hsa-miR-16-5p. *PLoS One* **10**, e0140488 (2015).
176. Floris, I., Kraft, J. & Altosaar, I. Roles of microRNA across prenatal and postnatal periods. *Int. J. Mol. Sci.* **17**, 1994 (2016).
177. Sun, J. *et al.* MicroRNA expression profiles of bovine milk exosomes in response to *Staphylococcus aureus* infection. *BMC Genomics* **16**, (2015).
178. Sun, Q. *et al.* Immune modulatory function of abundant immune-related microRNAs in microvesicles from bovine colostrum. *Protein Cell* **4**, 197–210 (2013).
179. Zhou, Q. *et al.* Immune-related microRNAs are abundant in breast milk exosomes. *Int. J. Biol. Sci.* **8**, 118–123 (2011).
180. Kosaka, N., Izumi, H., Sekine, K. & Ochiya, T. microRNA as a new immune-regulatory agent in breast milk. *Silence* **1**, 7 (2010).
181. Na, R. S. *et al.* Expressional analysis of immune-related miRNAs in breast milk. *Genet. Mol. Res.* **14**, 11371–11376 (2015).
182. Hanna, J., Hossain, G. S. & Kocerha, J. The potential for microRNA therapeutics and

- clinical research. *Frontiers in Genetics* vol. 10 (2019).
183. Zhou, Q. *et al.* Immune-related microRNAs are abundant in breast milk exosomes. *Int. J. Biol. Sci.* **8**, 118–23 (2012).
 184. Mirza, A. H. *et al.* Breast milk-derived extracellular vesicles enriched in exosomes from mothers with type 1 diabetes contain aberrant levels of microRNAs. *Front. Immunol.* **10**, (2019).
 185. Ojo-Okunola, A., Cacciatore, S., Nicol, M. P. & du Toit, E. The determinants of the human milk metabolome and its role in infant health. *Metabolites* **10**, (2020).
 186. Puhka, M. *et al.* Metabolomic profiling of extracellular vesicles and alternative normalization methods reveal enriched metabolites and strategies to study prostate cancer-related changes. *Theranostics* **7**, 3824–3841 (2017).
 187. Zebrowska, A., Skowronek, A., Wojakowska, A., Widlak, P. & Pietrowska, M. Metabolome of exosomes: Focus on vesicles released by cancer cells and present in human body fluids. *Int. J. Mol. Sci.* **20**, 3461 (2019).
 188. Williams, C., Palviainen, M., Reichardt, N.-C., Siljander, P. R.-M. & Falcón-Pérez, J. M. Metabolomics applied to the study of extracellular vesicles. *Metabolites* **9**, (2019).
 189. Zhao, H. *et al.* Tumor microenvironment derived exosomes pleiotropically modulate cancer cell metabolism. *Elife* **5**, e10250 (2016).
 190. Mecocci, S. *et al.* Anti-inflammatory potential of cow, donkey and goat milk extracellular vesicles as revealed by metabolomic profile. *Nutrients* **12**, 2908 (2020).
 191. Chen, W. *et al.* Lipidomic profiling of human milk derived exosomes and their emerging roles in the prevention of necrotizing enterocolitis. *Mol. Nutr. Food Res.* **n/a**, 2000845 (2021).
 192. Cargnello, M. & Roux, P. P. Activation and function of the MAPKs and their substrates, the MAPK-activated protein kinases. *Microbiol. Mol. Biol. Rev.* **75**, 50–83 (2011).
 193. Herrmann, K. & Carroll, K. An exclusively human milk diet reduces necrotizing enterocolitis. *Breastfeed. Med.* **9**, 184–190 (2014).
 194. Ward, T. L., Hosid, S., Ioshikhes, I. & Altosaar, I. Human milk metagenome: A functional capacity analysis. *BMC Microbiology* vol. 13 1–12 (2013).
 195. Floris, I., Kraft, J. D. & Altosaar, I. Roles of microRNA across prenatal and postnatal periods. *International Journal of Molecular Sciences* vol. 17 (2016).

196. Spong, C. Y. *et al.* Timing of indicated late-preterm and early-term birth. *Obstet. Gynecol.* **118**, 323–333 (2011).
197. Molinari, C. E. *et al.* Proteome mapping of human skim milk proteins in term and preterm milk. *J. Proteome Res.* **11**, 1696–1714 (2012).
198. Cattaneo, C. *et al.* Analysis of toll-like receptors in human milk: Detection of membrane-bound and soluble forms. *J. Immunol. Res.* **2019**, 4078671 (2019).
199. Wan, J. *et al.* Peptidome analysis of human skim milk in term and preterm milk. *Biochem. Biophys. Res. Commun.* **438**, 236–241 (2013).
200. Dallas, D. C., Murray, N. M. & Gan, J. Proteolytic systems in milk: Perspectives on the evolutionary function within the mammary gland and the infant. *J. Mammary Gland Biol. Neoplasia* **20**, 133–147 (2015).
201. Dvorak, B., Fituch, C. C., Williams, C. S., Hurst, N. M. & Schanler, R. J. Increased epidermal growth factor levels in human milk of mothers with extremely premature infants. *Pediatr. Res.* **54**, 15–19 (2003).
202. Montagne, P., Cuillière, M. L., Molé, C., Béné, M. C. & Faure, G. Immunological and nutritional composition of human milk in relation to prematurity and mothers' parity during the first 2 weeks of lactation. *J. Pediatr. Gastroenterol. Nutr.* **29**, (1999).
203. Ronayne de Ferrer, P. A., Baroni, A., Sambucetti, M. E., López, N. E. & Ceriani Cernadas, J. M. Lactoferrin levels in term and preterm milk. *J. Am. Coll. Nutr.* **19**, 370–373 (2021).
204. Hu, Y., Thaler, J. & Nieuwland, R. Extracellular vesicles in human milk. *Pharmaceuticals (Basel)*. **14**, (2021).
205. Leiferman, A., Shu, J., Upadhyaya, B., Cui, J. & Zempleni, J. Storage of extracellular vesicles in human milk, and microRNA profiles in human milk exosomes and infant formulas. *J. Pediatr. Gastroenterol. Nutr.* **69**, 235–238 (2019).
206. Alsaweed, M., Hartmann, P. E., Geddes, D. T. & Kakulas, F. Micronas in breastmilk and the lactating breast: Potential immunoprotectors and developmental regulators for the infant and the mother. *Int. J. Environ. Res. Public Health* **12**, 13981–4020 (2015).
207. Herwijnen, M. J. C. van *et al.* Abundantly present mirnas in milk-derived extracellular vesicles are conserved between mammals. *Frontiers in Nutrition* vol. 5 81 (2018).
208. Kupsco, A. *et al.* Human milk extracellular vesicle miRNA expression and associations

- with maternal characteristics in a population-based cohort from the Faroe Islands. *Sci. Rep.* **11**, 5840 (2021).
209. Do, D. N., Li, R., Dudemaine, P.-L. & Ibeagha-Awemu, E. M. MicroRNA roles in signalling during lactation: an insight from differential expression, time course and pathway analyses of deep sequence data. *Sci. Rep.* **7**, 44605 (2017).
 210. Shu, J., Chiang, K., Zemleni, J. & Cui, J. Computational Characterization of Exogenous MicroRNAs that Can Be Transferred into Human Circulation. *PLoS One* **10**, e0140587 (2015).
 211. Lefèvre, C., Venkat, P., Kumar, A., Modepalli, V. & Nicholas, K. R. Comparative analysis of milk microRNA in the therian lineage highlights the evolution of lactation. *Reprod. Fertil. Dev.* **31**, 1266 (2019).
 212. Zhou, Y. *et al.* Exosomal circRNAs contribute to intestinal development via the VEGF signalling pathway in human term and preterm colostrum. *Aging (Albany, NY)*. **13**, 11218–11233 (2021).
 213. He, B., Shi, J., Wang, X., Jiang, H. & Zhu, H. J. Label-free absolute protein quantification with data-independent acquisition. *J. Proteomics* **200**, 51–59 (2019).
 214. Meyer, J. Fast proteome identification and quantification from data-dependent acquisition–tandem mass spectrometry (DDA MS/MS) using free software tools. *Methods Protoc.* **2**, 8 (2019).
 215. Vahkal, B. *et al.* Review of methodological approaches to human milk small extracellular vesicle proteomics. *Biomolecules* **11**, (2021).
 216. Pluchino, S. & Smith, J. A. Explicating exosomes: Reclassifying the rising stars of intercellular communication. *Cell* vol. 177 225–227 (2019).
 217. Théry, C. *et al.* Minimal information for studies of extracellular vesicles 2018 (MISEV2018): a position statement of the International Society for Extracellular Vesicles and update of the MISEV2014 guidelines. *J. Extracell. Vesicles* **7**, 1535750 (2018).
 218. Chutipongtanate, S. & Greis, K. D. Multiplex biomarker screening assay for urinary extracellular vesicles study: A targeted label-free proteomic approach. *Sci. Rep.* **8**, (2018).
 219. Shao, D. *et al.* HBFP: a new repository for human body fluid proteome. *Database* **2021**, baab065 (2021).
 220. Castellote, C. *et al.* Premature delivery influences the immunological composition of

- colostrum and transitional and mature human milk. *J. Nutr.* **141**, 1181–1187 (2011).
221. bioinformatics.psb.ugent.be/venn.
222. Nielsen, S. D., Beverly, R. L., Underwood, M. A. & Dallas, D. C. Differences and similarities in the peptide profile of preterm and term mother’s milk, and preterm and term infant gastric samples. *Nutrients* vol. 12 (2020).
223. Zhang, F., Ge, W., Ruan, G., Cai, X. & Guo, T. Data-independent acquisition mass spectrometry-based proteomics and software tools: A glimpse in 2020. *Proteomics* **20**, 1900276 (2020).
224. Whitman, J. D. & Lynch, K. L. Optimization and comparison of information-dependent acquisition (IDA) to sequential window acquisition of all theoretical fragment ion spectra (SWATH) for high-resolution mass spectrometry in clinical toxicology. (2019).
225. Freiría-Martínez, L. *et al.* Proteomic analysis of exosomes derived from human mature milk and colostrum of mothers with term, late preterm, or very preterm delivery. *Anal. Methods* **15**, 4905–4917 (2023).
226. Boehmer, J. L. *et al.* The proteomic advantage: Label-free quantification of proteins expressed in bovine milk during experimentally induced coliform mastitis. *Vet. Immunol. Immunopathol.* **138**, 252–266 (2010).
227. Dallas, D. C. *et al.* Extensive in vivo human milk peptidomics reveals specific proteolysis yielding protective antimicrobial peptides. *J. Proteome Res.* **12**, 2295–2304 (2013).
228. Silverman, G. A. *et al.* The serpins are an expanding superfamily of structurally similar but functionally diverse proteins. Evolution, mechanism of inhibition, novel functions, and a revised nomenclature. *J. Biol. Chem.* **276**, 33293–33296 (2001).
229. Ménard, D. *et al.* Anti-inflammatory effects of epidermal growth factor on the immature human intestine. *Physiol. Genomics* **44**, 268–280 (2012).
230. Dallas, D. C., Underwood, M. A., Zivkovic, A. M. & German, J. B. Digestion of protein in premature and term infants. *J. Nutr. Disord. Ther.* **2**, 112 (2012).
231. Santoro, A. *et al.* SERPINE2 inhibits IL-1 α -induced MMP-13 expression in human chondrocytes: Involvement of ERK/NF- κ B/AP-1 pathways. *PLoS One* **10**, e0135979 (2015).
232. Liedel, J. L. *et al.* Mother’s milk-induced hsp70 expression preserves intestinal epithelial barrier function in an immature rat pup model. *Pediatr. Res.* **69**, 395–400 (2011).

233. Pistritto, G. *et al.* Expression and transcriptional regulation of caspase-14 in simple and complex epithelia. *Cell Death Differ.* **9**, 995–1006 (2002).
234. Denecker, G., Ovaere, P., Vandenabeele, P. & Declercq, W. Caspase-14 reveals its secrets. *J. Cell Biol.* **180**, 451–458 (2008).
235. Markiewicz, A., Sigorski, D., Markiewicz, M., Owczarczyk-Saczonek, A. & Placek, W. Caspase-14-From biomolecular basics to clinical approach. A review of available data. *Int. J. Mol. Sci.* **22**, (2021).
236. Abuharbeid, S., Czubayko, F. & Aigner, A. The fibroblast growth factor-binding protein FGF-BP. *Int. J. Biochem. Cell Biol.* **38**, 1463–1468 (2006).
237. Schiavinato, A. *et al.* EMILIN-3, peculiar member of elastin microfibril interface-located protein (EMILIN) family, has distinct expression pattern, forms oligomeric assemblies, and serves as transforming growth factor β (TGF- β) antagonist. *J. Biol. Chem.* **287**, 11498–11515 (2012).
238. Cho, S. X., Berger, P. J., Nold-Petry, C. A. & Nold, M. F. The immunological landscape in necrotising enterocolitis. *Expert Rev. Mol. Med.* **18**, e12 (2016).
239. Torres-Castro, P. *et al.* Modulation of the systemic immune response in suckling rats by breast milk TGF- β 2, EGF and FGF21 supplementation. *Nutrients* **12**, 1888 (2020).
240. Colitti, M. BCL-2 family of proteins and mammary cellular fate. *Anat. Histol. Embryol.* **41**, 237–247 (2012).
241. Zou, Y.-R., Kottmann, A. H., Kuroda, M., Taniuchi, I. & Littman, D. R. Function of the chemokine receptor CXCR4 in haematopoiesis and in cerebellar development. *Nature* **393**, 595–599 (1998).
242. Shalekoff, S., Gray, G. E. & Tiemessen, C. T. Age-related changes in expression of CXCR4 and CCR5 on peripheral blood leukocytes from uninfected infants born to human immunodeficiency virus type 1-infected mothers. *Clin. Diagn. Lab. Immunol.* **11**, 229–234 (2004).
243. Savulescu, D. M. *et al.* HLA antibody repertoire in infants suggests selectivity in transplacental crossing. *Am. J. Reprod. Immunol.* **84**, e13264 (2020).
244. Bhattacharjee, P. *et al.* Functional compensation of glutathione S-transferase M1 (GSTM1) null by another GST superfamily member, GSTM2. *Sci. Rep.* **3**, 2704 (2013).
245. Sharma, R., Yang, Y., Sharma, A., Awasthi, S. & Awasthi, Y. C. Antioxidant role of

- glutathione S-transferases: protection against oxidant toxicity and regulation of stress-mediated apoptosis. *Antioxid. Redox Signal.* **6**, 289–300 (2004).
246. Doare, K. Le, Holder, B., Bassett, A. & Pannaraj, P. S. Mother's Milk: A purposeful contribution to the development of the infant microbiota and immunity. *Frontiers in Immunology* (2018).
 247. Zhou, J.-K., Fan, X., Cheng, J., Liu, W. & Peng, Y. PDLIM1: Structure, function and implication in cancer. *Cell Stress* **5**, 119–127 (2021).
 248. Sharp, J. A., Lefèvre, C., Watt, A. & Nicholas, K. R. Analysis of human breast milk cells: gene expression profiles during pregnancy, lactation, involution, and mastitic infection. *Funct. Integr. Genomics* **16**, 297–321 (2016).
 249. Johnson, K. E. *et al.* Human milk variation is shaped by maternal genetics and impacts the infant gut microbiome. *bioRxiv* 2023.01.24.525211 (2023).
 250. Zhou, L. *et al.* Glycoprotein non-metastatic melanoma protein b (Gpnmb) is highly expressed in macrophages of acute injured kidney and promotes M2 macrophages polarization. *Cell. Immunol.* **316**, 53–60 (2017).
 251. Zhang, H. *et al.* GPNMB plays an active role in the M1/M2 balance. *Tissue Cell* **74**, 101683 (2022).
 252. Giovanazzi, A., van Herwijnen, M. J. C., Kleinjan, M., van der Meulen, G. N. & Wauben, M. H. M. Surface protein profiling of milk and serum extracellular vesicles unveils body fluid-specific signatures. *Sci. Rep.* **13**, 8758 (2023).
 253. Yamada, T., Inoshima, Y., Matsuda, T. & Ishiguro, N. Comparison of methods for isolating exosomes from bovine milk. *NOTE Clin. Pathol. J. Vet. Med. Sci* **74**, 1523–1525 (2012).
 254. Zhou, M., Weber, S. R., Zhao, Y., Chen, H. & Sundstrom, J. M. Methods for exosome isolation and characterization. in *Exosomes* 23–38 (Elsevier, 2020).
 255. Jung, H. H., Kim, J.-Y., Lim, J. E. & Im, Y.-H. Cytokine profiling in serum-derived exosomes isolated by different methods. *Sci. Rep.* **10**, 14069 (2020).
 256. Gagné, D. *et al.* Proteomics profiling of stool samples from preterm neonates with SWATH/DIA mass spectrometry for predicting necrotizing enterocolitis. *International Journal of Molecular Sciences* vol. 23 (2022).
 257. Adusumilli, R. & Mallick, P. Data conversion with ProteoWizard msConvert. *Methods*

- Mol. Biol.* **1550**, 339–368 (2017).
258. Kong, A. T., Lerevost, F. V, Avtonomov, D. M., Mellacheruvu, D. & Nesvizhskii, A. I. MSFragger: ultrafast and comprehensive peptide identification in mass spectrometry–based proteomics. *Nat. Methods* **14**, 513–520 (2017).
 259. da Veiga Lerevost, F. *et al.* Philosopher: a versatile toolkit for shotgun proteomics data analysis. *Nat. Methods* **17**, 869–870 (2020).
 260. Demichev, V., Messner, C. B., Vernardis, S. I., Lilley, K. S. & Ralser, M. DIA-NN: neural networks and interference correction enable deep proteome coverage in high throughput. *Nat. Methods* **17**, 41–44 (2020).
 261. Ashburner, M. *et al.* Gene Ontology: tool for the unification of biology. *Nat. Genet.* **25**, 25–29 (2000).
 262. Aleksander, S. A. *et al.* The Gene Ontology knowledgebase in 2023. *Genetics* **224**, (2023).
 263. Ewels, P. A. *et al.* The nf-core framework for community-curated bioinformatics pipelines. *Nature Biotechnology* vol. 38 276–278 (2020).
 264. Di Tommaso, P. *et al.* Nextflow enables reproducible computational workflows. *Nature Biotechnology* vol. 35 316–319 (2017).
 265. Dobin, A. *et al.* STAR: ultrafast universal RNA-seq aligner. *Bioinformatics* **29**, 15–21 (2013).
 266. Liao, Y., Smyth, G. K. & Shi, W. featureCounts: an efficient general purpose program for assigning sequence reads to genomic features. *Bioinformatics* **30**, 923–930 (2014).
 267. Risso, D., Ngai, J., Speed, T. P. & Dudoit, S. Normalization of RNA-seq data using factor analysis of control genes or samples. *Nat. Biotechnol.* **32**, 896–902 (2014).
 268. Peixoto, L. *et al.* How data analysis affects power, reproducibility and biological insight of RNA-seq studies in complex datasets. *Nucleic Acids Res.* **43**, 7664–7674 (2015).
 269. Wu, T. *et al.* clusterProfiler 4.0: A universal enrichment tool for interpreting omics data. *Innov.* **2**, 100141 (2021).
 270. Liberzon, A. *et al.* Molecular signatures database (MSigDB) 3.0. *Bioinformatics* **27**, 1739–1740 (2011).
 271. Subramanian, A. *et al.* Gene set enrichment analysis: a knowledge-based approach for interpreting genome-wide expression profiles. *Proc. Natl. Acad. Sci. U. S. A.* **102**, 15545–

- 15550 (2005).
272. Vahkal, B. *et al.* Gestational age at birth influences protein and RNA content in human milk extracellular vesicles. *J. Extracell. Biol.* **3**, e128 (2024).
273. Gephart, S. M., McGrath, J. M., Effken, J. A. & Halpern, M. D. Necrotizing enterocolitis risk: state of the science. *Adv. neonatal care Off. J. Natl. Assoc. Neonatal Nurses* **12**, 77–79 (2012).
274. Yee, W. H. *et al.* Incidence and timing of presentation of necrotizing enterocolitis in preterm infants. *Pediatrics* **129**, e298–e304 (2012).
275. Melnik, B. C., Stremmel, W., Weiskirchen, R., John, S. M. & Schmitz, G. Exosome-derived microRNAs of human milk and their effects on infant health and development. *Biomolecules* vol. 11 (2021).
276. Chiba, T. *et al.* Expression profiles of hsa-miR-148a-3p and hsa-miR-125b-5p in human breast milk and infant formulae. *Int. Breastfeed. J.* **17**, 1 (2022).
277. Wu, F. *et al.* Exploration of microRNA profiles in human colostrum. *Ann. Transl. Med.* **8**, 1170 (2020).
278. Wu, D. *et al.* Dietary depletion of milk exosomes and their microRNA cargos elicits a depletion of miR-200a-3p and elevated intestinal inflammation and chemokine (C-X-C Motif) ligand 9 expression in *Mdr1a(-/-)* mice. *Curr. Dev. Nutr.* **3**, nzz122 (2019).
279. Ng, P. C. *et al.* Comparative miRNA expressional profiles and molecular networks in human small bowel tissues of necrotizing enterocolitis and spontaneous intestinal perforation. *PLoS One* **10**, e0135737 (2015).
280. Huntzinger, E. & Izaurralde, E. Gene silencing by microRNAs: contributions of translational repression and mRNA decay. *Nat. Rev. Genet.* **12**, 99–110 (2011).
281. Diener, C., Keller, A. & Meese, E. The miRNA–target interactions: An underestimated intricacy. *Nucleic Acids Res.* gkad1142 (2023).
282. Bartel, D. P. MicroRNAs: Target recognition and regulatory functions. *Cell* **136**, 215–233 (2009).
283. Wu, S. *et al.* Multiple microRNAs modulate p21Cip1/Waf1 expression by directly targeting its 3' untranslated region. *Oncogene* **29**, 2302–2308 (2010).
284. Raymond, F. *et al.* Longitudinal human milk miRNA composition over the first 3 mo of lactation in a cohort of healthy mothers delivering term infants. *J. Nutr.* **152**, 94–106

- (2022).
285. Na, R. S. *et al.* Expressional analysis of immune-related miRNAs in breast milk. *Genet. Mol. Res.* **14**, 11371–11376 (2015).
 286. Fidler, G. *et al.* Circulating microRNA sequencing revealed miRNome patterns in hematology and oncology patients aiding the prognosis of invasive aspergillosis. *Sci. Rep.* **12**, 7144 (2022).
 287. Quillet, A. *et al.* Improving bioinformatics prediction of microRNA targets by ranks aggregation. *Frontiers in Genetics* vol. 10 (2020).
 288. Liu, J. *et al.* Wnt/ β -catenin signalling: function, biological mechanisms, and therapeutic opportunities. *Signal Transduct. Target. Ther.* **7**, 3 (2022).
 289. Kaeffer, B. Human breast milk miRNAs: Their diversity and potential for preventive strategies in nutritional therapy. *Int. J. Mol. Sci.* **24**, (2023).
 290. Alsaweed, M., Lai, C. T., Hartmann, P. E., Geddes, D. T. & Kakulas, F. Human milk miRNAs primarily originate from the mammary gland resulting in unique miRNA profiles of fractionated milk. *Sci. Rep.* **6**, 20680 (2016).
 291. Hicks, S. D., Confair, A., Warren, K. & Chandran, D. Levels of breast milk microRNAs and other non-Coding RNAs are impacted by milk maturity and maternal diet. *Frontiers in Immunology* vol. 12 (2022).
 292. Tremblay, É. *et al.* Gene expression profiling in necrotizing enterocolitis reveals pathways common to those reported in Crohn's disease. *BMC Med. Genomics* **9**, 6 (2016).
 293. Friedman, R. C., Farh, K. K.-H., Burge, C. B. & Bartel, D. P. Most mammalian mRNAs are conserved targets of microRNAs. *Genome Res.* **19**, 92–105 (2009).
 294. Ren, L.-L. *et al.* The distinct role of strand-specific miR-514b-3p and miR-514b-5p in colorectal cancer metastasis. *Cell Death Dis.* **9**, 687 (2018).
 295. Mitra, R., Lin, C.-C., Eischen, C. M., Bandyopadhyay, S. & Zhao, Z. Concordant dysregulation of miR-5p and miR-3p arms of the same precursor microRNA may be a mechanism in inducing cell proliferation and tumorigenesis: a lung cancer study. *RNA* **21**, 1055–1065 (2015).
 296. Li, T. *et al.* Activation of mucosal insulin receptor exacerbates intestinal inflammation by promoting tissue resident memory T cells differentiation through EZH2. *J. Transl. Med.* **22**, 78 (2024).

297. Khoramjoo, S. M. *et al.* Overview of three proliferation pathways (Wnt, Notch, and Hippo) in intestine and immune system and their role in inflammatory bowel diseases (IBDs). *Frontiers in Medicine* vol. 9 (2022).
298. Yilmaz, Ö. H. *et al.* mTORC1 in the Paneth cell niche couples intestinal stem-cell function to calorie intake. *Nature* **486**, 490–495 (2012).
299. Jiang, H., Grenley, M. O., Bravo, M.-J., Blumhagen, R. Z. & Edgar, B. A. EGFR/Ras/MAPK signaling mediates adult midgut epithelial homeostasis and regeneration in drosophila. *Cell Stem Cell* **8**, 84–95 (2011).
300. Yan, H. & Ajuwon, K. M. Butyrate modifies intestinal barrier function in IPEC-J2 cells through a selective upregulation of tight junction proteins and activation of the Akt signaling pathway. *PLoS One* **12**, e0179586 (2017).
301. Lawrence, R. M. Host-resistance factors and immunologic significance of human milk. in *Breastfeeding* (eds. Lawrence, R. A. & Lawrence, R. M. B. T.-B. (Ninth E.)) 145–192 (Elsevier, 2022).
302. Melnik, B. C., John, S. M. & Schmitz, G. Milk: An exosomal microRNA transmitter promoting thymic regulatory T cell maturation preventing the development of atopy? *Journal of Translational Medicine* vol. 12 43 (2014).
303. Melnik, B. C., John, S. M., Carrera-Bastos, P. & Schmitz, G. Milk: a postnatal imprinting system stabilizing FoxP3 expression and regulatory T cell differentiation. *Clin. Transl. Allergy* **6**, 18 (2016).
304. Carter, B. M. & Holditch-Davis, D. Risk factors for necrotizing enterocolitis in preterm infants: how race, gender, and health status contribute. *Adv. neonatal care Off. J. Natl. Assoc. Neonatal Nurses* **8**, 285–290 (2008).
305. Ng, P. C. *et al.* Plasma miR-1290 Is a novel and specific biomarker for early diagnosis of necrotizing enterocolitis—biomarker discovery with prospective cohort evaluation. *J. Pediatr.* **205**, 83-90.e10 (2019).
306. Wu, C.-P., Bi, Y.-J., Liu, D.-M. & Wang, L.-Y. Hsa-miR-375 promotes the progression of inflammatory bowel disease by upregulating TLR4. *Eur. Rev. Med. Pharmacol. Sci.* **23**, 7543–7549 (2019).
307. Buoli Comani, G. *et al.* miRNA-regulated gene expression differs in celiac disease patients according to the age of presentation. *Genes Nutr.* **10**, 482 (2015).

308. Tian, Y. *et al.* Stress responsive miR-31 is a major modulator of mouse intestinal stem cells during regeneration and tumorigenesis. *Elife* **6**, (2017).
309. Chen, J. *et al.* MiR-146a-5p mimic inhibits NLRP3 inflammasome downstream inflammatory factors and CLIC4 in neonatal necrotizing enterocolitis. *Front. cell Dev. Biol.* **8**, 594143 (2020).
310. Chen, Z., Gu, Q. & Chen, R. miR-146a-5p regulates autophagy and NLRP3 inflammasome activation in epithelial barrier damage in the in vitro cell model of ulcerative colitis through the RNF8/Notch1/mTORC1 pathway. *Immunobiology* **228**, 152386 (2023).
311. Lu, D. *et al.* Maternal fiber-rich diet promotes early-life intestinal development in offspring through milk-derived extracellular vesicles carrying miR-146a-5p. *J. Nanobiotechnology* **22**, 65 (2024).
312. Chen, X. *et al.* miR-146a-5p promotes epithelium regeneration against LPS-induced inflammatory injury via targeting TAB1/TAK1/NF- κ B signaling pathway. *Int. J. Biol. Macromol.* **221**, 1031–1040 (2022).
313. Marschner, D. *et al.* MicroRNA-146a regulates immune-related adverse events caused by immune checkpoint inhibitors. *JCI insight* **5**, (2020).
314. Huang, F. *et al.* miR-148a-3p mediates notch signaling to promote the differentiation and M1 activation of macrophages. *Frontiers in Immunology* vol. 8 (2017).
315. Chiba, T. *et al.* Suppression of milk-derived miR-148a caused by stress plays a role in the decrease in intestinal ZO-1 expression in infants. *Clin. Nutr.* **41**, 2691–2698 (2022).
316. Cheng, S. *et al.* MiR-375-3p alleviates the severity of inflammation through targeting YAP1/LEKTI pathway in HaCaT cells. *Biosci. Biotechnol. Biochem.* **84**, 2005–2013 (2020).
317. Hicks, S. D., Beheshti, R., Chandran, D., Warren, K. & Confair, A. Infant consumption of microRNA miR-375 in human milk lipids is associated with protection from atopy. *Am. J. Clin. Nutr.* **116**, 1654–1662 (2022).
318. Qian, W., Liu, Y., Li, X. & Pan, Y. MicroRNA-141 ameliorates alcoholic hepatitis-induced intestinal injury and intestinal endotoxemia partially via a TLR4-dependent mechanism. *Int J Mol Med* **44**, 569–581 (2019).
319. Li, X., Wang, Y., Wang, Y. & He, X. MiR-141-3p ameliorates RIPK1-mediated

- necroptosis of intestinal epithelial cells in necrotizing enterocolitis. *Aging (Albany, NY)*. **12**, 18073–18083 (2020).
320. Sun, L., Sun, M., Ma, K. & Liu, J. Let-7d-5p suppresses inflammatory response in neonatal rats with necrotizing enterocolitis via LGALS3-mediated TLR4/NF- κ B signaling pathway. *Am. J. Physiol. Physiol.* **319**, C967–C979 (2020).
321. Tremblay, É. *et al.* IL-17-related signature genes linked to human necrotizing enterocolitis. *BMC Res. Notes* **14**, 82 (2021).
322. Chen, Y., Lun, A. T. L. & Smyth, G. K. From reads to genes to pathways: differential expression analysis of RNA-Seq experiments using Rsubread and the edgeR quasi-likelihood pipeline. *F1000Research* **5**, 1438 (2016).
323. McCarthy, D. J., Chen, Y. & Smyth, G. K. Differential expression analysis of multifactor RNA-Seq experiments with respect to biological variation. *Nucleic Acids Res.* **40**, 4288–4297 (2012).
324. Robinson, M. D., McCarthy, D. J. & Smyth, G. K. edgeR: a Bioconductor package for differential expression analysis of digital gene expression data. *Bioinformatics* **26**, 139–140 (2010).
325. Chang, L. & Xia, J. MicroRNA regulatory network Analysis Using miRNet 2.0. *Methods Mol. Biol.* **2594**, 185–204 (2023).
326. Szklarczyk, D. *et al.* The STRING database in 2021: customizable protein–protein networks, and functional characterization of user-uploaded gene/measurement sets. *Nucleic Acids Res.* **49**, D605–D612 (2021).
327. Hulsen, T., de Vlieg, J. & Alkema, W. BioVenn – a web application for the comparison and visualization of biological lists using area-proportional Venn diagrams. *BMC Genomics* **9**, 488 (2008).
328. Swieboda, D. *et al.* Baby’s first macrophage: Temporal regulation of hofbauer cell phenotype influences ligand-mediated innate immune responses across gestation. *J. Immunol.* **204**, 2380–2391 (2020).
329. Torow, N., Marsland, B. J., Hornef, M. W. & Gollwitzer, E. S. Neonatal mucosal immunology. *Mucosal Immunol.* **10**, 5–17 (2017).
330. MohanKumar, K. *et al.* Gut mucosal injury in neonates is marked by macrophage infiltration in contrast to pleomorphic infiltrates in adult: evidence from an animal model.

- Am. J. Physiol. Liver Physiol.* **303**, G93–G102 (2012).
331. Dreschers, S., Ohl, K., Schulte, N., Tenbrock, K. & Orlikowsky, T. W. Impaired functional capacity of polarised neonatal macrophages. *Sci. Rep.* **10**, 624 (2020).
332. Franzoni, G. *et al.* Goat milk extracellular vesicles: immuno-modulation effects on porcine monocyte-derived macrophages in vitro. *Front. Immunol.* **14**, (2023).
333. Zhu, F. *et al.* Blockage of NLRP3 inflammasome activation ameliorates acute inflammatory injury and long-term cognitive impairment induced by necrotizing enterocolitis in mice. *J. Neuroinflammation* **18**, 66 (2021).
334. Liu, X. & Lieberman, J. A mechanistic understanding of pyroptosis: The fiery death triggered by invasive infection. in *Advances in Immunology* (ed. Alt, F. W. B. T.-A. in I.) vol. 135 81–117 (Academic Press, 2017).
335. Berghe, T. Vanden *et al.* Simultaneous targeting of IL-1 and IL-18 is required for protection against inflammatory and septic shock. *Am. J. Respir. Crit. Care Med.* **189**, 282–291 (2014).
336. Plaza-Zamora, J. *et al.* Polyamines in human breast milk for preterm and term infants. *Br. J. Nutr.* **110**, 524–528 (2013).
337. Pageot, L.-P. *et al.* Human cell models to study small intestinal functions: Recapitulation of the crypt-villus axis. *Microsc. Res. Tech.* **49**, 394–406 (2000).
338. Beaulieu, J.-F. & Ménard, D. Isolation, characterization, and culture of normal human intestinal crypt and villus cells. in *Methods in molecular biology (Clifton, N.J.)* vol. 806 157–173 (2012).
339. Tremblay, E. *et al.* Gene-expression profile analysis in the mid-gestation human intestine discloses greater functional immaturity of the colon as compared with the ileum. *J. Pediatr. Gastroenterol. Nutr.* **52**, 670–678 (2011).
340. Vidal, K., Labéta, M. O., Schiffrin, E. J. & Donnet-Hughes, A. Soluble CD14 in human breast milk and its role in innate immune responses. *Acta Odontol. Scand.* **59**, 330–334 (2001).
341. Funda, D. P. *et al.* CD14 Is expressed and released as soluble CD14 by human intestinal epithelial cells in vitro: Lipopolysaccharide activation of epithelial cells revisited. *Infect. Immun.* **69**, 3772 LP – 3781 (2001).
342. Ward, T. L., Goto, K. & Altosaar, I. Ingested soluble CD14 contributes to the functional

- pool of circulating sCD14 in mice. *Immunobiology* **219**, 537–546 (2014).
343. Ruemmele, F. M. *et al.* Lipopolysaccharide modulation of normal enterocyte turnover by toll-like receptors is mediated by endogenously produced tumour necrosis factor alpha. *Gut* **51**, 842–8 (2002).
344. Francoeur, C., Escaffit, F., Vachon, P. H. & Beaulieu, J.-F. Proinflammatory cytokines TNF- α and IFN- γ alter laminin expression under an apoptosis-independent mechanism in human intestinal epithelial cells. *Am. J. Physiol. Liver Physiol.* **287**, G592–G598 (2004).
345. Schwartz, S., Beaulieu, J. F. & Ruemmele, F. M. Interleukin-17 is a potent immunomodulator and regulator of normal human intestinal epithelial cell growth. *Biochem. Biophys. Res. Commun.* **337**, 505–509 (2005).
346. Chanput, W., Mes, J. J. & Wichers, H. J. THP-1 cell line: an in vitro cell model for immune modulation approach. *Int. Immunopharmacol.* **23**, 37–45 (2014).
347. Baxter, A. A. *et al.* Analysis of extracellular vesicles generated from monocytes under conditions of lytic cell death. *Sci. Rep.* **9**, 7538 (2019).
348. Chen, X. *et al.* NEK7 interacts with NLRP3 to modulate the pyroptosis in inflammatory bowel disease via NF- κ B signaling. *Cell Death Dis.* **10**, 906 (2019).
349. Kale, J., Osterlund, E. J. & Andrews, D. W. BCL-2 family proteins: changing partners in the dance towards death. *Cell Death Differ.* **25**, 65–80 (2018).
350. Trzpis, M., McLaughlin, P. M. J., de Leij, L. M. F. H. & Harmsen, M. C. Epithelial cell adhesion molecule: more than a carcinoma marker and adhesion molecule. *Am. J. Pathol.* **171**, 386–395 (2007).
351. Djurisic, S. & Hviid, T. V. F. HLA class Ib molecules and immune cells in pregnancy and preeclampsia. *Frontiers in Immunology* vol. 5 (2014).
352. Fang, X., Zheng, P., Tang, J. & Liu, Y. CD24: from A to Z. *Cell. Mol. Immunol.* **7**, 100–103 (2010).
353. Tesfaigzi, Y. & Daheshia, M. CD14. in *Encyclopedia of Respiratory Medicine* (eds. Laurent, G. J. & Shapiro, S. D. B. T.-E. of R. M.) 343–347 (Academic Press, 2006).
354. Hall, P. E., Lathia, J. D., Miller, N. G. A., Caldwell, M. A. & French-Constant, C. Integrins are markers of human neural stem cells. *Stem Cells* **24**, 2078–2084 (2006).
355. Mizrak, D., Brittan, M. & Alison, M. R. CD133: molecule of the moment. *J. Pathol.* **214**, 3–9 (2008).

356. Dawod, B. & Marshall, J. S. Cytokines and soluble receptors in breast milk as enhancers of oral tolerance development. *Frontiers in Immunology* vol. 10 (2019).
357. Buchheister, S. *et al.* CD14 plays a protective role in experimental inflammatory bowel disease by enhancing intestinal barrier function. *Am. J. Pathol.* **187**, 1106–1120 (2017).
358. Dvorak, B. Milk epidermal growth factor and gut protection. *J. Pediatr.* **156**, S31–S35 (2010).
359. Fazioli, F. *et al.* Eps8, a substrate for the epidermal growth factor receptor kinase, enhances EGF-dependent mitogenic signals. *EMBO J.* **12**, 3799–3808 (1993).
360. Jeffery, V., Goldson, A. J., Dainty, J. R., Chieppa, M. & Sobolewski, A. IL-6 signaling regulates small intestinal crypt homeostasis. *J. Immunol.* **199**, 304–311 (2017).
361. Wei, J. & Besner, G. E. M1 to M2 macrophage polarization in heparin-binding epidermal growth factor-like growth factor therapy for necrotizing enterocolitis. *J. Surg. Res.* **197**, 126–138 (2015).
362. Wei, J., Meng, Z., Li, Z., Dang, D. & Wu, H. New insights into intestinal macrophages in necrotizing enterocolitis: the multi-functional role and promising therapeutic application. *Front. Immunol.* **14**, 1261010 (2023).
363. Bernhard, S. *et al.* Interleukin 8 elicits rapid physiological changes in neutrophils that are altered by inflammatory conditions. *J. Innate Immun.* **13**, 225–241 (2021).
364. Benmoussa, A. *et al.* Concentrates of two subsets of extracellular vesicles from cow's milk modulate symptoms and inflammation in experimental colitis. *Sci. Rep.* **9**, 14661 (2019).
365. Yu, P. *et al.* Pyroptosis: mechanisms and diseases. *Signal Transduct. Target. Ther.* **6**, 128 (2021).
366. Fattinger, S. A. *et al.* Gasdermin D is the only Gasdermin that provides protection against acute Salmonella gut infection in mice. *Proc. Natl. Acad. Sci.* **120**, e2315503120 (2023).
367. Zhang, J. *et al.* Epithelial Gasdermin D shapes the host-microbial interface by driving mucus layer formation. *Sci. Immunol.* **7**, eabk2092 (2022).
368. Swindell, W. R. *et al.* RNA-Seq analysis of IL-1B and IL-36 responses in epidermal keratinocytes identifies a shared MyD88-dependent gene signature. *Front. Immunol.* **9**, (2018).
369. Welsh, J. A. & Joshua A Welsh Sean M Cook, J. J. MPAPASS software collection.

- protocols.io* (2020).
370. Welsh, J. A. *et al.* MPAPASS software enables stitched multiplex, multidimensional EV repertoire analysis and a standard framework for reporting bead-based assays. *Cell Reports Methods* **2**, 100136 (2022).
 371. Vachon, P. H. & Beaulieu, J.-F. Transient mosaic patterns of morphological and functional differentiation in the Caco-2 cell line. *Gastroenterology* **103**, 414–423 (1992).
 372. Guezguez, A., Paré, F., Benoit, Y. D., Basora, N. & Beaulieu, J.-F. Modulation of stemness in a human normal intestinal epithelial crypt cell line by activation of the WNT signaling pathway. *Exp. Cell Res.* **322**, 355–364 (2014).
 373. Tremblay, E. *et al.* Gene expression profiles of normal proliferating and differentiating human intestinal epithelial cells: A comparison with the Caco-2 cell model. *J. Cell. Biochem.* **99**, 1175–1186 (2006).
 374. Zhuang, J., Dinsdale, D. & Cohen, G. M. Apoptosis, in human monocytic THP.1 cells, results in the release of cytochrome c from mitochondria prior to their ultracondensation, formation of outer membrane discontinuities and reduction in inner membrane potential. *Cell Death Differ.* **5**, 953–962 (1998).
 375. Livak, K. J. & Schmittgen, T. D. Analysis of relative gene expression data using real-time quantitative PCR and the $2^{-\Delta\Delta C(T)}$ Method. *Methods* **25**, 402–408 (2001).
 376. Willems, E., Leyns, L. & Vandesompele, J. Standardization of real-time PCR gene expression data from independent biological replicates. *Anal. Biochem.* **379**, 127–129 (2008).
 377. Yuksel, S., Yigit, A. A., Cinar, M., Atmaca, N. & Onaran, Y. Oxidant and antioxidant status of human breast milk during lactation period. *Dairy Sci. Technol.* **95**, 295–302 (2015).
 378. Lu, P. *et al.* Maternal aryl hydrocarbon receptor activation protects newborns against necrotizing enterocolitis. *Nat. Commun.* **12**, 1042 (2021).
 379. Swanson, L. *et al.* TLR4 signaling and macrophage inflammatory responses are dampened by GIV/Girdin. *Proc. Natl. Acad. Sci.* **117**, 26895–26906 (2020).
 380. Abaandou, L., Quan, D. & Shiloach, J. Affecting HEK293 cell growth and production performance by modifying the expression of specific genes. *Cells* **10**, (2021).
 381. Yang, S. *et al.* Programmed death of intestinal epithelial cells in neonatal necrotizing

- enterocolitis: a mini-review. *Front. Pediatr.* **11**, (2023).
382. Barnett, K. C., Li, S., Liang, K. & Ting, J. P.-Y. A 360° view of the inflammasome: Mechanisms of activation, cell death, and diseases. *Cell* **186**, 2288–2312 (2023).
383. Chen, R. *et al.* Expression and possible role of Silent Mating Type Information Regulation 2 Homolog 1 in post-necrotizing enterocolitis stricture in vivo and in vitro. *Front. Pediatr.* **10**, (2022).
384. Cheng, K. & Kalluri, R. Guidelines for clinical translation and commercialization of extracellular vesicles and exosomes based therapeutics. *Extracell. Vesicle* **2**, 100029 (2023).
385. Gupta, D., Zickler, A. M. & El Andaloussi, S. Dosing extracellular vesicles. *Adv. Drug Deliv. Rev.* **178**, 113961 (2021).
386. Webber, J. & Clayton, A. How pure are your vesicles? *J. Extracell. vesicles* **2**, (2013).
387. Filler, R. *et al.* Milk-derived exosomes prevent activation of inflammatory pathways in the lung during necrotizing enterocolitis. *Pediatrics* **149**, 893 (2022).
388. Yun, B., Kim, Y., Park, D.-J. & Oh, S. Comparative analysis of dietary exosome-derived microRNAs from human, bovine and caprine colostrum and mature milk. *J. Anim. Sci. Technol.* (2021).
389. Kankaanpää, S. *et al.* Comparative analysis of the effects of different purification methods on the yield and purity of cow milk extracellular vesicles. *J. Extracell. Biol.* **3**, e149 (2024).
390. Buratta, S. *et al.* Protein and lipid content of milk extracellular vesicles: A comparative overview. *Life* vol. 13 (2023).
391. Welsh, J. A. *et al.* Minimal information for studies of extracellular vesicles (MISEV2023): From basic to advanced approaches. *J. Extracell. vesicles* **13**, e12404 (2024).
392. Lesage, F. & Thébaud, B. Mesenchymal stromal cell-derived extracellular vesicles for neonatal lung disease: Tiny particles, major promise, rigorous requirements for clinical translation. *Cells* vol. 11 (2022).
393. Lotfy, A., AboQuella, N. M. & Wang, H. Mesenchymal stromal/stem cell (MSC)-derived exosomes in clinical trials. *Stem Cell Res. Ther.* **14**, 66 (2023).
394. Tan, F. *et al.* Clinical applications of stem cell-derived exosomes. *Signal Transduct. Target. Ther.* **9**, 17 (2024).

395. Zempleni, J. Extracellular vesicles and methods of using. (2018).
396. Qiu, C. *et al.* Nebulized milk exosomes loaded with siTGF- β 1 ameliorate pulmonary fibrosis by inhibiting EMT pathway and enhancing collagen permeability. *J. Nanobiotechnology* **22**, 434 (2024).
397. Jing, R. *et al.* Milk-derived extracellular vesicles functionalized with anti-tumour necrosis factor- α nanobody and anti-microbial peptide alleviate ulcerative colitis in mice. *J. Extracell. Vesicles* **13**, e12462 (2024).
398. Melnik, B. C., Weiskirchen, R. & Schmitz, G. Milk exosomal microRNAs: friend or foe?—a narrative review. *ExRNA; Vol 4 (October 31, 2022) ExRNA* (2022).
399. Piephoff, S. Biomanufacturing human milk components to improve early-life nutrition. *Nat. Biopharma Deal.* (2024).
400. Gilliland, H. C. B. T. Mother's milk: many parents rely on infant formula to feed their newborns. Could cell culture technology produce something closer to human breast milk? *MIT Technol. Rev.* **124**, 32+ (2021).
401. Valentine, C. J. *et al.* Lactational stage of pasteurized human donor milk contributes to nutrient limitations for infants. *Nutrients* **9**, (2017).

Curriculum vitae

DEGREES

- University of Ottawa, PhD Biochemistry** 2019/9-Present
Thesis title: “*Term-dependent changes in human milk extracellular vesicle composition – immunomodulatory effects in vitro*”
- University of Winnipeg, MSc Bioscience, Technology and Public Policy** 2014/9-2017/6
GPA 4.3 (on a 4.5 scale)
Thesis title: “*Exploring the role of insulin like peptide 5 and its cognate receptor in the immune system*”
- University of Leicester, BSc Medical Biochemistry** 2011/10-2014/6
2.1 Honours degree classification
Thesis title: “*Using molecular visualization and site-directed mutagenesis to improve Angiopoietin-2 binding to Tie-2*”

EMPLOYMENT

- Co-Principal Investigator – Research grant-based project** 2024/5-present
Children’s Hospital of Eastern Ontario Research Institute, and Prolacta, Pasadena, USA
- Junior Researcher – A liquid corneal glue-filler as an alternative to transplantation in high-risk patients** 2021/1-2022/6
Estonian University of Life Sciences, Tartu, Estonia
- Technician – Research and Development** 2017/9-2019/8
Intrinsic Analytics Inc., Winnipeg, Manitoba
- Laboratory Instructor** (Courses: Cells and Cellular Processes, Anatomy and Physiology, Evolution, Ecology and Biodiversity) 2014/9-2017/5
Department of Biology, Faculty of Science, University of Winnipeg

PUBLICATIONS

- Vahkal B**, Altosaar I, Ariana A, Jabbour J, Pantieras F, Daniel R, Tremblay E, Sad S, Beaulieu JF, Côté M, and Ferretti E, Human milk extracellular vesicles modulate inflammatory response and cell survival in intestinal and immune cells. *Pediatric Research*. In press. 2024
- Vahkal B**, Altosaar I, Hoang HD, Alain T, Barisani D, Côté M, Beaulieu JF, Ferretti E. Shielding against necrotizing enterocolitis: Insights from gestational-age-specific profiling of human milk extracellular vesicle microRNAs. *Scientific Reports*. Under review. 2024

Ariana A*, **Vahkal B***, Abu-Kwaik J, Abualhaj N, Laroche G, Bo Y, Benlarbi M, Finzi A, Abdelnour A, Côté M, Abu-Dayyeh I. Side-by-side comparison of plasma recognition and neutralization of Spike coronavirus glycoproteins from Sinopharm, Comirnaty, Covishield, Sputnik V and Spikevax COVID-19 vaccine recipients in Jordan. *Vaccines*. In preparation. 2024

Vahkal B, Altosaar I, Tremblay E, Gagné D, Hüttman N, Minic Z, Côté M, Blais A, Beaulieu JF, Ferretti E. Gestational age at birth influences protein and RNA content in human milk extracellular vesicles. *Journal of Extracellular Biology*, 3 (1), e128. 2024

Pickering B, ..., **Vahkal B**, ...et al. Divergent SARS-CoV-2 variant emerges in white-tailed deer with deer-to-human transmission. *Nature Microbiology*. 7 (12):2011-24. 2022

Hechter D, **Vahkal B**, Tiede T, Good SV. Reviewing the physiological roles of the novel hormone-receptor pair INSL5-RXFP4: a protective energy sensor? *Endocrinology*. 69 (1), R45-R62. 2022

Vahkal B, Kraft J, Ferretti E, Chung M, Beaulieu JF, Altosaar I. Review of Methodological Approaches to Human Milk Small Extracellular Vesicle Proteomics. *Biomolecules*. 11 (6), 833. 2021

Vahkal B, Yegorov S, Onyilagha C, Donner J, Reddick D, Shrivastav A, Uzonna J, Good SV. Immune System Effects of Insulin-Like Peptide 5 in a Mouse Model. *Frontiers in Endocrinology*. 11, 610672. 2021

Altosaar I and **Vahkal B**. Plant biochemistry mysteries – food science in the epoch of IT (*Taimede biokeemia müsteerium – toitlustus IT epohhil*) Proceedings, Forest University (*Metsaülikool*), Ed. Kadi Kass. 2020

Al Nafea H, **Vahkal B**, Zelmer K, Yegorov S, Bogerd J, Good SV. Japanese medaka as a model for studying the relaxin family genes involved in neuroendocrine regulation: insights from the expression of fish-specific paralogues of rln3 and insl5 and rxfp3/4-type receptors. *Molecular and Cellular Endocrinology*. 487, 2-11. 2019

CONFERENCE PUBLICATIONS

Vahkal B, Ferretti E, Beaulieu JF, Altosaar I, Côté M. Human milk extracellular vesicle cargo is influenced by timing of birth. *ISEV2023 Abstract Book. J. Extracell. Vesicles 2023*, 12 (S1), e12329. 2023/5

Vahkal B, Ferretti E, Beaulieu JF, Kraft J, Altosaar I. Proteome in human milk: Term- dependent changes in exosome composition and 2020

modulation of inflammatory markers in vitro. *Frontiers Event Abstracts, Virtual ISRHML Research Workshop*.

Vahkal B, Ferretti E, Altosaar I, Beaulieu JF. Proteome and microRNAs in human milk: Term-dependent changes in exosome composition. *The FASEB Journal*. 34 (S1), pp. 1-1. 2020

PRESENTATIONS

Canadian Society for Molecular Biosciences 66th Annual Meeting 2023/5
Poster Presentation: “*Characterizing the protein cargo of human milk extracellular vesicles*”, Ottawa, Canada

International Society for Extracellular Vesicles Annual Meeting 2023/5
Oral Presentation: “*Human milk extracellular vesicle cargo is influenced by timing of birth*”, Seattle, USA

Euronanomed Final Symposium 2022/3
Poster Presentation: “*A liquid corneal glue-filler as an alternative to transplantation in high-risk patients*”, Virtual

The International Society for Research in Human Milk and Lactation 20th Biennial Conference. 2021/8
Oral Presentation: “*Term-dependent changes in human milk EV composition – immunomodulatory effects in vitro*”, Virtual

The International Society for Research in Human Milk and Lactation Virtual Research Workshop. 2020/8
Oral Presentation: “*Proteome in human milk: Term- dependent changes in exosome composition and modulation of inflammatory markers in vitro*”, Virtual

Experimental Biology 2020/4
Poster Presentation: “*Proteome and microRNAs in human milk: Term-dependent changes in exosome composition*”, Virtual

8th International Conference on Relaxin and Related Peptides 2018/5
Oral and Poster Presentations: “*Exploring the role of INSL5 and its cognate receptor in the immune system*”, Cabo San Lucas, Mexico

18th International Congress of Comparative Endocrinology 2017/6
Oral Presentation: “*Potential role of INSL5 and RXFP4 in the immune system*”, Lake Louise, Canada

Beyond Sciences Initiative (BSI) Conference 2017/2
Oral Presentation: “*Exploring the role of INSL5 and RXFP4 in the immune system*”, Winnipeg, Canada

Project Pulse Winnipeg Panel Presentation: “ <i>University Panel</i> ”, Winnipeg, Canada	2016/5
Prairie University Biology Symposium Oral Presentation: “ <i>Relaxin Family of Peptides</i> ”, University of Lethbridge, Canada	2016/2

COMMUNITY AND VOLUNTEER ACTIVITIES

Organizing Committee Member, Canadian Extracellular Vesicle Online Symposium, and Society Virtual	2021/6-2024/1
International Society for Extracellular Vesicles Annual Meeting, Milk EVs Poster Session Co-chair Seattle, USA	2023/5
Animal Care Committee (UACC) Student Board Member University of Winnipeg	2016/5-2017/5
Peer-reviewer Proceedings of Manitoba's Science and Engineering Research	2016/5-2017/4
Let's Talk Science (LTS) Outreach Volunteer University of Winnipeg	2015/9-2017/4
Conference Coordinator Beyond Sciences Initiative (BSI) Conference, Winnipeg branch	2017/1-2017/2

AWARDS

Biotalent Student Work Placement Program	2024/5-2024/8
University of Ottawa Admission Scholarship	2019/9-2023/9
Ontario Graduate Scholarship	2021/1-2022/5
University of Ottawa, Faculty of Medicine Conference Grant	2021/8
Relaxin and Related Peptides Conference Award Best Poster	2018/5
Relaxin and Related Peptides Conference Travel Grant	2018/5
University of Winnipeg Teaching Assistantship	2014/9-2017/5
University of Winnipeg Graduate Travel Award	2017/5
University of Winnipeg Graduate Scholarship	2014/9-2017/4
Donna Young Teaching Award	2016/9
University of Winnipeg Student Association Travel Grant	2016/2
Prairie University Biology Symposium – 2nd prize	2016/2